From the

Institute for Cardiovascular Prevention, Ludwig-Maximilians University

DISSERTATION

zum Erwerb des Doctor of Philosophy (Ph.D.) an

der

Medizinischen Fakultät der

Ludwig-Maximilians-Universität zu München

Cell-specific roles of ACKR3 in atherosclerosis

submitted by

Selin Gencer

from

Malatya, Turkey

2021

First supervisor: Prof. Dr. Christian Weber

Second supervisor: Prof. Dr. Jürgen Bernhagen

Third supervisor: Dr. Siegfried Ussar

Further supervisors: Dr. Emiel van der Vorst, Prof. Yvonne Döring

Dean: Prof. Dr. Thomas Gudermann

Date of oral defense: 20.05.2022

Publications arising from the projects presented in this thesis:

Gencer S, Döring Y, Jansen Y, Bayasgalan S, Schengel O, Müller M, Peters LJF, Weber C, van der Vorst EPC. **Adipocyte-Specific ACKR3 Regulates Lipid Levels in Adipose Tissue**. *Biomedicines*. 2021 Apr 6;9(4):394. doi: 10.3390/biomedicines9040394. PMID: 33917642; PMCID: PMC8067615.

Gencer S, Jansen Y, Bayasgalan S, Yan Y, Bianchini M, Cimen I, Müller M, Peters LJF, Megens RTA, Duchene J, Lemnitzer P, Soehnlein O, Weber C, Döring Y, van der Vorst EPC. **Endothelial ACKR3 drives atherosclerosis by promoting immune cell adhesion to vascular endothelium**. *Basic Research in Cardiology* (currently in revision).

Table of contents

Abstract

Cardiovascular diseases have been responsible for the majority of deaths worldwide for a long time. Atherosclerosis is the main pathology behind cardiovascular diseases and its treatment is the key to curb the world's leading killer. Atherosclerosis is characterized by lesion development in medium- to large-sized arteries and its major drivers are hyperlipidemia and inflammation. Patients with hyperlipidemia are recognized to be at risk for atherosclerosis and therefore treated with cholesterol lowering medication, such as statins. Nonetheless, inflammation is also a strong driver of atherosclerosis and research aimed at identifying novel anti-inflammatory therapeutic targets for atherosclerosis treatment is still ongoing. The chemokine system heavily contributes to numerous aspects of atherosclerotic inflammation, therefore chemokines and chemokine receptors are scrutinized in the search for novel therapeutic candidates. The atypical chemokine receptor-3 (ACKR3) gained significant interest in this field as it was revealed to be an alternative receptor for the atherosclerotic chemokine CXCL12. Although CXCL12 and its other receptor CXCR4 have been studied in the context of atherosclerosis, investigation of ACKR3 in this disease model remains to be explored in detail.

This study elucidated the role of ACKR3 in atherosclerosis *in vivo* with regards to its cell type specific functions. In doing so, cell specific deficiency of the receptor was accomplished in hyperlipidemic mice prone to develop atherosclerosis. Endothelial specific deficiency of ACKR3 limited atherosclerosis formation in mice, whereas its deficiency in smooth muscle cells, hematopoietic cells, adipocytes and hepatocytes did not significantly contribute to atherosclerosis. ACKR3 in the endothelium regulated cell adhesion and thereby modulated the entry of circulating immune cells into the sub-endothelial space of the arteries. This effect was reflected by reduced lesional macrophage accumulation and therefore lesion development in mice lacking endothelial ACKR3. Further analyses revealed that ACKR3 mediated ICAM and VCAM driven endothelial adhesion via the MAPK and NF-kB pathways. We also established that ACKR3 has an adverse impact on PPAR-γ signalling both in endothelial cells and in adipocytes. ACKR3 deficiency in the adipocytes limited lipid accumulation within the tissue by modulating the activity of the lipoprotein lipase via ANGPTL4 and PPAR-γ. Interestingly, ACKR3 deficiency did not affect CXCL12 concentrations in any of the mouse models.

Overall, this study establishes a significant and novel role of the endothelial ACKR3 in diet induced atherosclerosis. These findings indicate that the endothelial ACKR3 has the potential to be further investigated in therapeutic research for atherosclerosis. Furthermore, ACKR3 is characterized as a functional and signalling receptor. The role of ACKR3 in adipose tissue lipid accumulation suggests that adipocyte specific ACKR3 may be a noteworthy target to study in further disease models, such as obesity and metabolic syndrome.

List of figures

List of tables

List of abbreviations

µl	Microliter
µM	Micromolar
4-OHT	4-Hydroxytamoxifen
AAV	Adeno associated virus
ACKR	Atypical chemokine receptors
ad	Adipocyte
ADM	Adrenomedullin
aEC	Arterial endothelial cell
Angptl4	Angiopoietin-like 4
ApoE	Apolipoprotein E deficient
AT	Adipose tissue
BAM22	Bovine adrenal medulla 22
BCA	Bicinchoninic acid assay
Bmx	Bone marrow x promoter
BSA	Bovine serum albumin
cDNA	Copy deoxyribonucleic acid
CNS	Central nervous system
Cre	Cre recombinase
CreER	Cre fused to an estrogen receptor
CreERT	CreER induced by tamoxifen
CVD	Cardiovascular disease
DAPI	4′,6-diamidino-2-phenylindole
ddPCR	Droplet digital polymerase chain reaction
dH2O	Deionized water
dNTP	Deoxynucleoside triphosphate
EC	Endothelial cell
EDTA	Ethylene-diamine-tetraacetic acid

EPC	Endothelial progenitor cell
ER	Estrogen receptor
Erk1/2	Extracellular Signal-Regulated Kinase 1/2
EtOH	Ethanol
EVB	Evans blue
FPLC	Fast-performance liquid chromatography
g	Gravitational (centrifugal) force
gDNA	genomic DNA
GDP	Guanosine diphosphate
GPCR	G-protein coupled receptors
GRK	G protein coupled receptor kinases
GTP	Guanosine triphosphate
GWAS	Genome wide association study
h	Hepatocyte
HBSS	Hank's Balanced Salt Solution
HCAEC	Human coronary artery endothelial cell
HDL	High density lipoproteins
HEK	Human embryonic kidney
HIV	Human immunodeficiency virus
HRP	Horseradish peroxidase
ht	Hematopoietic compartment
HUVEC	Human umbilical vein endothelial cell
IBD	Inflammatory bowel disease
ICAM	Intracellular adhesion molecule
IDL	Intermediate density lipoproteins
IL	Interleukin
IL-1β	Interleukin-1β
LDL	Low density lipoproteins

LOX-1	Lectin-like oxLDL receptor-1
loxP	Locus of X over P1
LPL	Lipoprotein lipase
M	Molar
MAPK	Mitogen activated protein kinase
mg	Milligram
MgCl2	Magnesium Chloride
MIF	Macrophage inhibitory factor
ml	Mililiter
mM	Milimolar
MPTC	Maastricht Pathology Tissue Collection
NF-kB	Nuclear factor kappa B
ng	nanograms
nM	Nanomolar
nm	nanometer
OD	Optical density
oxLDL	Oxidized LDL
PBS	Phosphate buffered saline
PCR	Polymerase chain reaction
PECAM	platelet endothelial cell adhesion molecule
PFA	Paraformaldehyde
PM	Phosphomolybdic
PPAR-γ	Peroxisome proliferator-activated receptor-gamma
PT	Phosphotungstic
RNA	Ribonucleic acid
rpm	Rotations per minute
RT	Room temperature
SEM	Standard error of the mean

siRNA	Silencing RNA
SMC	Smooth muscle cell
SNS	Sympathetic nervous system
SR	Scavenger receptors
TBST	Tris-buffered saline with Tween 20
TNF-α	Tumor necrosis factor-alpha
U	Units
VCAM	Vascular adhesion molecule
VLDL	Very low density lipoproteins
vWF	von Willebrand factor
WD	Western diet
WHO	World Health Organization

1. Introduction

1.1 Cardiovascular Diseases: A Global Concern

Cardiovascular diseases (CVDs) refer to a spectrum of disorders, which significantly compromise the health of heart and blood vessels, such as coronary artery disease, heart failure, arrhythmia, heart attack, lower extremity arterial disease and stroke (Flora & Nayak, 2019). A report by the World Health Organization (WHO) evaluating foremost reasons of death worldwide reveals that CVDs are the top ranked causes of death (World Health Organization, 2020). They identified ischemic heart disease as the 'world's biggest killer', followed by stroke (Figure 1). It is also evident that the number of deaths have been increasing from 2000 to 2019. These facts highlight the need for more effective prevention and treatment strategies for CVDs. Therefore, a better understanding of the main pathology behind CVDs is needed. Atherosclerosis is a disease leading to plaque formation in arteries and it is the primary cause of CVDs (Frostegård, 2013). Atherosclerosis can lead to arterial narrowing, ischemic cardiovascular diseases and thrombotic complications (Weber & Noels, 2011).

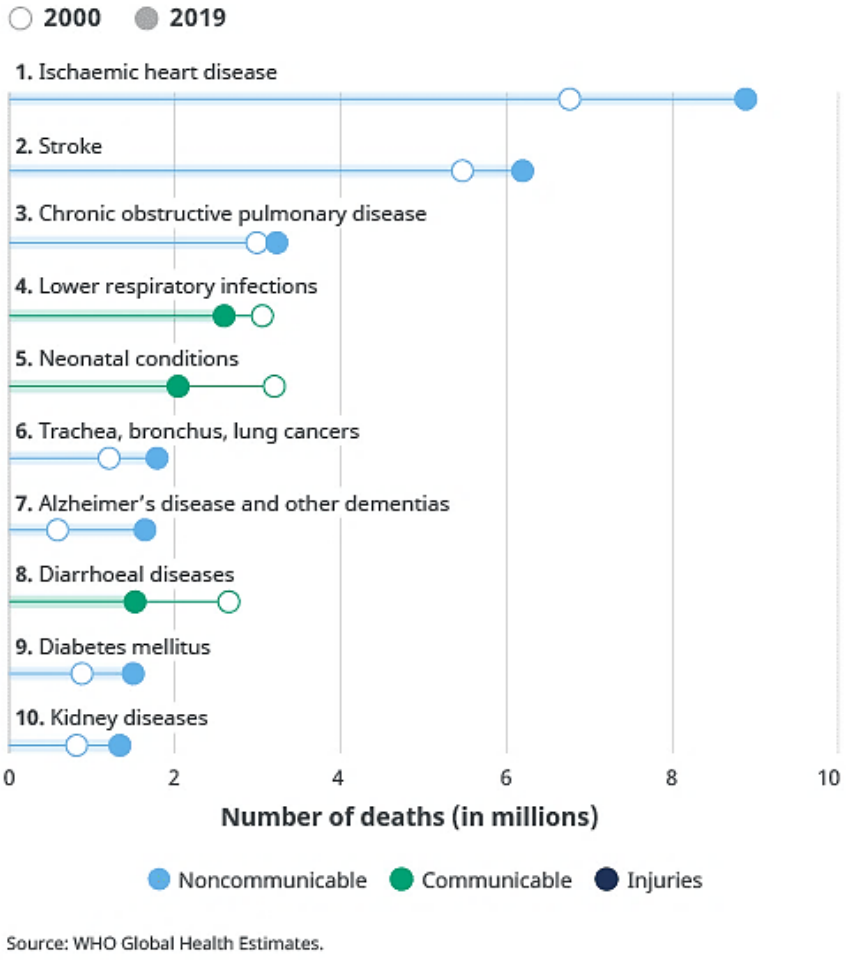

Figure 1: Leading causes of death globally.

WHO identifies CVDs as the leading cause of death globally, according to their report 2000-2019. Adopted from WHO's Global Health Estimates (World Health Organization, 2020).

1.2 Atherosclerosis

The vascular disease termed ‘atherosclerosis’ is best defined as the hardening and narrowing of arteries as a result of plaque formation inside the arterial walls (Figure 2) (Rafieian-Kopaei et al., 2014). Atherosclerotic plaques affect medium and large sized arteries and they commonly occur at arterial bifurcations, where disturbed blood flow associated with higher hemodynamic shear stress is observed (Khatana et al., 2020). The plaques are characterized by the accumulation of lipids and immune cells underneath the endothelial lining of the arteries, known as the arterial wall (Figure 2). Therefore, dysregulation of lipid metabolism and chronic inflammation are recognized as two main factors in atherosclerosis development (Malekmohammad et al., 2021). Currently, the golden standard therapy for atherosclerosis is the mitigation of lipid levels in patients together with hypertension treatment. Nevertheless, research for effective anti-inflammatory therapeutics for atherosclerosis is still ongoing. The importance of this approach is proven by the CANTOS trial, which demonstrated a significant decrease in cardiovascular complications in canakinumab (monoclonal antibody against IL-1ß) treated patients targeting a highly inflammatory molecule in comparison to placebo treated patients (Ridker et al., 2017). Progression and severity of atherosclerosis may differ on an individual basis, especially with regards to the presence of atherosclerotic risk factors. Main risk factors are, for example, hyperlipidemia, high blood pressure, smoking, obesity, insulin resistance, older age, stress, family history, etc. (Herrington et al., 2016; Rafieian-Kopaei et al., 2014).

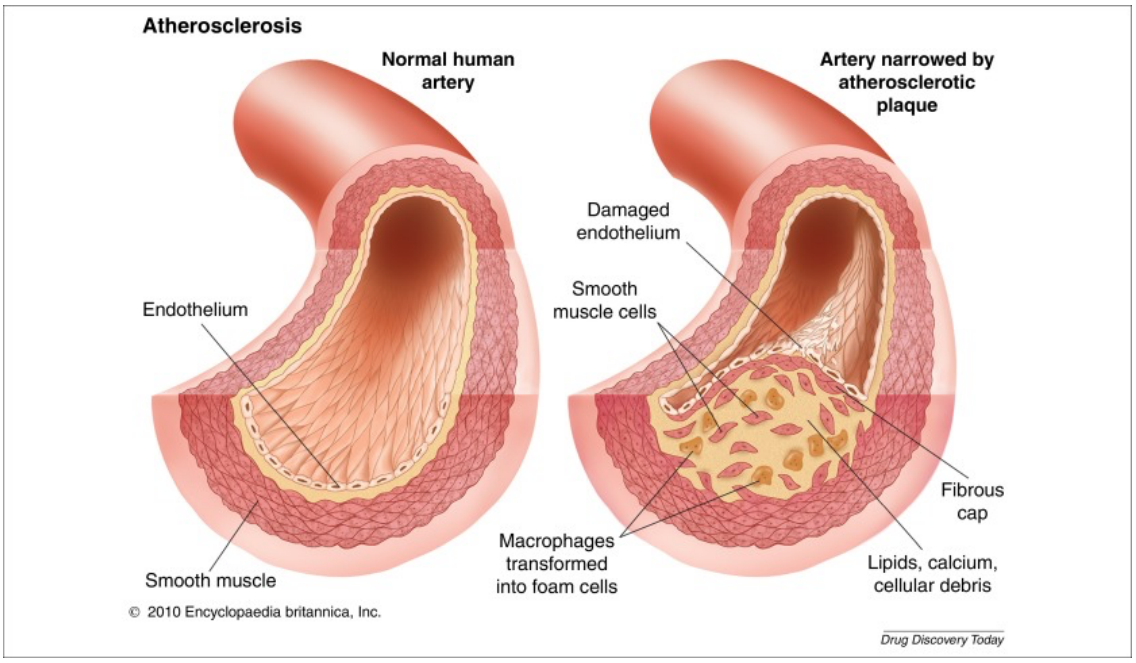

Figure 2: Normal artery versus narrowed artery by an atherosclerotic plaque.

This image compares a healthy artery and a narrowed artery with an atherosclerotic plaque. Lipid laden atheroma formation is observed in the sub-endothelial space. The plaque contains foam cells, lipids, calcium and cellular debris. The image is adopted from Subbotin, 2016 (Subbotin, 2016).

Atherosclerosis is a slowly progressing disease over a long period of time and it can advance to a serious degree without demonstrating symptoms in patients. By the time patients experience symptoms, the disease may have reached advanced stages with a high risk of potentially fatal clinical manifestations, such as occlusion of the arteries leading to downstream hypoxia or rupture of the plaques leading to thrombosis (Gatto & Prati, 2020). Atherosclerosis can lead to thrombus formation, ischemic heart disease, coronary heart disease, myocardial infarction, stroke, as well as sudden death (Toth, 2008).

1.2.1 Pathobiology of Atherosclerosis

The progression of atherosclerotic lesions initiates with the formation of fatty streaks (Rafieian-Kopaei et al., 2014), which develop as a result of arterial entry of excessive lipids in the circulation (Figure 3, A). As mentioned above, hyperlipidemia is a known risk factor for atherosclerosis and it refers to abnormally augmented lipid levels in the blood (Nelson, 2013). Hyperlipidemia is evaluated by measuring the total cholesterol and triglyceride levels from the blood samples of fasted patients, which may be done via the assessment of plasma lipoproteins (Nelson, 2013). Lipids on their own are insoluble in the plasma due to their hydrophobic nature and are therefore carried by lipoproteins in the circulation, which are also responsible for transporting the lipids to cells (Olson, 1998). Lipoproteins are the products of lipids binding to special proteins called apolipoproteins (Lestavel & Fruchart, 1994) and there are five major types of lipoproteins based on their density: chylomicrons, very low density lipoproteins (VLDL), intermediate density lipoproteins (IDL), low density lipoproteins (LDL) and high density lipoproteins (HDL) (Eisenberg, 1983). Chylomicrons are the biggest lipoproteins in size and they are dispensed from the intestines to deliver dietary lipids to other cells (Mansbach & Siddiqi, 2010). VLDL, on the other hand, carries lipids from the liver to other organs and in doing so, it is hydrolyzed into IDL and LDL in the plasma (Mahley et al., 1984). LDL is the main transporter of cholesterol in the circulation (Mahley et al., 1984). Last but not least, HDL, the smallest lipoprotein, is responsible for reverse cholesterol transport, a process that allows extraction of cholesterol from tissues to be returned to the liver (Tall, 1998). Due to the roles of LDL and HDL, their quantities in the patients' blood samples are evaluated as risk factors for atherosclerosis; patients with a low HDL concentration (<40mg/dL) or/and a high LDL concentration (>190mg/dL) are considered to be at increased risk for arterial plaque formation (Hao & Friedman, 2014).

Under regular circumstances, circulating and intracellular levels of LDL are balanced (Rafieian-Kopaei et al., 2014). However, this balance may be compromised if LDL load in circulation reaches surplus as a result of varying factors, such as excessive calorie consumption or genetic family history (Soran et al., 2018). LDL dependent lipid transport to cells requires lipoprotein recognition by the cells, which is enabled by lipoprotein receptors. However, surplus of LDL may delay its clearance and lead to its oxidization (oxLDL), which as a result interferes with its recognition and uptake by the cells (Lestavel & Fruchart, 1994). Excess LDL in the circulation can enter and accumulate in the sub-endothelial space of the arteries leading to the formation oxLDL (Pirillo et al., 2013). oxLDL in the sub-endothelial space activates tissue resident macrophages, which

release inflammatory cytokines, such as tumor necrosis factor-alpha (TNF-α) or interleukin-1β (IL-1β). This leads to the activation of the vascular endothelium, which subsequently initiates a cascade of pro-atherosclerotic events (Figure 3, A). Furthermore, hemodynamic shear stress can also lead to vascular endothelial damage, which causes endothelial inflammation (Davies, 2009). This biomechanical stress is exacerbated at regions of disturbed blood flow, such as arterial divisions, as well as pathological factors, such as hypertension. (Davies, 2009). Activated endothelium releases inflammatory cytokines and chemokines, such as CCL2, in order to recruit immune cells to eliminate the root cause of inflammation; oxLDL (Harrington, 2000). Chemokines are chemotactic cytokines which heavily contribute to several stages of atherosclerosis and will be discussed in detail in the next chapter.

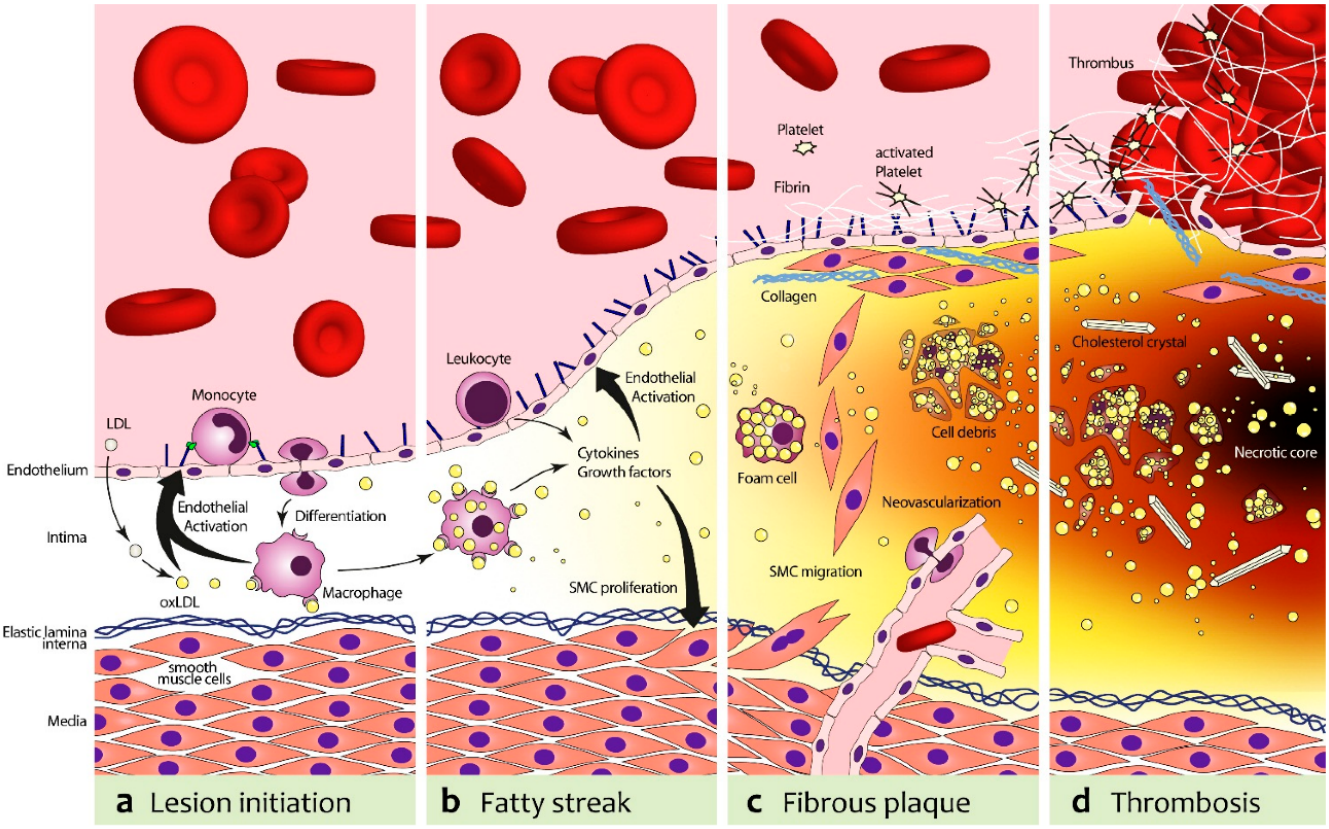

Figure 3: Step-wise progression of atherosclerosis.
LDL breaches the vascular endothelium and becomes oxidized in the arterial intima. Endothelium is activated and it recruits immune cells which infiltrate into the intima and turn into foam cells leading to fatty streak formation. As atherosclerosis formation advances, SMCs migrate to the luminal side and necrotic core forms as a result of apoptotic macrophage accumulation. Eventually, atherosclerosis can result in plaque rupture and thrombosis. This image was adopted from Steinl & Kaufmann, 2015 (Steinl & Kaufmann, 2015).

One of the foremost immune cells to infiltrate the inflamed endothelium are monocytes (Figure 3, A) (Randolph, 2009). Infiltration of immune cells into the arterial intima occurs though a process called transmigration and it requires passage of the cells through the vascular endothelium. Dur-

ing this process, permeability of the vascular endothelium is a critical factor determining the integrity of the endothelial barrier function, as it regulates the trafficking of lumen materials and cells into the vessels (Sluiter et al., 2021). Transmigration of the immune cells is a highly regulated mechanism and it occurs through several steps: capture, rolling, firm adhesion and transmigration (Figure 4) (Gerhardt & Ley, 2015). During this process, activated endothelium at the site of inflammation upregulates the surface expression of adhesion molecules in order to capture and arrest circulating immune cells. Adhesion molecules, such as E-selectin and P-selectin mediate the rolling and tethering of the immune cells, whereas intracellular adhesion molecule (ICAM) and vascular adhesion molecule (VCAM) are responsible for the firm adhesion of the immune cells to the vascular endothelium (Figure 4) (Blankenberg et al., 2003). Adhesion of the leukocytes onto the endothelium is a crucial part of their trans-endothelial migration and the presence of ICAM-1 as well as VCAM-1 on the endothelium of atherosclerotic lesions have been steadily reported (Blankenberg et al., 2003). Endothelial ICAM-1 and VCAM-1 bind to leukocyte function associated antigen-1 (LFA-1) (Figure 4) and very late antigen-4 (VLA-4) present on the surface of the immune cells, respectively (Yusuf-Makagiansar et al., 2002).

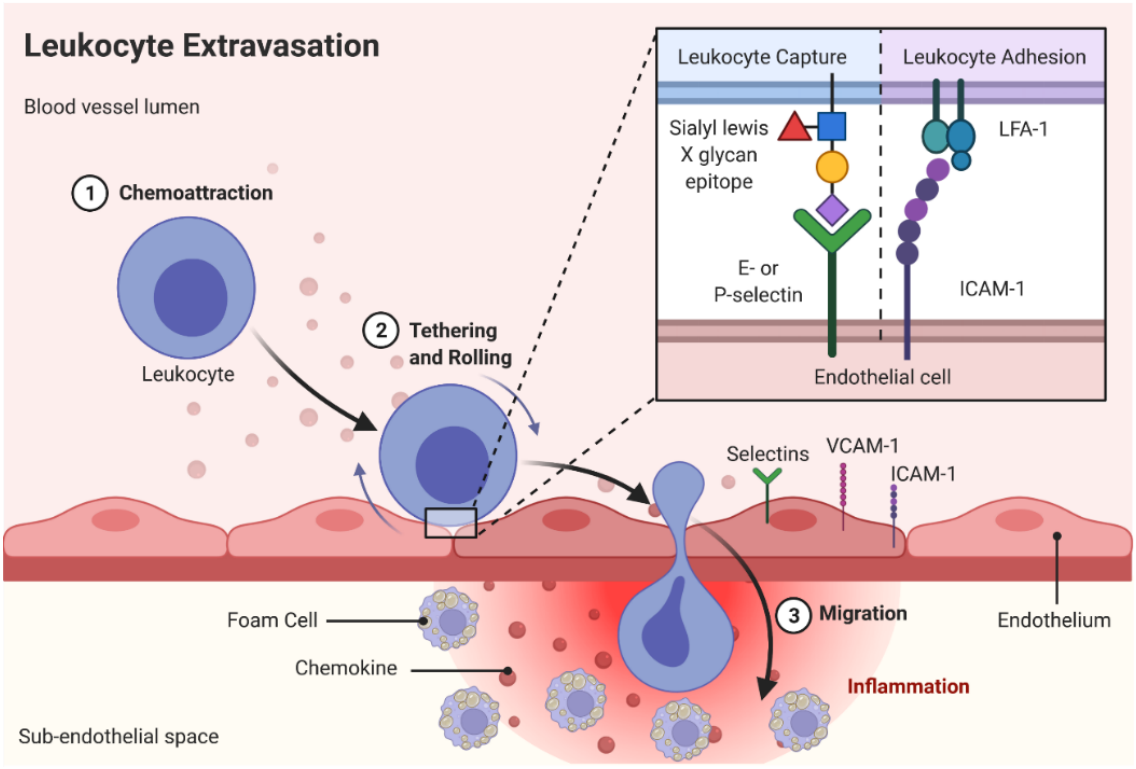

Figure 4: Trans-endothelial migration of immune cells at the vascular wall.

Infiltration of the circulating immune cells into the sub-endothelial space requires chemo-attraction of the leukocytes, followed by tethering and rolling, adhesion and finally transmigration through the vascular endothelium. The capture step is mediated by the endothelial selectins, whereas during the adhesion step, endothelial ICAM and VCAM molecules play a critical role binding to LFA-1 and VLA-4 molecules on the surface of immune cells, respectively. Created with BioRender.com.

Once in the sub-endothelial space, monocytes differentiate into macrophages (Lestavel & Fruchart, 1994; Ley et al., 2011). These macrophages are capable of recognizing oxLDL via their scavenger receptors (SR), such as CD36, lectin-like oxLDL receptor-1 (LOX-1), as well as clearing the oxLDL by means of phagocytosis (Chistiakov et al., 2016; Yu et al., 2013). Upon engulfing the oxLDL, macrophages hydrolyze it into cholesterol via their lysosomes, which then needs to be removed from macrophages via cholesterol efflux (Chistiakov et al., 2016). However, when the uptake of cholesterol is larger than the efflux of cholesterol in macrophages, they become loaded with lipids and form the so called foam cells (Bobryshev, 2006). These foam cells are indicators of very early steps of lesion formation, as the aggregation of these foam cells in the arteries lead to visible fatty streaks (Figure 3, B) (Stary et al., 1994). Such fatty streaks can evolve into atheromas by the accumulation of lipids as well as the migration of adjacent smooth muscle cells (SMCs) at the luminal side of the vascular wall, which form a collagen rich fibrous cap by synthesizing extracellular matrix (Figure 3, C) (Libby et al., 1996). At this stage, cell debris and neovascularization within the plaque can be observed (Figure 3, C). Over time, oxLDL clearing macrophages become loaded with lipids and may become apoptotic, which signals the necessity of their clearance by other macrophages through a process named efferocytosis (Seimon & Tabas, 2009). Essentially, this is a smart way of limiting cellularity in the plaque and therefore inhibiting its growth (Seimon & Tabas, 2009). Nevertheless, efferocytosis may become inefficient in lesions which have significantly advanced. In such cases, impaired efferocytosis leads to increased accumulation of foam cells, which eventually become necrotic and form a necrotic core within lesions (Figure 3, D) (Kojima et al., 2017). Moreover, cholesterol crystals are visible in the plaques at this stage (Figure 3, D). Necrotic cores are a hallmark of vulnerable plaques, which may lead to plaque rupture and subsequent thrombosis (Naghavi et al., 2003). Another factor that can determine the vulnerability or alternatively the stability of the plaque is the thickness of fibrous cap formed by the SMC; thinner fibrous cap may be indicative of a plaque that is prone to rupture and vice versa (Seneviratne et al., 2013).

1.3 The Chemokine System

1.3.1 Chemokines & Chemokine Receptors

Chemokines are a subset of cytokines that possess the ability to prompt chemotaxis on immune cells, hence they are also known as chemotactic cytokines (Hughes & Nibbs, 2018). Chemokines are secreted proteins that are very small in size, 8-10 kDa, and they are grouped into four families based on the pattern of their cysteine residues: C, CC, CXC and CX_3C chemokines (Tripathi & Poluri, 2020). In these classes, C represents the cysteine residue and X represents any amino acid. The three dimensional structure of the chemokines was identified for the first time in 1990 with the chemokine CXCL8 (L referring to ligand), also known as interleukin-8 (IL-8) (Clore et al., 1990). All classes of chemokines share a common basic structure; a signaling domain (N-terminal) and a core domain made up of an N-loop, three stranded ß-sheets and a helix at the C-terminal (Figure 5, A) (Clore et al., 1990). The C chemokines have two cysteine residues, one at the C terminus and one at the N terminus, whereas the CC chemokines have two neighboring cysteine residues at their N terminus (Figure 5, B). Such neighboring cysteine residues are divided by one amino acid (X) in the CXC chemokines and three amino acids (XXX) in the CX_3C chemokines (Figure 5, B).

Chemokines signal through seven transmembrane cell surface receptors which are categorized into two classes: the classical chemokine receptors: G-protein coupled receptors (GPCRs), as well as the non-classical chemokine receptors: atypical chemokine receptors (ACKRs) (Gencer et al., 2019). GPCRs make up the biggest portion of the cell surface proteins and they owe their name to their ability to signal through G proteins (Edward Zhou et al., 2019). Chemokines bind to the N terminus of the GPCRs, which is located on the outside of the cell (Hanlon & Andrew, 2015). Upon ligand binding, GPCRs go through a conformational change which enables them to bind to G-proteins; these are constituted by three subunits (α, ß and γ). The α subunit of the G protein then hydrolyzes guanosine triphosphate (GTP) to guanosine diphosphate (GDP) and subsequently dissociates from its ß and γ subunit dimer. Activated G protein then initiates a signaling cascade; the α subunit can activate adenylyl cyclase and its downstream signaling, whereas the ßγ subunit can summon G protein coupled receptor kinases (GRKs) to phosphorylate the GPCR and induce a negative feedback loop via ß-arrestin dependent clathrin mediated endocytosis of the receptor (Gurevich & Gurevich, 2019; Hanlon & Andrew, 2015). Downstream signaling of GPCRs can regulate many transcription factors and therefore gene expression. This feature of GPCRs allows them to control many physiological responses in the cells, such as proliferation, differentiation, development, cell survival, angiogenesis and cell migration (Marinissen & Gutkind, 2001). Due to their various roles, extensive presence as well as their easy access positioning (cell surface), GPCRs are regarded as attractive therapeutic targets for pharmacological treatment of many pathological conditions.

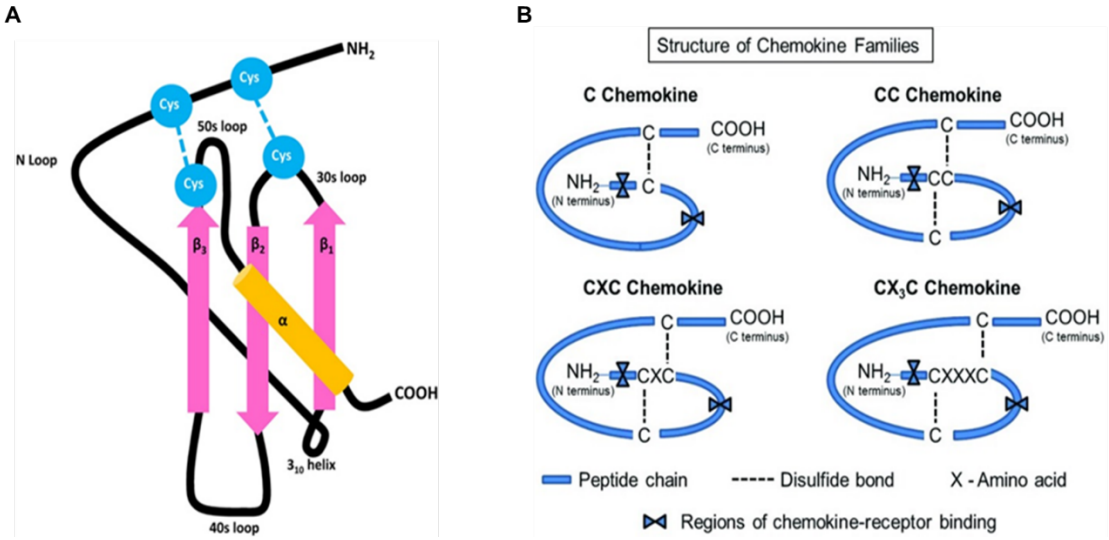

Figure 5: Structure of chemokines.

A. Commonly shared basic tertiary structure of the chemokines consisting of an N terminus, alpha helix, three ß sheets and a C terminus. **B.** Classification and structure of the chemokines into four subgroups based on their cysteine residue positioning. Image **A** was adopted from Metzemaekers et al (Metzemaekers et al., 2018) and image **B** was adopted from Balaji et al. (Balaji et al., 2015).

In addition to GPCRs, chemokines can also bind ACKRs. ACKRs are seven transmembrane receptors which are structurally very similar to GPCRs, however they lack the ability to signal through G proteins (Graham et al., 2012). This inability stems from the fact that the ACKRs lack the canonical DRYLAIV motif with the following amino acid sequence: Asp-Arg-Tyr-Leu-Ala-Ile-Val (Ulvmar et al., 2011). Instead of classical GPCR signaling, ACKRs have been evaluated for their ability to scavenge their ligands by receptor internalization, therefore they are also known as decoy receptors (Bachelerie, Graham, et al., 2014). ACKRs are described to recruit ß-arrestin upon ligand binding, which in turn initiates receptor internalization by acting as a clathrin adaptor (Galliera et al., 2004). This characteristic of the ACKRs allow them to regulate the bioavailability of their chemokines and therefore indirectly modulate their signaling and thus signaling dependent effects. Five major members of the ACKR family have been identified: ACKR1 (DARC), ACKR2 (D6), ACKR3 (CXCR7), ACKR4 (CCX-CKR) and ACKR5 (CCRL2) (Quinn et al., 2018). The decoy function of the ACKRs can serve in two different ways; for example, ACKR1 is known to aid in establishing concentrations of chemokines via chemokine transportation (Pruenster et al., 2009), whereas, ACKR2 is known to degrade its ligands (Fra et al., 2003).

1.3.2 The Chemokine System in Atherosclerosis

Hyperlipidemia and other risk factors play a significant role in the initiation of atherosclerosis, however, the main pathological driver of atherosclerotic lesion progression is chronic inflammation. Orchestration of the inflammation driven by the immune system relies heavily on the participation of the chemokine system. Chemokines and their receptors are best known for their chemotactic abilities, which is essential in the process of immune cell recruitment to the sites of inflammation (Baggiolini et al., 1997). Nonetheless, their roles are not limited to immune cell recruitment during the inflammatory events in atherosclerosis.

Under homeostatic conditions, the chemokine system is responsible for controlling cellular trafficking in many tissues, proliferation, survival and differentiation of various cells, as well as homing of stem cells (Cuesta-Gomez et al., 2021; Lapidot & Kollet, 2002; Raman et al., 2011). In addition to their essential roles during homeostatic conditions, chemokines and their receptors are extensively involved in the regulation of many inflammatory tasks. Their implications in recruitment, activation, differentiation, phagocytosis and adhesion of immune cells are well established (van der Vorst et al., 2019). Especially in the context of atherosclerotic inflammation, the chemokine system plays a key role in various stages, which also renders them as significant therapeutic targets (Figure 6).

Arterial entry of immune cells during atherosclerosis is a key step that fuels the growth of lesions and chemokines released by the activated endothelium aid this step in numerous ways. For example, the chemokine CXCL1, also known as GRO-α, and its receptor CXCR2 were shown to enhance monocyte mobilization, recruitment and accumulation during atherosclerosis (Figure 6) (Boisvert et al., 2006; Huo et al., 2001; Soehnlein et al., 2013). Furthermore, the chemokine CCL2 (monocyte chemoattractant protein-1) and its receptor CCR2 have been established to promote atherosclerosis through their roles in monocyte trafficking and adhesion, as well as lesional macrophage accumulation (Figure 6) (Boring et al., 1998; Winter et al., 2018). As mentioned before, endothelial barrier function is another important factor allowing passage of immune cells into the arterial intima. Our research group revealed that the chemokine receptor CXCR4 expressed by the arterial endothelial cells is essential in the maintenance of the endothelial integrity and its absence exacerbated endothelial permeability and atherosclerosis in hyperlipidemic mice (Figure 6) (Döring et al., 2017). Chemokines released by other cell types have also been implicated in the progression of atherosclerosis. For example, the chemokine CCL3 was reported to be produced by activated macrophages, platelets, neutrophils, as well as mast cells (Gencer, Evans, et al., 2021; Weber, 2005) and it was shown to contribute to plaque progression by mediating neutrophil adhesion and accumulation in lesions (Figure 6) (de Jager et al., 2013). Platelet derived CCL5 was also reported to drive monocyte arrest onto the endothelium in various studies, implying its importance in atherosclerosis (Figure 6) (Schober et al., 2002; von Hundelshausen et al., 2001). Apart from these chemokines, CCL17 and its receptor were shown to be important in the recruitment of T cells (Andrew et al., 2001) and CCL17 expressed by dendritic cells was reported to drive atherosclerosis by limiting the homeostasis of regulatory T cells (Weber et al., 2011). Furthermore, analyses with human patient samples also highlighted the modulation of several

chemokines. For example, inflammatory chemokine CXCL8, was detected to be increased in the sera of patients with atherosclerosis and it was shown to be important in neutrophil extracellular trap formation via its receptor CXCR2. (An et al., 2019) Moreover, CXCR3 ligands CXCL9, CXCL10 and CXCL11 were observed in human atherosclerotic plaque samples during the whole course of plaque progress (Zernecke et al., 2008). CXCR3 inhibition in murine models by means of genetic or pharmacological manipulation revealed its pro-atherosclerotic role via T cell recruitment and migration into atherosclerotic plaques (van Wanrooij et al., 2008; Veillard et al., 2005). Another important chemokine with various inflammatory roles in atherosclerosis is the macrophage inhibitory factor (MIF), which is also an atypical chemokine (Schober et al., 2008). MIF is expressed by many cell types, such as T cells, monocytes, macrophages, endothelial cells, SMCs, neutrophils, dendritic cells and B cells, and it binds to several receptors including CD74, CXCR2, CXCR4 and ACKR3 (Bernhagen et al., 2007; Grieb et al., 2014; Lue et al., 2002; Schober et al., 2008; Sinitski et al., 2019; van der Vorst et al., 2015). MIF is known to be highly inflammatory and it has been reported to impact leukocyte-endothelium adhesion, vascular inflammation as well as monocyte recruitment (Figure 6) (Chen et al., 2004; Gencer, Evans, et al., 2021; Sinitski et al., 2019). Furthermore, its genetic ablation in atherosclerotic mice depicted clear reduction in atherosclerosis along with diminished SMC proliferation (Pan et al., 2004), also suggesting a role for MIF in plaque stability (Schober et al., 2004).

In addition to the above mentioned examples of chemokines and chemokine receptors, recent advances in the field revealed the chemokine CXCL12 as an important target for cardiovascular research. In 2007, an extensive genome wide association study (GWAS) reported by Samani and colleagues revealed a significant association between the genetic locus of *Cxcl12* and coronary artery disease, as well as myocardial infarction (Samani et al., 2007). This finding clearly underpinned the importance of the chemokine CXCL12 in CVDs and it also highlighted the potential roles of its receptors CXCR4 and ACKR3. CXCL12 is an important chemokine which plays key roles both in homeostasis and in disease. Mouse embryo studies revealed that the CXCL12-CXCR4 axis is essential in the embryonic development, as their lack resulted in lethal developmental defects, such as impaired hematopoiesis (Ma et al., 1998; Tachibana et al., 1998). The essential role of CXCL12 has also been implicated in hematopoietic stem cell homing, leukocyte recruitment and neovascularization in ischemic tissues (Nagasawa, 2007; Yamaguchi et al., 2003; Yellowley, 2013). Furthermore, our research group disclosed that CXCL12 released by the arterial endothelial cells had a pro-atherosclerotic role in hyperlipidemic mice, as its endothelial deficiency and thereby decrease in the circulation lead to reduced plaque sizes as well as greater collagen content within the plaques (Döring et al., 2019). This suggested that endothelial CXCL12 mediates the expansion of atherosclerotic lesions and renders the plaques more vulnerable by modulating the collagen levels within the plaques.

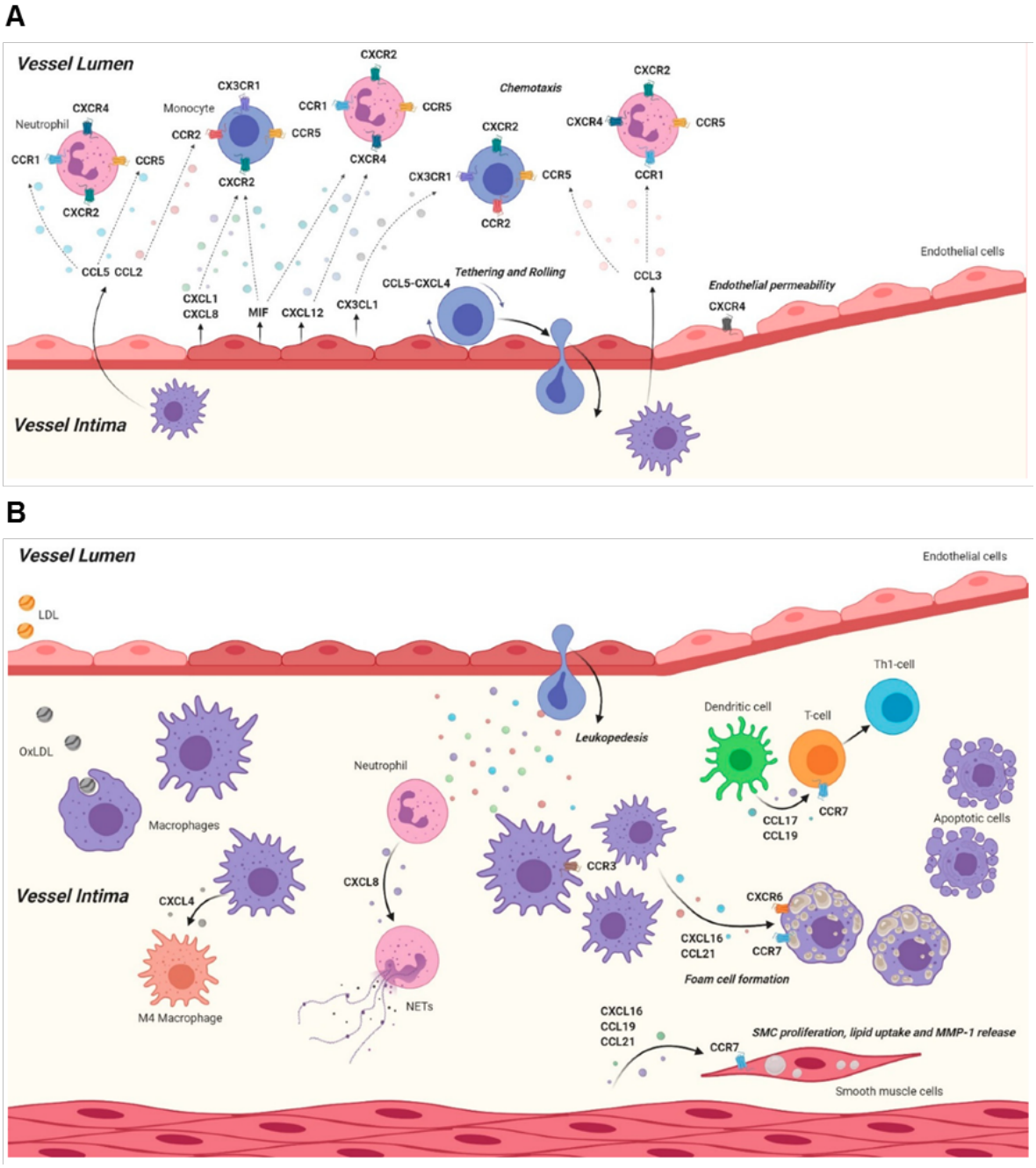

Figure 6: Overview of the roles of the chemokine system in various stages of atherosclerosis.

A. Activated endothelium releases various chemokines which interact with the chemokine receptors expressed on leukocyte subsets for immune cell recruitment. Such chemokine-receptor interactions are also important in the trans-endothelial migration and infiltration of the immune cells into the sub-endothelial space of the artery. Moreover, the chemokine system can also regulate other factors such as endothelial permeability. **B.** The chemokine-receptor interactions are further involved in other stages of atherosclerosis that take place inside the vessel wall, such as monocyte to macrophage differentiation, neutrophil extracellular trap formation, SMC proliferation and migration as well as foam cell formation. These images were adopted from (Gencer, Evans, et al., 2021).

1.4 ACKR3

As mentioned in section 1.3.1, ACKR3 is an atypical chemokine receptor, which, by definition, lacks G protein mediated signaling (Bachelerie, Ben-Baruch, et al., 2014). It was first recognized for its role as a co-receptor enabling the entry of several human immunodeficiency virus (HIV) strains into brain derived cells (Shimizu et al., 2000). ACKR3 is expressed in various cell types, such as endothelial cells, epithelial cells, neurons, SMCs, cardiomyocytes, adipocytes, osteocytes and immune cell subsets, although it was previously thought to be absent in leukocytes (Berahovich et al., 2014; Berahovich et al., 2010; Gencer et al., 2019; Gerrits et al., 2008; Li et al., 2014; Shimizu et al., 2011). ACKR3 was initially named as RDC-1 and later as CXCR7 due to its structural resemblance to CXC receptors (Wang et al., 2018). However, due to its ability to scavenge its ligands and its inability to induce GPCR signaling pathway, it was classified as an ACKR.

Although it is best known for its binding to the chemokine CXCL12 (SDF-1), ACKR3 has a number of ligands: CXCL11 (also known as I-TAC) and MIF are also recognized to ligate ACKR3 (Alampour-Rajabi et al., 2015; Burns et al., 2006). Apart from these, adrenomedullin (ADM) and bovine adrenal medulla 22 (BAM22) are also documented as ACKR3 ligands (Ikeda et al., 2013; Kapas & Clark, 1995; Klein et al., 2014). The ligand CXCL11 also binds CXCR3 and its release can be upregulated by interferons (Van Raemdonck et al., 2015). This chemokine is reported to be involved in infection as well as cancer processes (Puchert et al., 2020; Tokunaga et al., 2018; Torraca et al., 2015; Wang et al., 2018). CXCL12 is perhaps the most studied ligand of ACKR3, potentially due to its wide ranging expression in addition to numerous roles in homeostasis as well as disease settings, as partly explained in section 1.3.2. In addition to this point, CXCL12 was found to have a high affinity to ACKR3, which is nearly 10 fold higher compared to CXCR4 (Balabanian et al., 2005). This is complemented by the finding that ACKR3 also has a higher affinity to CXCL12 compared to CXCL11 (Burns et al., 2006). CXCL12 was observed to be enhanced under pathological conditions, such as ischemia, inflammation, autoimmune diseases and tumor angiogenesis (Karin, 2010; Li & Ransohoff, 2009). As mentioned above, CXCL12 is especially important in the research of CVDs and atherosclerosis (Döring et al., 2019). CXCL12 further binds CXCR4 and elicits GPCR signaling (Busillo & Benovic, 2007). Another chemokine that shares mutual receptors with CXCL12 is the atypical chemokine MIF. As mentioned before, MIF can bind to CXCR4, ACKR3, CXCR2 and CD74 and it is involved in inflammatory as well as autoimmune diseases (Lue et al., 2002). ADM, on the other hand, is a hormone with mitogenic features (meaning it can induce cell division) and it is also recognized as a vasodilator (Kitamura et al., 1993; Wang et al., 2018). Interestingly, ADM is a crucial factor for proper cardiac development; according to a study, *Adm*$^{-/-}$ mouse embryos died at midgestation with cardiovascular abnormalities (Caron & Smithies, 2001). On the other hand, overexpression of *Adm* leads to cardiac hyperplasia in mouse embryos (Wetzel-Strong et al., 2014). Moreover, BAM22 is broadly present in the central nervous system (CNS) (Pittius et al., 1984) and it can bind opioid receptors (Boersma et al., 1994). Its interaction with ACKR3 was shown to increase circadian glucocorticoid

oscillation and anxiolytic like behavior in mice, revealing an impact of ACKR3 on emotional behavior (Ikeda et al., 2013). Recently another study elucidated that ACKR3 is actually activated by many opioid peptides in the CNS and thereby capable of scavenging an array of neuromodulators (Meyrath et al., 2020). Altogether, these facts indicate that ACKR3 is a broad spectrum receptor binding various kinds of ligands which are involved in a plethora of physiological functions. Furthermore, these ligands of ACKR3 are also capable of binding several other receptors, each of which can further regulate numerous other pathways. Although ACKR3 was regarded as a 'silent' sink for its ligands in the early days, it is now well established that ACKR3 is also capable of cell signaling.

The GPCR signalling motif DRYLAIV is reported to be DRYLSIT (Asp-Arg-Tyr-Leu-Ser-Ile-Thr) in ACKR3 (Graham et al., 2012; Wang et al., 2018). Although this implies that ACKR3 cannot signal through G proteins like other GPCRs, one study claimed that ACKR3 can signal though G-i/o proteins in primary rodent astrocytes and subsequently increase intracellular calcium concentration (Odemis et al., 2012). Another study showed very recently that ACKR3 ligand binding results in the activation of GRK2 mediated by G protein ßγ subunits which then leads to receptor phosphorylation (Nguyen et al., 2020). Interestingly, ACKR3 was also described to form heterodimers with CXCR4, a GPCR sharing the mutual ligand CXCL12 (Décaillot et al., 2011; Levoye et al., 2009). Through this connection, ACKR3 is suggested to modulate CXCL12-CXCR4 signaling, potentially also directly CXCR4 mediated GPCR signaling. Other studies also stated that ACKR3 scavenges its ligands, such as CXCL11 and CXCL12, which suggests another route for modulating the signaling pathways of its ligands as well as the potential of establishing chemokine gradients (Luker et al., 2012; Naumann et al., 2010; Wang et al., 2012). Furthermore, ACKR3 has been established to recruit ß-arrestins, which can induce mitogen activated protein kinase (MAPK) signaling (Gravel et al., 2010; Ishizuka et al., 2021; Nguyen et al., 2020; Rajagopal et al., 2010). Indeed, ACKR3 dependent MAPK signaling through ERK1/2 and Akt activation has been shown in numerous cell lines (Alampour-Rajabi et al., 2015; Li et al., 2019; Lin et al., 2014; Odemis et al., 2012).

1.4.1 ACKR3 in health and disease

As mentioned above, ACKR3 was initially recognized for its role in enabling HIV infection, revealing a significant role of ACKR3 in pathological conditions. One of the best known and most studied pathological roles of ACKR3 is its involvement in cancer. ACKR3 expression is revealed to be upregulated in cancerous cells, tumor microenvironment as well as tumor vasculature (Smit et al., 2021). Studies also showed that ACKR3 stimulates growth of cancer cells as well as cancer metastasis (Miao et al., 2007; Würth et al., 2014). The receptor has also been observed to be enhanced with malignancy (Hattermann et al., 2010) and it is suggested to be a prognostic marker (D'Alterio et al., 2010; Gebauer et al., 2011; Schrevel et al., 2012). To this date, ACKR3 has been detected in numerous cancer types, such as lung, breast, cervix, myeloid cell, pancreas and prostate cancer (Sánchez-Martín et al., 2013). Apart from HIV infection and cancer, involvement of

ACKR3 was reported in several other diseases, such as the inflammatory bowel disease (IBD) (Werner et al., 2011) and rheumatoid arthritis (Watanabe et al., 2010).

Remarkably, strong evidence disclosed that ACKR3 is of utmost importance for the proper development of the cardiovascular system. For example, constitutive *Ackr3*$^{-/-}$ *(Cxcr7*$^{-/-}$*)* mice died at birth with defects in the cardiac system, such as ventricular septal defects (an abnormal hole in the heart between ventricles) and malformation of semilunar valves reported by Sierro et al. (Sierro et al., 2007). Furthermore, the study reported that these findings were repeated by a congenital endothelial cell knockout (via Tie2-cre) of the receptor, indicating the importance of the endothelial ACKR3 in cardiac development. Another study reported that 70% of *Ackr3*$^{-/-}$ mice died within their birth week due to cardiac hyperplasia, whereas *Ackr3* deletion in adult mice revealed myocardial degeneration and fibrosis (Gerrits et al., 2008). These findings were further confirmed by another study in which *Ackr3*$^{-/-}$ mice died prenatally as a result of enlarged aortic and pulmonary valves as well as ventricular septal defects (Yu et al., 2011). This study also confirmed similar findings upon a constitutive endothelial deletion of ACKR3, once more depicting the importance of endothelial ACKR3 in cardiac development. Remarkably, as mentioned above, an ACKR3 ligand, ADM, was also shown to be very crucial for cardiac development. It was suggested that ACKR3 may be a decoy receptor for ADM and thereby regulate cardiac development (Klein et al., 2014). In line with this concept, ACKR3 was found to be important in vascular homeostasis as well as cardiac remodelling after myocardial infarction in murine studies (Hao et al., 2017). This role of ACKR3 is attributed to its impact on endothelial proliferation and angiogenesis (Dai et al., 2011).

The fact that the main ligand of ACKR3, CXCL12, was revealed to be strongly associated with CVDs (refer to section 1.3.2) underpinned the significance of ACKR3 in CVDs. Since then, multiple studies suggested various roles of ACKR3 in the pathological processes of atherosclerosis. In an apolipoprotein E deficient (*Apoe*$^{-/-}$) mouse model, ACKR3 expression was detected in atherosclerotic plaque macrophages in the aorta of mice but not in healthy aorta samples (Ma et al., 2013). This study further identified that ACKR3 expression was enhanced during monocyte to macrophage differentiation and augmented macrophage phagocytosis was reported in ACKR3 activated macrophages via agonist treatments, whereas this effect was abrogated via ACKR3 silencing. This finding implied a potential role for ACKR3 in the immune cell compartment during atherosclerosis as monocyte to macrophage differentiation as well as macrophage phagocytosis are key events in atherosclerosis that could be targeted to halt atherosclerotic progression. Moreover, another study investigated the role of ubiquitous ACKR3 in atherosclerosis employing a wire-induced carotid artery injury model in mice (Li et al., 2014). This study disclosed that genetic ablation of ACKR3 from all somatic cells resulted in increased serum lipid levels concomitant with monocytosis. Further investigation revealed that ACKR3 had an impact on adipose tissue (AT) lipid uptake leading to the conclusion that ACKR3 in AT regulated circulating lipid levels. Treatment of mice with an ACKR3 ligand (CCX771) was reported to decrease blood lipid levels as well as atherosclerotic lesion sizes in the aortic roots (Li et al., 2014). Monocytosis was also attenuated, leading to the theory that it was induced by hyperlipidemia. These findings suggested an atheroprotective role of ACKR3, although its cell specific roles still remained to be elucidated. Another striking finding was the fact that SMCs could migrate towards the ACKR3 ligand CXCL11,

a process that was inhibited with either ACKR3 antagonist treatment or ß-arrestin silencing (Rajagopal et al., 2010). Migration of cells was always attributed to GPCR mediated signaling, however this study highlighted that ACKR3 was capable of inducing cell migration in SMCs through ß-arrestin activation. SMC migration during atherosclerosis establishes fibrous cap formation and thereby aids in plaque stabilization. Therefore, this finding suggests a potential role of SMC specific ACKR3 in atherosclerosis.

Last but not least, the impact of ACKR3 on cell adhesion was confirmed many times including different cell types, such as endothelial progenitor cells and cancerous cells (Dai et al., 2011; Gentilini et al., 2019; Jiang et al., 2020; Ma et al., 2016; Yan et al., 2012). Cell adhesion is a crucial step during the trans-endothelial migration of immune cells in atherosclerotic lesion development. This step enables accumulation of foam cells in the arteries which in turn fuels lesion progression. Interfering with immune cell adhesion onto atherosclerotic arteries could present a therapeutic approach in the treatment of atherosclerosis. Therefore, ACKR3 in the vascular endothelium or on the immune cells could be potentially involved in endothelium-leukocyte adhesion and provide a mechanism to target atherosclerosis.

1.5 Study Rationale & Aim

Atherosclerosis is the foundation of CVDs, which have been the top ranked causes of death worldwide for a very long time. Therefore, effective treatment of atherosclerosis is of crucial necessity. Current treatment methods of atherosclerosis include drug administration to mitigate atherosclerotic risk factors, such as hyperlipidemia and hypertension. Nonetheless, by the time patients experience CVD related discomfort, the disease often has already progressed so far that such preventive treatment methods may not be fully effective any longer. Moreover, since inflammation is a major driver of atherosclerosis, conventional treatment methods of CVD risk factors leave room for improvement. Therefore, novel therapeutic approaches targeting atherosclerotic inflammatory pathways are needed in order to firmly intervene with disease progression. To this end, the chemokine system comes into focus because of its extensive roles in atherosclerotic inflammation. The effectiveness of this approach is evident by the CANTOS trial, which successfully established that targeting IL-1ß in order to combat inflammation dampened cardiovascular risk (Ridker et al., 2017). A chemokine-receptor axis that has gained significant attention in the cardiovascular research field is the CXCL12-CXCR4/ACKR3 axis. Previously, our research group as well as others investigated the roles of CXCL12 and its GPCR receptor CXCR4 in atherosclerosis. These studies established that both CXCL12 and CXCR4 in the vascular compartment are significantly involved in atherosclerosis. The role of ACKR3, however, remains to be a big gap in this research field, which needs immediate attention. ACKR3 is recognized to be involved in various disease models and its crucial role in the cardiac development has been well established. Furthermore, recent findings as summarized above strongly suggest a significant role of ACKR3 in atherosclerotic processes. In order to understand how ACKR3 may be involved in atherosclerosis, this study is designed to scrutinize the receptor with regards to its cell specific roles as opposed to a bulk study involving various cell types at once. In doing so, a well-established *in vivo* atherosclerotic mouse model (*Apoe*$^{-/-}$) is employed. These mice develop atherosclerotic lesions when introduced to western diet (WD). Furthermore, investigation of cell-specific ACKR3 in this mouse model is achieved with the cre-lox recombination technology, allowing site specific deletion of the flanked *Ackr3* gene via the enzyme Cre recombinase activity. We utilized this model in order to study the role of endothelial (*BmxCre*), SMC (*SmmhcCre*), adipocyte (*AdipoqCre*) and hepatocyte (*AlbuminCre*) specific ACKR3 in atherosclerosis, as well as hematopoietic ACKR3 via bone marrow transplantation using *UniCre* mice. Mapping cell specific roles of the receptors allows thorough understanding of its roles in addition to predictions of possible complications or side effects in case the receptor is planned to be targeted therapeutically.

2. Material and Methods

2.1 Materials

2.1.1 Animals

Table 1: List of mouse models used in *in-vivo* experiments

Species	Origin	Background Strain	Stock Number
Mouse	Jackson Laboratories	*Apoe*$^{-/-}$	#002052
Mouse	ChemoCentryx, Inc. (Mountain View, CA)	*Ackr3*$^{fl/fl}$	N/A
Mouse	Dr. R. Adams (MPI Münster, Germany)	*BmxCre*^{ERT2}	N/A
Mouse	Jackson Laboratories	*AdipoqCre*^{ERT2}	#025124
Mouse	Jackson Laboratories	*SmmhcCre*^{ERT2}	#019079
Mouse	Taconic Laboratories	*Cre*^{ERT2} (Gt(ROSA)26)	#10471-F #10471-M
Mouse	Janvier Labs	C57Bl/6J	N/A

2.1.2 Cell Culture

Table 2: List of cell culture materials

Material	Source	Catalog Number
Human Coronary Artery Endothelial Cells (HCAEC)	Lonza	Cat# CC-2585
Reagent Pack Subculture Reagents	Lonza	Cat# CC-5034
EGMTM -2 MV Microvascular Endothelial Cell Growth Medium-2 BulletKitTM	Lonza	Cat# CC-3202

2.1.3 Antibodies

Table 3: List of antibodies

Antibody	Source	Catalog Number
APC anti-human CD54 Antibody	BioLegend	Cat# 353111
PE anti-human CD106 Antibody	BioLegend	Cat# 305805
Anti-mouse Ly6C Alexa Fluor488 (clone HK1.4)	BioLegend	Cat#128022
Anti-mouse Ly6G PE (clone 1A8)	BioLegend	Cat#127608
Anti-mouse/human CD11b PE/Cy7 (clone M1/70)	BioLegend	Cat#101216
PE anti-human/mouse CXCR7 Antibody	BioLegend	Cat# 331103
CXCR7 Recombinant Rabbit Monoclonal Antibody (SN65-09)	ThermoFisher	Cat# MA5-32281
Anti-Mouse/Human Mac-2 (Galectin-3), Purified (Clone M3/38) (rat IgG2a)	Cedarline Labs	Cat# CL8942AP
Monoclonal Anti-Actin, α-Smooth Muscle - FITC antibody produced in mouse	Sigma-Aldrich	Cat# F3777-.5ML
p-NFκB p65 Antikörper (27.Ser 536)	SantaCruz	Cat# sc-136548
Anti-NF-kB p65 antibody	Abcam	Cat# ab16502
Recombinant Anti-ERK1 + ERK2 antibody [EPR17526]	Abcam	Cat# ab184699
Recombinant Anti-ERK1 (phospho T202) + ERK2 (phospho T185) antibody [EPR19401]	Abcam	Cat# ab201015
PPAR-gamma (Phospho-Ser112) Polyclonal Antibody	Mybiosource	Cat# MBS9402552
Recombinant Anti-PPAR gamma antibody [EPR18516] (ab178860)	Abcam	Cat# ab178860
Purified Hamster Anti-Mouse CD54 Clone3E2	BD Pharmingen	Cat# 553250
Anti-Von Willebrand Factor antibody	Abcam	Cat# ab11713

Cy™3 AffiniPure Donkey Anti-Rat IgG (H+L)	Jackson ImmunoResearch	Cat# 712-165-150
APC anti-mouse CD45 Antibody (clone 30-F11)	BioLegend	Cat# 103111
CD45 Monoclonal Antibody (30-F11), APC-eFluor 780, eBioscience™	eBioscience	Cat# 47-0451-82
CD115 (c-fms) Monoclonal Antibody (AFS98)	eBioscience	Cat# 14-1152-82
Ly-6G/Ly-6C Monoclonal Antibody (RB6-8C5), PerCP-Cyanine5.5	eBioscience	Cat# 45-5931-80
CD11b Monoclonal Antibody (M1/70), PE-Cyanine7	eBioscience	Cat# 25-0112-82
CD45R (B220) Monoclonal Antibody (RA3-6B2), eFluor 450	eBioscience	Cat# 48-0452-82
CD3e Monoclonal Antibody (145-2C11)	eBioscience	Cat# 14-0031-82

2.1.4 Chemicals, buffers and solutions

Table 4: List of chemicals, buffers and solutions

Chemical/Buffer/Solution/Reagent	Source	Catalog Number / Description
Antibody blocking solution (ABS)	Lab	6ml PBS + 1% BSA + 3 drops of horse serum
Antibody staining solution	Lab	6ml PBS + 90 µl blocking solution
Antigen retrieval solution A	Lab	21,01g citric acid in 1L deionized water (dH_2O)
Antigen retrieval solution B	Lab	29,4g sodium citrate in 1L dH_2O
Red blood cell lysis buffer	Lab	8.26g ammoniumchloride + 1g potassiumbicarbonate + 200ul 0.5M EDTA added up to 1L dH_2O, pH 7.2

Hank's buffer	Lab	HBSS, 0.5 mM EDTA, 0.1% BSA
Oil Red O	Sigma-Aldrich	Cat# O0625-25G
Hematoxylin	Sigma-Aldrich	Cat# H9627-25G
Eosin Y solution 0.5 %	Carl Roth	Cat# X883.1
Paraformaldehyde	Sigma-Aldrich	Cat# P6148
Xylene	Merck	Cat# 108297
Ethanol	Merck	Cat# V1.00983.1000
Methanol	Roth	Cat# 8388.1
Gibco Phosphate Buffered Saline (PBS)	ThermoFisher	Cat# 10010023
Gibco HBSS, calcium, magnesium, no phenol red	ThermoFisher	Cat# 14025100
Restore™ Western Blot Stripping Buffer	ThermoFisher	Cat# 21059
M-PER Mammalian protein extraction reagent	ThermoFisher	Cat# 78503
Pierce™ 20X TBS Tween™ 20 Buffer	ThermoFisher	Cat# 28360
Cell Lysis Buffer (10X) #9803	Cell Signaling Technologies	Cat# 9803S
10x Tris/Glycine Buffer for Western Blots and Native Gels	BioRad	Cat# 1610734
10x Tris/Glycine/SDS #1610732	BioRad	Cat# 1610732
Weigert's Iron Hematoxylin Stock Solution A	Lab	5gr hematoxylin + 500ml 95% ethanol
Weigert's Iron Hematoxylin Stock Solution B	Lab	5.8gr ferric chloride dissolved in 50ml dH_2O + 500ml dH_2O + 5ml acetic acid
Acid Fuchsin, 1% Aqueous Solution	Lab	1gr acid fuchsin in 100ml dH_2O
Aniline Blue Stock Solution	Lab	6.25gr aniline blue + 5ml acetic acid + 245ml dH_2O
Biebrich Scarlet, 1% Aqueous Solution	Lab	10gr biebrich scarlet in 1L dH_2O
Phosphomolybdic (PM)-Phosphotungstic(PT) Acid Solution	Lab	3.125 gr PM acid + 3.125 gr PT acid + 250ml dH_2O

2-propanol 99%	Merck	Cat# 1.096342511
Bouin's solution	Sigma Aldrich	Cat# HT10132
Opti-MEM™ I Reduced Serum Medium	ThermoFisher	Cat# 31985070
Glycerine	Roth	Cat# 3908.2

2.1.5 Kits and miscellaneous

Table 5: List of kits and further products

Kits / Products	Source	Catalog Number
Gelatine	Sigma	Cat# G-1890
Mounting Medium	Dako	Cat# S3023
Stainless Steel Beads, 5mm	Qiagen	Cat# 69989
DirecT-ZOL™ RNA MICROPREP	ZymoResearch	Cat# R2062
Tamoxifen	Sigma-Aldrich	Cat# T5648-5G
ProLong™ Diamond Antifade Mountant with DAPI	ThermoFisher	Cat# P36962
Tissue-Tek O.C.T. compound	Sakura	Cat# 94-4583
siPORT™ NeoFX™ Transfection Agent	Invitrogen by Life Technologies	Cat# AM4510
Hoechst	Invitrogen by Life Technologies	Cat# H3570
Droplet Generation Oil for Probes	BioRad	Cat# 1863005
ddPCR™ Droplet Reader Oil	BioRad	Cat# 1863004
DG8™ Cartridges for QX200™/QX100™ Droplet Generator	BioRad	Cat# 1864008
DG8™ Gaskets for QX200™/QX100™ Droplet Generator	BioRad	Cat# 1863009
iScript™ cDNA Synthesis Kit, 100 x 20 µl rxns	BioRad	Cat# 1708891
Hitachi 704 Analyzer-cholesterol	Roche Diagnostics	Cat# 11489232
Hitachi 704 Analyzer-triglycerides	Roche Diagnostics	Cat# 11488872
Mouse CXCL12/SDF-1 alpha Quantikine ELISA Kit	R&D Systems	Cat# MCX120

ddPCR Supermix for Probes (No dUTP)	BioRad	Cat# 1863024
Human/Mouse MAPK Phosphorylation Array	RayBiotech	Cat# AAH-MAPK-1-8
Human 18s (Hs99999901_s1)	ThermoFisher	Cat# 4331182
Human ACKR3 (Hs00664172_s1)	ThermoFisher	Cat# 4331182
Human PPARG (Hs01115513_m1)	ThermoFisher	Cat# 4331182
Silencer™ Negative Control No. 1 siRNA, AM4611	ThermoFisher	Cat# AM4611
Silencer validated siRNA CXCR7, AM51331	Ambion by Life Technologies	Cat# AM51331
CountBright Absolute Counting Beads	ThermoFisher	Cat# C36950
Western Diet	sniff	Cat# E15721-347
Halt™ Phosphatase Inhibitor Cocktail (100x)	ThermoFisher	Cat# 78420
Halt™ Protease Inhibitor-Cocktails	ThermoFisher	Cat# 87785
Lipoprotein Lipase Assay Kit (Fluorometric) (ab204721)	Abcam	Cat# ab204721
NF kappaB p65 (pS536 + Total) ELISA Kit	Abcam	Cat# ab176663
AAV-ALB(1.9)-EGFP	Vector Labs	Cat# VB1586
Pierce™ BCA™ Protein-Assay	ThermoFisher	Cat# 23225
CXCR7 Agonist, VUF11207 - Calbiochem	Merck	Cat# 239824-10MG
12% Mini-PROTEAN® TGX™ Precast Protein Gels	Bio-Rad	Cat# 4561043
Precision Plus Protein™ WesternC™ blotting standard	Bio-Rad	Cat# 1610376
SuperSignal™ West Pico PLUS Chemiluminescent Substrate	ThermoFisher	Cat# 34579
Bovine Serum Albumin	Merck	Cat# A9418-50G
GoTaq Flexi DNA Polymerase	Promega	Cat# M8308
dNTP mix	Fermentas	Cat# R0182
100 bp marker	Fermentas	Cat# SM0321

2.2 Methods

All materials mentioned in the Methods section below are documented in the Materials section above, unless otherwise stated.

2.2.1 Mice

Ackr3-floxed (Ackr3$^{fl/fl}$) mice were crossed with *Apoe$^{-/-}$* mice to generate *Ackr3$^{fl/fl}$Apoe$^{-/-}$* mice. For arterial endothelial cell-specific deletion of *Ackr3*, *Ackr3$^{fl/fl}$Apoe$^{-/-}$* mice were crossed with BmxCre-^{ERT2} expressing mice (*BmxCre*). SMC specific deletion of *Ackr3* was accomplished by crossing *Ackr3$^{fl/fl}$Apoe$^{-/-}$* mice with SmmhcCre^{ERT2} expressing mice (*SmmhcCre*). Adipocyte specific deletion of *Ackr3* was accomplished by crossing *Ackr3$^{fl/fl}$Apoe$^{-/-}$* mice with AdipoqCre^{ERT2} expressing mice (*AdipoqCre*). *Cre^{ERT2}Ackr3$^{fl/fl}$Apoe$^{-/-}$* (*UniCre*) mice, a ubiquitous model, were used for bone marrow transplantation study (refer to section 1.2.3) The knockouts were induced with daily tamoxifen injections (Sigma; 1.5 mg per 20g body weight, dissolved in corn oil) for 5 consecutive days. Liver specific knockout of ACKR3 was succeeded by injecting 1x10^{11} adeno associated virus (AAV) (expressing iCre driven by a liver ALB (1.9) promoter) into *Ackr3$^{fl/fl}$Apoe$^{-/-}$* mice. For atherosclerosis development, mice were put on a 4 or 12-week WD containing 21% fat and 0.15% to 0.2% cholesterol (Sniff Diets). All mice were on a C57BL/6J background. All animals were bred and housed in the local animal facility under specific pathogen free (SPF) conditions. Prior to the start of the WD, all mice were fed a normal chow diet. All animal experiments were approved by the local ethical committee (Regierung von Oberbayern, Sachgebiet 54, Germany; Az. 55.2.1.54-2532-177-2016 and ROB-55.2-2532.Vet_02-18-96).

2.2.2 Genotyping

Genotyping of mice as described in Table 1, such as assessment of Cre expression, *Ackr3* flox and *Ackr3* knockout, was carried out utilizing tail samples. *Ackr3* knockout genotyping in mice subjected to bone marrow transplantation (2.2.4) was carried out in spleen samples due to high blood content. Tail and spleen samples were first digested at 55°C in 500 µl lysis buffer containing 50 µl proteinase K for 3 to 4 hours at 600 rotations per minute (rpm). Samples were then proceeded to deoxyribonucleid acid (DNA) extraction as follows: tubes were inverted 20-30 times and centrifuged at 14,000 rpm for 10 minutes. Supernatants were added to tubes containing 550 µl isopropanol. Tubes were again inverted 20-30 times to ensure mixing and a white precipitate was observed. Samples were centrifuged at 14,000 rpm for 2 minutes and supernatant was discarded. 2 mililiter (ml) of ethanol (EtOH) was added to the pellets and incubated at room temperature (RT) for 3 minutes. EtOH was then discarded and tubes were evaporated at RT overnight. 80 µl of distilled water was added to the tubes and samples were vortexed vigorously. Samples were then stored at 20°C until analysis. Analysis was accomplished with a QIAxcel Advanced System gel electrophoresis examination of polymerase chain reaction (PCR) samples. PCR was performed containing primers designed to detect control (wildtype) or mutant alleles. A general PCR reaction mix for all samples was prepared containing the following components with final

concentrations unless specified otherwise: 1X green GoTaq Flexi buffer, 1,5 mM magnesium chloride ($MgCl_2$), 0,2 mM deoxynucleoside triphosphates (dNTPs), 0,5 µM forward primer, 0,5 µM reverse primer, 0,05 U/µl Gotaq DNA polymerase and 200 nanograms (ng) of genomic DNA (gDNA). Details of the PCR primers and cycling conditions will be specified for each genotyping below.

***Apoe* Genotyping**

Forward wildtype primer: 5' GCC TAG CCG AGG GAG AGC CG 3'

Reverse wildtype primer: 5' TGT GAC TTG GGA GCT CTG CAG C 3'

Forward mutant primer: 5' GCC TAG CCG AGG GAG AGC CG 3'

Reverse mutant primer: 5' GCC GCC CCG ACT GCA TCT 3'

Cycling was performed in steps as follows: 5 minutes at 94°C, 30 seconds at 94°C, 30 seconds at 60°C, 30 seconds at 72°C, repeat steps 2 to 4 for 35 cycles, 5 minutes at 72°C, 5 minutes at 21°C.

***Ackr3* Flox Genotyping**

Forward primer: 5' GGA ACC CAG GCG AAG TCT GAG 3'

Reverse primer: 5' CCT GTA CTT CAG TAG GAG TCC AC 3'

In this protocol, 100 ng of gDNA was used. Cycling was performed in steps as follows: 3 minutes at 94°C, 30 seconds at 94°C, 30 seconds at 55°C, 45 seconds at 72°C, repeat steps 2 to 4 for 35 cycles, 5 minutes at 72°C, 5 minutes at 21°C.

***BmxCre*^{ERT2} Genotyping**

Forward primer: 5' AAA TAC CTT CAG TTT TCA TCT 3'

Reverse primer: 5' TTG CGA ACC TCA TCA CTC GTT 3'

In this protocol, 400 ng of gDNA was used. Cycling was performed in steps as follows: 2 minutes at 94°C, 30 seconds at 94°C, 30 seconds at 58°C, 1 minute at 72°C, repeat steps 2 to 4 for 35 cycles, 5 minutes at 72°C, 5 minutes at 21°C.

***SmmhcCre*^{ERT2} Genotyping**

Forward wildtype primer: 5' TGA CCC CAT CTC TTC ACT CC 3'

Reverse wildtype primer: 5' AAC TCC ACG ACC ACC TCA TC 3'

Forward mutant primer: 5' TGA CCC CAT CTC TTC ACT CC 3'

Reverse mutant primer: 5' AGT CCC TCA CAT CCT CAG GTT 3'

Cycling was performed in steps as follows: 5 minutes at 94°C, 30 seconds at 94°C, 30 seconds at 60°C, 30 seconds at 72°C, repeat steps 2 to 4 for 35 cycles, 5 minutes at 72°C, 5 minutes at 21°C.

***Cre*^{ERT2} Genotyping**

Forward wildtype primer: 5' CAT GTC TTT AAT CTA CCT CGA TGG 3'

Reverse wildtype primer: 5' CTC TTC CCT CGT GAT CTG CAA CTC C 3'

Forward mutant primer: 5' CCA TCA TCG AAG CTT CAC TGA AG 3'

Reverse mutant primer: 5' GGA GTT TCA ATA CCC GAG ATC ATG C 3'

In this protocol, 500 ng of gDNA was used. Cycling was performed in steps as follows: 15 minutes at 95°C, 45 seconds at 94°C, 1 minute at 60°C, 1 minute at 72°C, repeat steps 2 to 4 for 35 cycles, 5 minutes at 72°C, 5 minutes at 10°C.

***AdipoqCre*^{ERT2} Genotyping**

Forward wildtype primer: 5' CCG CAT CTT CTT GTG CAG T 3'

Reverse wildtype primer: 5' ATC ACG TCC TCC ATC ATCC 3'

Forward mutant primer: 5' GAG TCT GCC TTT CCC ATG AC 3'

Reverse mutant primer: 5' TCC CTC ACA TCC TCA GGT TC 3'

Cycling was performed in steps as follows: 2 minutes at 95°C, 20 seconds at 94°C, 15 seconds at 65°C, 10 seconds at 10°C, repeat steps 2 to 4 for 10 cycles, 15 seconds at 94°C, 15 seconds at 60°C, 10 seconds at 72°C, repeat steps 6 to 8 for 28 cycles, 2 minutes at 72°C, 5 minutes at 72°C, 5 minutes at 21°C.

***Ackr3* Knockout Genotyping**

Forward primer: 5' GAG TCA ATT GAG TGG GCA AGG 3'

Reverse primer: 5' GCT ACA TTG CTT TCT TGA AGA AACC 3'

In this protocol, 400 ng of gDNA was used. Cycling was performed in steps as follows: 2 minutes at 95°C, 30 seconds at 95°C, 30 seconds at 63°C, 2 minutes 30 seconds at 68°C, repeat steps 2 to 4 for 35 cycles, 5 minutes at 72°C, 5 minutes at 12°C. Representative knockout genotyping of mice are shown in Appendix A.

2.2.3 Anesthesia

Mice were sacrificed via anesthesia administration as follows: 90-120mg ketamine per kg of mouse, 6-8mg xylazine per kilogram (kg) of mouse. The components of the anesthesia were provided by the animal facility of Institute for Cardiovascular Prevention (IPEK), LMU upon the approval of the local ethical committee issued ethical statement for the mouse experiments.

2.2.4 Bone Marrow Transplantation

Mice were treated with the following antibiotic solution for 4 weeks in their drinking water (protected from light) prior to irradiation: 1:1 neomycin (100mg/ml in sterile dH_2O) and polymyxin (0.1g/ml in sterile dH_2O). All mice were irradiated twice in an X-ray machine (FAXITRON CP-160) by the following program: 5Gy; kV160; mA 6.3; time 8.5; level 7. Post-irradiation, mice received bone marrow from *Cre^{ERT2-}Ackr3$^{fl/fl}$Apoe$^{-/-}$* and *Cre^{ERT2+}Ackr3$^{fl/fl}$Apoe$^{-/-}$* mice via intravenous injection. Bone marrow from donor mice was prepared as follows: femurs and tibia of donor mice were collected without fractures and the bones were sterilized in 70% ethanol for 30 seconds and washed in PBS. The marrow of the bones was carefully extracted under sterile conditions and a single cell suspension was prepared in sterile PBS by filtering the bone marrow using a 70µm cell strainer. Syringes were prepared with 100uL of cell suspension (maximum amount of 2.5x10^6 cells per 100µl and a minimum amount of 1.5x10^6 cells per 100µl). After 4 weeks of recovery time, mice were treated with tamoxifen (1.5 mg per 20g body weight, dissolved in corn oil) for 5 consecutive days. Mice were then subjected to 12 weeks of Western Diet (WD) containing 21% fat and 0.15% to 0.2% cholesterol.

2.2.5 Atherosclerotic Lesion Analysis

Atherosclerotic plaque sizes were examined in regions which are predisposed to developing lesions: the aortic root, the aortic arch and the aorta. Heart samples collected from mice were first fixated in 4% PFA and then embedded using Tissue-Tek compound to cryo-section the aortic roots areas of the hearts into 4 µm thick sections. Aortic arch samples were fixated in the same fashion and embedded in paraffin for sectioning into 4 µm thick sections using the microtome. Aortic root and arch sections collected on slides were stained with hematoxylin & eosin to visualize atherosclerotic lesions. The sizes of the lesions were evaluated on ImageJ Software using 3 sections per mouse. Aortas were prepared en face and stained with Oil Red O to visualize lipid loaded lesions. The sizes of the lesions were also evaluated on ImageJ Software. Lesion stability was characterized via the Masson Trichrome stained aortic root samples (see section 2.2.6 Masson Trichrome Staining) via Leica Software. Cellular composition of the plaques characterized by the amount of macrophages and SMCs in the lesions, as well as adhesion molecule (ICAM) expression were evaluated via immunofluorescent stainings on the aortic root samples. Antigen retrieval was performed on the samples prior to immunofluorescent stainings. Antigen retrieval working solution was prepared by mixing 630ml dH2O with 12,6ml solution A and 57,4ml solution B, followed by the addition of 350uL Tween 20 Buffer. Samples were washed in PBS. The antigen retrieval working solution was pre-heated in the microwave and the samples were boiled in the

working solution for 10 minutes at 90Watt in the microwave. Samples were again washed in PBS after cooling down. Macrophages were identified with anti Mac-2 antibody, whereas SMCs were identified with anti SMC antibody. Secondary antibodies were then used to fluorescently tag the mentioned primary antibodies. Nuclei were identified via 1:2000 diluted Hoechst staining for 5 minutes or by labeling nuclei with DAPI in the mounting medium. Lesion composition was analyzed on ImageJ Software. All lesion sample images were taken with a Leica DM4000 microscope attached with a Leica DFC 365FX camera. NF-kB expression in endothelial cells found in aortic root lesions was examined via immunohistochemical stainings with van Willebrand factor (vWF) and phospho-NF-kB p65 antibodies. Images were taken with Thunder Imaging Systems (Leica Microsystems) and analyzed with ImageJ Software.

2.2.6 Masson Trichrome staining

Working solutions are as follows:

Weigert's Iron Hematoxylin Working Solution: 1:1 stock solution A and stock solution B (refer to Table 4).

Biebrich Scarlet-Acid Fuchsin Working Solution: 222.5ml Biebrich Scarlet (1% stock) 222.5 mL + 25ml Acid Fuchsin (1% stock) + 2.5 ml Acetic Acid

Aniline Blue Working Solution: 250ml aniline stock solution + 5ml acetic acid

Tissue samples were incubated in Bouin's solution overnight and washed in dH_2O. Samples were then stained in Weigert's Iron Hematoxylin working solution for 7 minutes and washed. This was followed by staining in Biebrich Scarlet-Acid Fuchsin sorking solution for 1 minute. Samples were washed again and incubated in PM-PT acid solution for 30 minutes. Samples were then stained with Aniline Blue working solution for 7 minutes and washed again. Samples were incubated in 1% acetic acid solution for 4 minutes. Stained samples were then dipped into 96% ethanol, followed by 100% ethanol and then into xylene and finally mounted with mounting medium. Images were taken with a Leica DM4000 microscope attached with a Leica DFC 365FX camera and analyzed on Leica Software.

2.2.7 Oil Red O Staining

Oil Red O stock solution was prepared by dissolving 1 gram of Oil Red O in 200ml 2-propanol. Working solution for the Oil Red O staining was then prepared with 180ml Oil Red O stock solution added into 120ml dH_2O. The solution was filtered after 1-hour incubation time. Kaiser's glycerin jelly was prepared by mixing 4 grams of gelatin in 21ml dH_2O followed by addition of 25ml glycerin. Samples were washed in 60% 2-propanol for 10 minutes and then stained in Oil Red O working solution for 15 minutes. Samples were again washed in 60% 2-propanol followed by washing in dH_2O. Samples were mounted with Kaiser's glycerin jelly. Images were taken with a Leica DM4000 microscope attached with a Leica DFC 365FX camera and analyzed on ImageJ Software.

2.2.8 *Ex vivo* Perfusion Assay

Adhesion of immune cells onto the vascular endothelium lacking ACKR3 was examined by *ex-vivo* perfusion of carotid arteries with pre-labeled bone marrow cells according to the protocol published by van der Vorst et al. (van der Vorst et al., 2017). Briefly, carotid arteries extracted from control and endothelial ACKR3 deficient mice were attached onto vessel chambers and cell tracker green labelled bone-marrow cells were perfused through the artery. The assay employed 2-photon excitation microscopy. Mounted carotid arteries were then washed with HBSS and imaged using a LeicaSP5IIMP two-photon laser scanning microscope with a Ti:Sapphire Laser (Spectra Physics MaiTai Deepsee) tuned at 800nm and a 20×NA1.00 (Leica) water dipping objective. Spectral detection was performed using Hybrid Diode detectors (n=4) tuned for maximum intensity of the (auto)fluorescence signal of the vessel wall and clear detection of cell tracker green: second harmonics generation of collagen (395-405nm), autofluorescence; (470-490nm), cell tracker green + autofluorescence; (500-550nm), autofluroescence (570-600nm). Adhered cell tracker positive leukocytes were counted manually by three observers in 3D sections of the arterial wall. 3D image processing was performed using LASX software including 3D analysis plugin (Leica).

2.2.9 Intravital Microscopy

The right jugular vein was cannulated with a catheter to inject antibodies. After revealing the left carotid artery, 1 µg antibody to each CD11b, Ly6C and Ly6G were consecutively administered to tag myeloid cells, neutrophils and classical monocytes, respectively. Recordings were started 3 minutes after antibody injection. Intravital microscopy was performed using an Olympus BX51 microscope equipped with a Hamamatsu 9100-02 EMCCD camera and a 10x saline-immersion objective. For image acquisition and analysis, Olympus Cell-R software was used.

2.2.10 Leukocyte Infiltration Assay

Circulating leukocyte tracking assay was executed according to the protocol described in Winter et al., 2018 (Winter et al., 2018). Briefly, mice were intravenously injected with a rat anti-CD45 antibody and sacrificed 2 hours after injection. Hearts were collected and the aortic roots were cryosectioned as described above. The aortic root samples were then stained with an anti-rat secondary antibody to identify the pre-labelled blood-borne leukocytes which infiltrated into the atherosclerotic lesions in the 2-hour timeframe. Images were taken with a Leica DM4000 microscope attached with a Leica DFC 365FX camera and analyzed on Leica Software.

2.2.11 *In vivo* Endothelial Permeability Assay

0.5% Evans blue (EVB) was prepared in 0.9% saline solution and the solution was filter-sterilized. Mice were intravenously injected with the EVB solution (40mg/kg) and sacrificed 30 minutes after injection. Mice were then perfused with phosphate-buffered saline (PBS) prior to organ collection in order to analyze the retained amount of EVB in the lung, aorta and aortic arch samples. Aortic

arches were fixed with 4% PFA for 30 minutes and placed on objective slides to be imaged. Excitation peaks of EVB are 470 and 540 nm and the emission peak is at 680 nm. Tilescan z-stacks of the whole aortic arch samples were joined together and processed using Imaris 8.4 (Oxford Instruments). The endothelial EVB positive signal was quantified as a volume after 3D segmentation based on appropriate fluorescence intensity thresholding. Aortas and lungs were weighed, air dried for half a day, fixed with formamide and cut into small pieces. The organs were then incubated at 56°C shaking for 24 hours in order to release the retained EVB into the solution. Optical density (OD) of the formamide solutions containing the EVB were measured with a plate reader at 620 nm and the results were normalized to tissue weights.

2.2.12 Flow Cytometry

Whole blood was collected from mice in EDTA-buffer tubes. Red blood cells were lysed with the lysis buffer mentioned in Table 4 for 2-5 minutes prior to the staining procedure. Hematopoietic cell populations in blood samples were stained as follows: anti-CD45, anti-CD115, anti-Gr1, anti-CD11b, anti-B220 and anti-CD3. Cell populations were gated and analyzed as follows on FlowJo Software: leukocytes (CD45+), neutrophils (CD45+CD115-Gr1high), monocytes (CD45+CD11b+CD115+), T cells (CD45+ CD115- Gr1-B220-CD3+) and B cells (CD45+ CD115-Gr1-CD3-B220+). Flow cytometry analysis on cell culture experiments were performed as follows: post *in-vitro* treatments, the cells were washed and trypsinized to be collected as single cell suspensions. The samples were stained with the following antibodies: anti-ICAM, anti-VCAM and anti-E-selectin. All samples were analyzed with FACS Canto II together with FACSDiva software (BD Biosciences).

2.2.13 Tissue Homogenization

Mice were sacrificed and were fully perfused with PBS prior to organ collection in order to remove blood from the tissues. AT and liver samples were weighed and washed with ice cold PBS. Tissue samples were homogenized with a bead-based tissue lyser using 500µl cell lysis buffer (including protease and phosphatase inhibitors) per 250 mg of tissue. After homogenization, samples were centrifuged at 10,000 x g for 10 minutes at 4°C. Total protein content of the homogenates was measured via a commercially available BCA assay kit according to the manufacturer's protocol.

2.2.14 Protein Isolation and Total Protein Measurement

Lysis of cell culture samples was achieved with M-PER™ Mammalian Protein Extraction Reagent (see Table 4) according to the manufacturer's protocol. Briefly, following the completion of the *in-vitro* assays, the cells were washed and trypsinized to be collected for protein isolation. Since the *in-vitro* experiments were performed in 6-well plates, 200ul of the protein extraction reagent (minimum amount according to the manufacturer's protocol) containing 1X protease and phosphatase inhibitors was used for the cells collected from each well. The samples were incubated on ice and shaken gently for 5 minutes. Samples were then centrifuged at 14,000 × g for 5-10 minutes to

pellet the cell debris. The supernatants were collected in a new tube to proceed with total protein level measurement. The total protein level of tissue homogenate as well as cell culture samples was analyzed via a commercially available BCA assay kit according to the manufacturer's protocol. Briefly, standards were prepared by diluting the bovine serum albumin (BSA) stock provided in the kit. BCA working reagent was prepared by mixing 50 parts of reagent A with 1 part of reagent B of the kit. Working reagent was added to the samples with a 1:8 ratio, respectively. Samples were then incubated at 37°C for 30 minutes. The absorbance was measured at 550nm on a TECAN infinite 200pro plate reader.

2.2.15 Measurement of Lipid Levels

Cholesterol and triglyceride levels were quantified in EDTA-plasma and homogenized tissue using enzymatic assays according to the manufacturer's protocol. Briefly, plasma samples of mice fed with 4 weeks of WD were diluted 1:5 for cholesterol measurement, whereas samples were not diluted for triglyceride measurement. Plasma samples of mice fed with 12 weeks of WD were diluted 1:20 for cholesterol measurement and 1:5 for triglyceride measurement. Standard curve was established by diluting a series of the standard sample (c.f.a.s., Cobas® 10759350 190). 200µl of either cholesterol or triglyceride reagents were added to 5µl of sample on a 96-well plate and the mixes were incubated 30 minutes in dark at room temperature. The absorbance was measured at 505nm on a plate reader.

2.2.16 Lipoprotein Lipase Activity Measurement

Lipoprotein lipase (LPL) activity in AT homogenate samples was quantified by a commercially available LPL kit according to the manufacturer's protocol. LPL activity was normalized to total protein levels of the AT homogenate samples.

2.2.17 Fast-Performance Liquid Chromatography

The amount of the lipoprotein fractions (vLDL, LDL, HDL) in mouse plasma samples was measured via fast-performance liquid chromatography (FPLC) (gel filtration on Superose 6 column (GE Healthcare)). Lipoprotein fractions were separated and assessed based on the flow-through time. Cholesterol levels were quantified as described before.

2.2.18 Cell Culture

Human Primary Coronary Artery Endothelial Cells (HCAECs) were kept at 37 °C and 5% CO2 under sterile conditions in a humidified incubator. Thawing, sub-culturing and medium refreshing were performed according to the manufacturer's protocol. In order to silence *Ackr3*, cells were transfected with either 30 nM negative control siRNA (Silencer™ Negative Control No. 1 siRNA) or 30 nM ACKR3 siRNA (Silencer validated siRNA CXCR7) with the following sequence: Sense GGAUGACACUAAUUGUUAGtt and Antisense CUAACAAUUAGUGUCAUCCtt. Transfection

was performed via siPORT™ NeoFX™ Transfection Agent (see Table 5) according to the manufacturer's protocol. Briefly, 6µl of the siPORT reagent was used per well on a 6-well plate and a reverse transfection protocol was followed. The siPORT reagent and siRNA were mixed in Opti-MEM medium and added to the wells prior to adding the cells to the wells. Cells were incubated in 37°C until seeding equal amounts to the wells containing the siRNA-transfection reagent mix. Cells were transfected for 48-72 hours and the transfection efficiency was evaluated by analyzing the gene expression via droplet digital PCR. Protein expression was also analyzed via western blot. VUF treatments were done at 1uM concentration. All cells were stimulated with 10ng/ml TNFα 2-4 hours. ACKR3 transfected HEK cells were kindly donated by Prof. Alexander Faussner. The cells were treated with tetracycline for 24 hours to induce *Ackr3* expression and treated with 10ng/ml TNFα for 1 hour before evaluating the impact of ACKR3 overexpression.

2.2.19 ELISA

In order to measure circulating CXCL12 levels, plasma samples were analyzed with a commercially available Mouse CXCL12/SDF-1 alpha Quantikine ELISA Kit, according to the manufacturer's instructions. Phosphorylation of NF-kB p65 subunit in cell culture protein isolates was measured via a commercially available NF kappaB p65 (pS536 + Total) ELISA Kit, according to the manufacturer's instructions.

2.2.20 RNA Isolation

Total RNA was isolated from cell culture samples, mouse aortic arch samples as well as mouse AT samples using a commercially available RNA isolation kit from Zymoresearch according to the manufacturer's protocol. The quality (A_{260}/A_{280}) and the quantity (ng/µl) of the RNA samples were analyzed via NanoPhotometer N60/N50 (Implen). A ratio of ~2 for A_{260}/A_{280} was accepted as good quality RNA.

2.2.21 cDNA Synthesis

Prior to cDNA synthesis, all RNA samples were diluted to the equal concentrations. cDNA synthesis was achieved via a commercially available iScript cDNA synthesis kit according to the manufacturer's protocol. Briefly, 20 µL reaction mixes were prepared using <1µg RNA and the reaction protocol was as follows: priming was performed for 5 minutes at 25°C, reverse transcription was performed for 20 minutes at 46°C and reverse transcriptase inactivation was executed for 1 minute at 95°C.

2.2.22 Droplet Digital PCR

Digital PCR was executed on the QX200 Droplet Digital PCR (ddPCR) system from Bio-Rad. 20µL reaction mixes consisted of the following: 10µl of 2X ddPCR SuperMix for probes, 1µL of 20X FAM labeled primer/probe for the target gene, 1µl of 20X VIC labeled primer/probe for the housekeeping gene, RNase-/DNase-free water and the cDNA sample. Droplet generation was

achieved using the QX200 droplet generator as follows: 20µl reaction mix and 70µl droplet generation oil for probes were added onto cartridges, covered with gaskets and inserted into the droplet generator. 42µl of the droplet solution including up to 20,000 droplets was collected from the droplet generator and transferred to the appropriate PCR plate. Cycling was performed in the ddPCR cycler with the following conditions: 10 min at 95°C (enzyme activation), 30 seconds at 94°C (denaturation) and 1 min at 60°C (annealing/extension) for 40 cycles, 10 min at 98°C (enzyme deactivation). The PCR plate was then inserted into the droplet reader. Analysis was done on QuantaSoft software.

2.2.23 Imaging of ACKR3 in Human Atherosclerotic Endothelium

Human atherosclerotic plaque samples obtained during carotid endarterectomy collected in the Maastricht Pathology Tissue Collection (MPTC) in line with the Dutch Code for Proper Secondary use of Human Tissue (http://www.fmwv.nl) and the local Medical Ethical Committee (protocol number 16-4-181). This study conforms to the Declaration of Helsinki, all participants have given informed written consent prior to the inclusion. Sections were stained immunohistochemically as follows: sections were washed in PBS followed by antigen retrieval and permeabilization by boiling the sections in 10mM sodium citrate buffer (pH=6) containing 0.05% Tween-20. Slides were washed with PBS again and tissue sections were blocked with a 1% BSA solution for 30 minutes at room temperature. Samples were then incubated with the primary antibodies Willebrand factor (vWF) and CXCR7 (ACKR3) overnight at 4°C, washed in PBS and incubated with the secondary antibody (1:300) 1 hour at room temperature. Nuclei were stained via 1:2000 diluted Hoechst solution for 5 minutes.

2.2.24 Western Blot

All protein samples were diluted to the same concentration and mixed with sample loading buffer. The mixes were boiled at 95°C for 5 minutes. Samples and the blotting standard were loaded onto 12% gels. Western blot was carried out with Mini Trans-Blot® Cell and Criterion™ Blotter according to the manufacturer's protocol (Bio-Rad). Briefly, protein separation was accomplished by gel electrophoresis with running buffer (Tris/Glycine/SDS) for about 1 hour with 100-150 Volts (V). Proteins were then transferred from the gel to the membrane in transfer buffer (Tris/Glycine buffer with 20% methanol added) for 1 hour at 100V. The membrane was blocked with 5% bovine serum albumin (BSA) in Tris-buffered saline with Tween 20 (TBST) buffer for 1 hour. Primary antibody incubation (p-Erk1/2, p-p65-NFkB, p-PPAR-γ) was carried out overnight at 4°C. The membrane was then washed with TBST buffer and incubated with the HRP-labelled anti-rabbit secondary antibody for 1 hour at room temperature. After washing with TBST buffer, the membrane was developed with a chemiluminescent substrate. After the acquisition of the phosphoprotein signal, the membrane was washed in TBST and stripped for 30 minutes with a stripping buffer followed by 1 hour blocking with 5% BSA solution. Next, the membrane was incubated with antibodies (t-Erk1/2, t-p65-NFkB and t-PPAR-γ) for 1 hour followed by 1-hour secondary antibody incubation, both at room temperature. The signal was captured as explained above. Analysis of

phospho and total protein signals was done on ImageJ and the phospho-protein band was normalized by dividing it to total protein band.

2.2.25 Phosphorylation Array

Protein samples of control and *Ackr3* silenced HCAEC lysates were analyzed for the changes in the phosphorylation of MAPK pathway proteins via a commercially available Human/Mouse MAPK Phosphorylation Array kit, according to manufacturer's protocol.

2.2.26 Statistical Analysis

All data are expressed as mean ±SEM. Statistical analyses were performed using GraphPad Prism version 7.0 or higher (GraphPad Software, Inc.). Outliers were identified with an outlier test ROUT=1 and the distribution of the data was tested via the D'Agostino-Pearson omnibus normality test. Statistical significance was tested via unpaired Student's t-test with Welch correction for normally distributed data and Mann-Whitney U test for non-normally distributed data. A result of <0.05 for p-value was considered statistically significant.

3. Results

The development of mouse models for atherosclerosis studies allowed researchers to investigate potential therapeutic concepts *in vivo*. In 1992, an atherosclerosis mouse model was developed based on the deficiency of ApoE, which is a lipoprotein receptor ligand facilitating the uptake of chylomicrons and vLDL by the lipid receptors in the liver (Zhang et al., 1992). Absence of ApoE leads to accumulation of cholesterol-rich particles in the circulation leading to hyperlipidemia, a known risk factor for atherosclerosis. As a result, *Apoe*$^{-/-}$ mice develop atherosclerotic lesions, which is even more pronounced upon high-fat diet feeding (Lo Sasso et al., 2016).

Furthermore, the use of the Cre (Cre recombinase)-*loxP* (locus of X over P1) technology enabled researches to study target genes in a cell specific manner. The enzyme Cre recombinase recognizes *loxP* sites (34 basepair specific DNA sequences) and excises the floxed DNA sequence (DNA sequence flanked by two *loxP* sites ($^{fl/fl}$)), which leads to the deletion of the targeted gene (Kim et al., 2018) (Figure 7, A). In order to carry out a spatial deletion of the target gene, Cre is expressed by a cell-specific promoter. For example, the promoter *Bmx* targets arterial endothelial cells, whereas *Smmhc* targets SMCs, *Adipoq* targets adipocytes and *Albumin* hepatocytes (Figure 7B). In addition to site specificity, gene editing by Cre can also be controlled temporally. Cre can be fused to an estrogen receptor (CreER) with a mutated ligand binding domain, which then allows the Cre to be induced in the presence of tamoxifen (CreER^{T}) but not natural ER ligand estrogens (Brocard et al., 1997; Metzger & Chambon, 2001). A more sensitive version of the CreER^{T} to the active metabolite of tamoxifen (4-Hydroxytamoxifen (4-OHT)) is named CreER^{T2} (Indra et al., 1999; Kim et al., 2018). For simplicity purposes, the CreER^{T2} mouse models in this study will be referred to as X-Cre, where X represents the name of the promoter.

In order to study the cell-specific roles of ACKR3 in atherosclerosis, *Ackr3*$^{fl/fl}$*Apoe*$^{-/-}$ mice were crossbred with *Apoe*$^{-/-}$ mice expressing cell specific Cre recombinase to allow tamoxifen induced deletion of *Ackr3* in specific cell types as depicted in Figure 7B. Upon intraperitoneal tamoxifen injections, mice were placed on a Western Diet (WD) containing 21% fat and 0.15% to 0.2% cholesterol for either 4 or 12 weeks to assess early or advanced stage atherosclerotic lesion development, respectively.

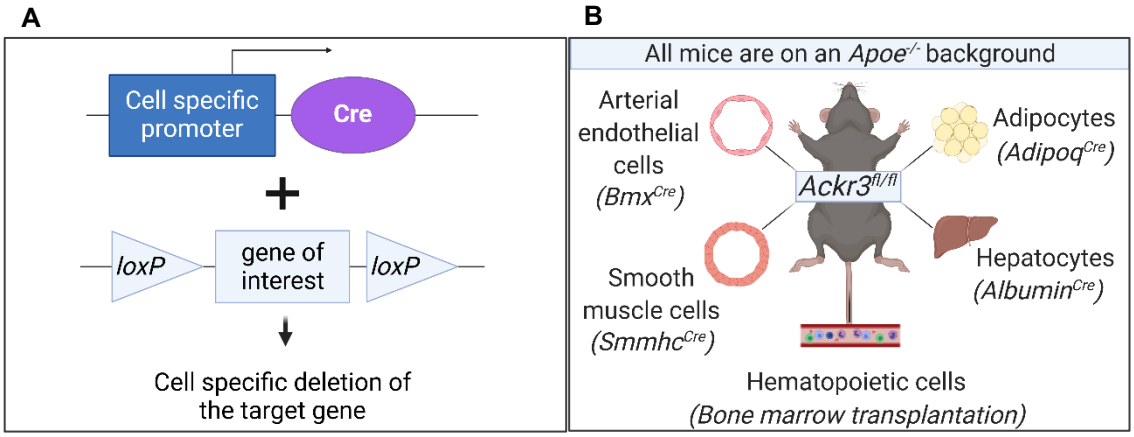

Figure 7: Models of cell-specific ACKR3 deficiency studies in atherosclerotic mice.

A. The tissue specific mechanism of Cre-*loxP* system. **B.** ACKR3 was studied in arterial endothelial cells via *Bmx*^{Cre}, smooth muscle cells via Smmhc^{Cre}, adipocytes via *Adipoq*^{Cre} and hepatocytes via *Albumin*^{Cre} in *Apoe*$^{-/-}$ mice on WD. Furthermore, studying ACKR3 in hematopoietic cells during WD was accomplished with a bone marrow transplantation from *Uni*^{Cre} mice into *Apoe*$^{-/-}$ mice (created with BioRender.com).

3.1 The role of arterial endothelial ACKR3 in atherosclerosis

ACKR3 is a crucial receptor for the development of the cardiovascular system; postnatally, it was shown to be expressed specifically in cardiomyocytes and vascular endothelial cells (Gerrits et al., 2008). Moreover, ACKR3 deficient mice suffered cardiovascular defects and died at or soon after birth (Gerrits et al., 2008; Sierro et al., 2007). Further studies confirmed the expression and the importance of ACKR3 in endothelial cells (Berahovich et al., 2014; Hao et al., 2017). Previously, our research group studied the impact of vascular CXCR4, alternative receptor of the main ACKR3 ligand CXCL12, during atherosclerosis (Döring et al., 2017). The study revealed a protective role of endothelial CXCR4, leaving endothelial ACKR3 to be elucidated. In this chapter, we will focus on the role of arterial endothelial cell specific ACKR3 (aEC-ACKR3) in atherosclerosis.

3.1.1 Assessment of atherosclerotic lesion sizes

Ackr3$^{fl/fl}$*Apoe*$^{-/-}$ and *Bmx*^{Cre}*Apoe*$^{-/-}$ were crossed to generate *Bmx*^{Cre}*Ackr3*$^{fl/fl}$*Apoe*$^{-/-}$ mice, which were then treated with tamoxifen for 5 consecutive days and subsequently subjected to 4 or 12 weeks of WD feeding (Figure 8, A). Lesion sizes were analyzed in the aortic roots of 4-week WD fed mice and in the aortic roots, arches and the aortas of 12-week WD fed mice (Figure 8, B). It could be revealed that aEC-ACKR3 deficiency in *Apoe*$^{-/-}$ mice fed a 4-week WD led to significantly reduced atherosclerotic lesion sizes in the aortic roots compared to control mice (Figure 8, C-D), indicating a pro-atherosclerotic role for aEC-ACKR3. This pro-atherosclerotic effect was confirmed in mice fed a 12-week WD, as deficiency of aEC-ACKR3 resulted in significantly decreased lesion sizes in the aortic roots (Figure 8, E-F). Likewise, lesion sizes were significantly smaller in the arches (Figure 8, G-H) of aEC-ACKR3 deficient mice, compared to controls. No significant changes were observed in the aortas of control and aEC-ACKR3 deficient mice (Figure 8, I). Apart

from this, blood cholesterol and triglyceride levels did not change between the two genotypes upon 12 weeks of WD (Table 7). Surprisingly however and in sharp contrast to the observed effects on atherosclerotic lesion size, aEC-ACKR3 deficient mice developed neutrophilia upon 4 weeks of WD feeding as well as leukocytosis attributed to significantly elevated counts of neutrophils and B cells upon 12 weeks of WD feeding (Table 6 & 7).

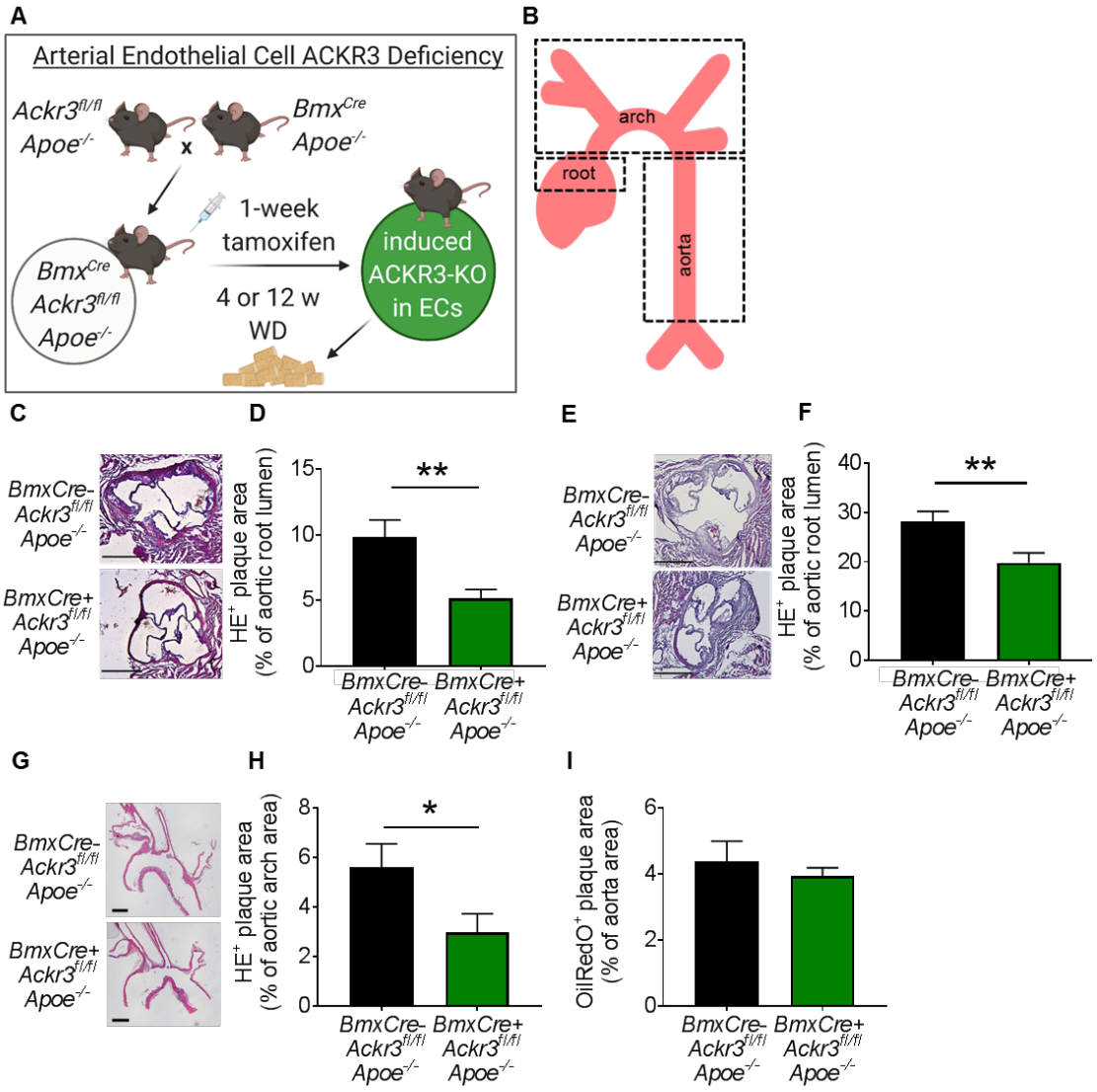

Figure 8: Endothelial ACKR3 deficiency attenuates atherosclerotic lesions in Apoe$^{-/-}$ mice.

A. Schematic representation of the 4 and 12-week WD experimental setup (created with BioRender.com). **B.** Schematic representation of the studied atherosclerosis prone regions. Aortic root and aortic arch lesions were visualized via hematoxylin & eosin (H&E) staining, whereas the lipid deposits in the aortas were visualized with an Oil Red O staining. **C-D.** Representative images (**C**; scale bar: 500 µm) and quantification (**D**) of atherosclerotic lesion sizes in the aortic roots of mice fed with 4 weeks of WD (n=22-32). **E-F.** Representative images (**E**; scale bar: 500 µm) and quantification (**F**) of atherosclerotic lesion sizes in the aortic roots of mice fed 12 weeks of WD (n=12-14). **G-H.** Representative images (**G**; scale bar: 500 µm) and quantification (**H**) of atherosclerotic lesion sizes in the aortic arches of mice fed 12 weeks of WD (n=12-14). **I.** Quantification of atherosclerotic lesion sizes in the aortas of mice fed 12 weeks of WD (n=12-14). Bar graphs represent ±SEM. *p<0.05, **p<0.01.

3.1.2 Atherosclerotic plaque composition and stability analysis

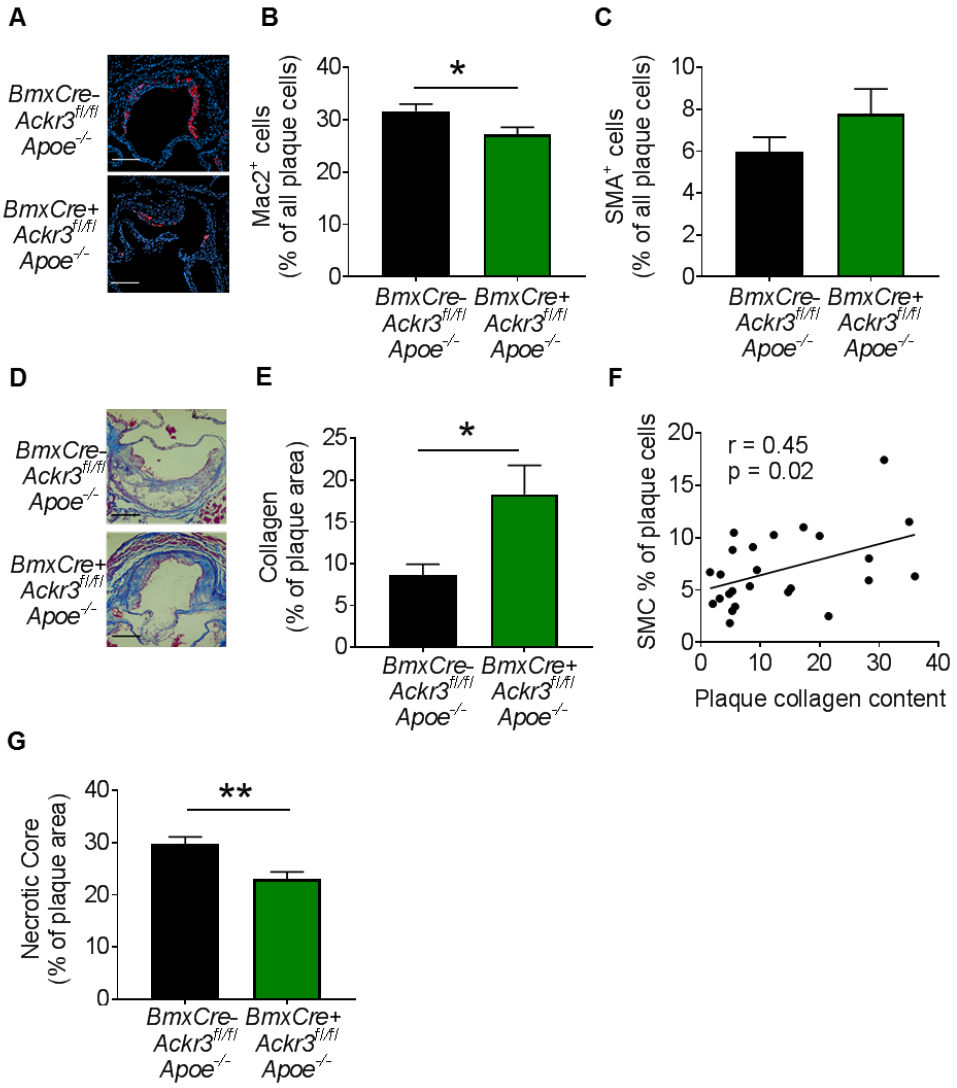

Figure 9: Endothelial ACKR3 deficiency improves plaque composition and stability in Apoe$^{-/-}$ mice.

A-B. Representative images (**A**; scale bar: 250 µm, red=MAC2, blue=DAPI) and quantification (**B**) of macrophage (MAC2+) content in the aortic roots (n=12). **C.** Quantification of SMC (SMA+) content in the aortic roots (n=12-13). **D-E.** Representative images of Masson Trichrome staining (**D**; scale bar: 250 µm, blue=collagen, red=muscle fibers, cytoplasm, keratin) and quantification (**E**) of collagen (n=12-14) in the aortic roots (n=12-13). **F.** Pearson r correlation of lesional SMC content and collagen content in atherosclerotic lesions (r=0.45, p=0.02), (n=25). **G.** Quantification of necrotic core content in the aortic roots (n=12-13). Bar graphs represent ±SEM. *p<0.05, **p<0.01.

In order to further characterize the plaques, cell composition of the advanced lesions (12-week WD) was analyzed by evaluating the number of macrophages (MAC2+) and SMCs (SMA+) in the plaques. Analyses disclosed that aEC-ACKR3 deficient mice had significantly less macrophage content inside their plaques compared to control mice (Figure 9, A-B). Meanwhile, SMC quantity within lesions showed an insignificant trend towards an increase in aEC-ACKR3 deficient mice

(Figure 9, C). Plaque stability analysis through Masson Trichrome staining revealed a significantly increased amount of collagen in plaques of aEC-ACKR3 deficient mice (Figure 9, D-E). Intraplaque collagen content also correlated positively with the SMC content (Figure 9, F). Furthermore, lesions of the aEC-ACKR3 deficient mice contained significantly less necrotic cores (Figure 9, G). Altogether, these findings establish that aEC-ACKR3 drives a pro-atherosclerotic cellular composition in lesions as well as a more unstable plaque phenotype.

3.1.3 Investigation of the main ACKR3 ligand CXCL12 levels

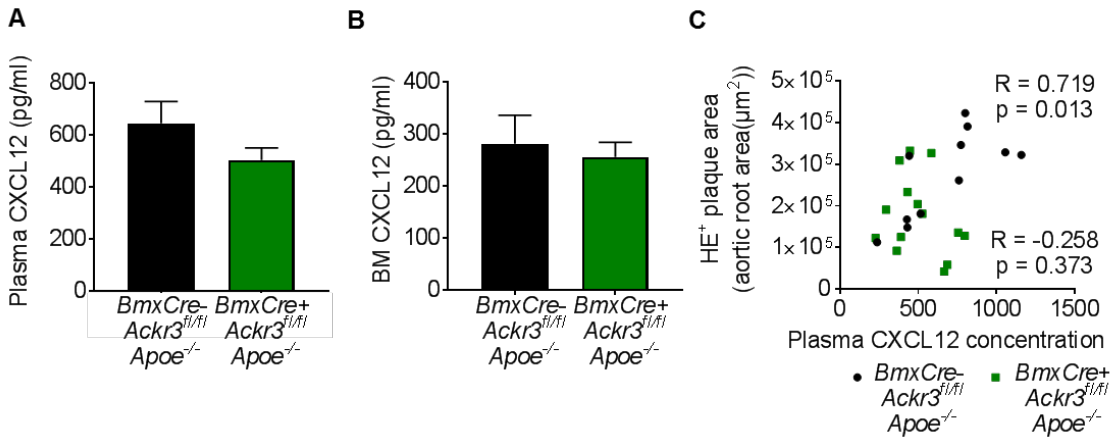

Figure 10: Endothelial ACKR3 deficiency does not impact CXCL12 levels.

A. Plasma CXCL12 levels (n=12-14). **B.** Bone marrow CXCL12 levels (n=12-14). **C.** Pearson r correlation of plasma CXCL12 levels and aortic root lesion content in mice fed 12 weeks of WD (R=0.719, p=0.013), (n=12-14). Bar graphs represent ±SEM.

ACKR3 has two main chemokine ligands; CXCL11 and CXCL12, which further bind to CXCR3 and CXCR4, respectively (Burns et al., 2006). In some studies, ACKR3 was reported to regulate the bioavailability of its ligands by scavenging its chemokine ligands (Boldajipour et al., 2008; Naumann et al., 2010). In this study, we used mice on a C57BL/6 (B6) background which were reported to not express CXCL11 (Sierro et al., 2007). We also confirmed this lack of CXCL11 in our mice via ELISA analysis in plasma samples (Appendix C). The other ligand, CXCL12 is a chemotactic cytokine which is described to regulate homing and recruitment of hematopoietic progenitor cells (Döring et al., 2014). Accordingly, potential changes in CXCL12 gradient upon aEC-ACKR3 deficiency could be responsible for the observed leukocytosis in knockout mice. Therefore, we investigated the levels of the main ACKR3 ligand CXCL12 in the plasma samples of mice in order to understand how aEC-ACKR3 deficiency affected circulating CXCL12 levels. Interestingly, CXCL12 levels did not differ between control and aEC-ACKR3 deficient mice in the plasma (Figure 10, A). Next, we investigated the levels of CXCL12 in bone marrow and found no differences between the two groups (Figure 10, B). These results confirm that aEC-ACKR3 deficiency did not lead to any changes of CXCL12 gradient or levels. Previously, we established that circulating CXCL12 originating from endothelial cells drives atherosclerosis in *Apoe*$^{-/-}$ mice (Doring et al., 2019). Analysis of a link between circulating CXCL12 levels and atherosclerotic

lesion sizes indeed confirmed a positive and significant correlation between the two factors in our control mice (Figure 10, C). Surprisingly, this correlation was lost in the absence of endothelial ACKR3 (Figure 10, C), suggesting that the interaction between circulating CXCL12 and aEC-ACKR3 drives atherosclerosis regardless of significant changes in plasma/bone marrow CXCL12 levels. Apart from CXCL11 and CXCL12, MIF was also reported to bind ACKR3 (Alampour-Rajabi et al., 2015). Although a decrease was observed in the plasma levels of MIF in aEC-ACKR3 deficient mice, no significant changes were disclosed (Appendix D).

3.1.4 Assessment of leukocyte infiltration into lesions

Mice with aEC-ACKR3 deficiency disclosed less macrophage content within their lesions. We theorized that aEC-ACKR3 may be involved in leukocyte extravasation through the vascular endothelium, which may lead to differences in lesional macrophage accumulation. To test this theory, we performed a leukocyte infiltration assay as described by Winter et al. (Winter et al., 2018). Briefly, control and aEC-ACKR3 deficient mice were fed with a 4-week WD and subsequently injected intravenously with an anti-CD45 antibody. Injection of this antibody into the bloodstream labeled the leukocytes in the circulation and therefore allowed identification of blood-borne leukocytes. Later, the antibody was tracked in the atherosclerotic lesions as an indicator of newly recruited circulating leukocytes that infiltrated the lesions (Figure 11, A). Immunohistochemical analysis of the aortic root lesions revealed that aEC-ACKR3 deficient mice had significantly less leukocyte infiltration into their lesions compared to control mice (Figure 11, B-C), confirming a role of aEC-ACKR3 in the arterial invasion of immune cells.

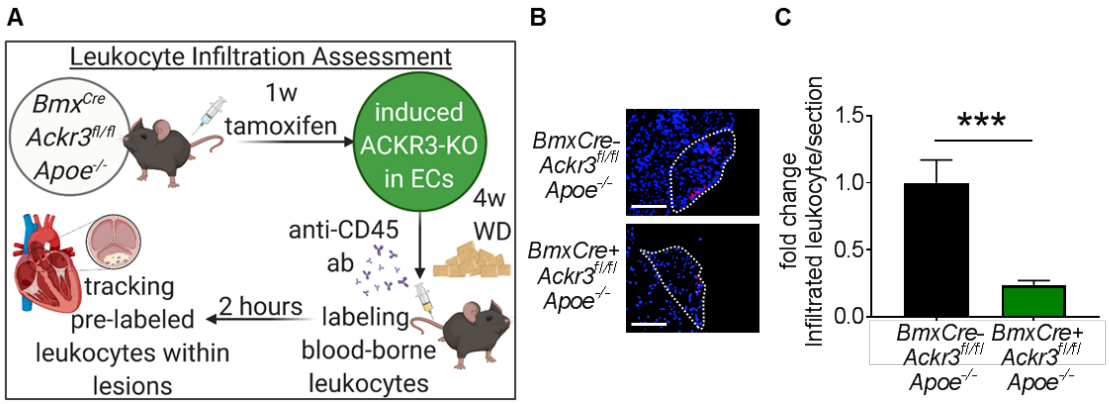

Figure 11: Endothelial ACKR3 deficiency significantly reduces immune cell infiltration into atherosclerotic lesions.

A. Schematic representation of the leukocyte tracking experimental setup (created with BioRender.com). **B-C.** Representative pictures (**B**; scale bar: 250 µm, dotted line= atherosclerotic lesion) and fold change (**C**) of infiltrated leukocytes in aortic root lesions (n=7-10). Bar graphs represent ±SEM. ***p<0.001.

3.1.5 Examination of vascular integrity

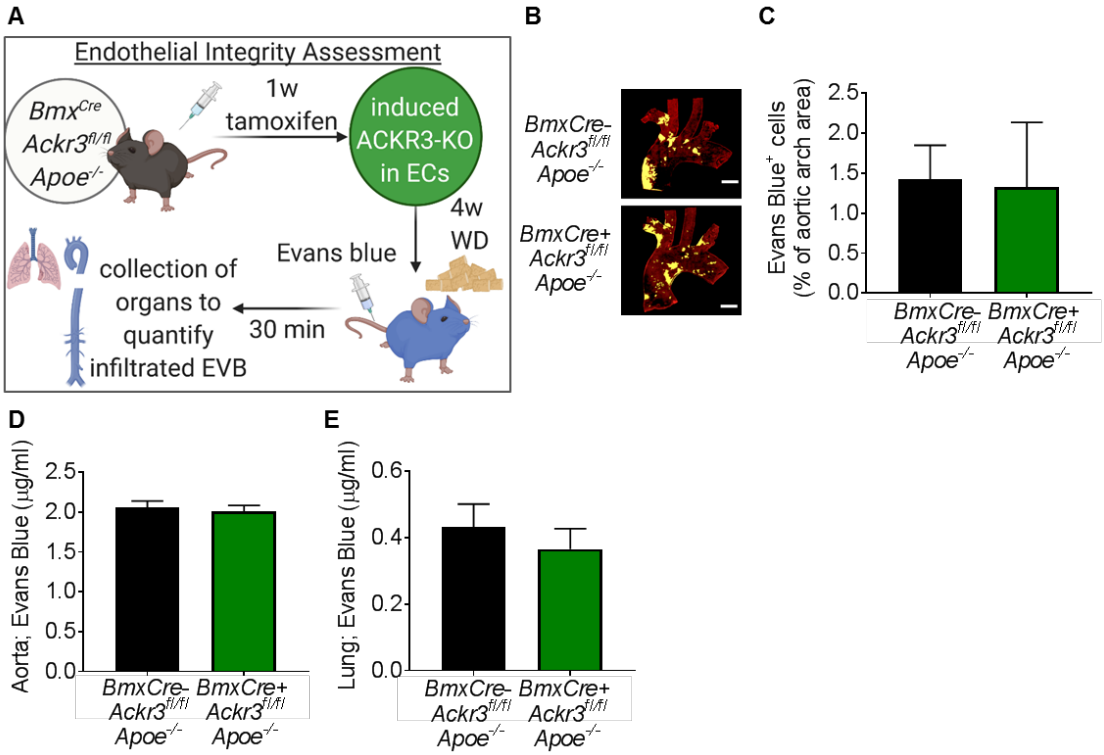

Figure 12: Endothelial ACKR3 deficiency does not affect vascular endothelial permeability.

A. Schematic representation of the endothelial permeability experiment (created with BioRender.com). **B-C.** Representative images (B; yellow=Evans Blue) and quantification (**C**) of infiltrated EVB in the aortic arches (n=4-5). **D.** Quantification (µg/ml) of infiltrated EVB in the lysates of aortas (n=7) and **E.** lungs (n=6). Bar graphs represent ±SEM.

Investigation of the vascular CXCR4 revealed that the endothelial CXCR4 deficiency resulted in the loss of endothelial barrier function leading to arterial leakage (Döring et al., 2017). In order to understand how the alternate CXCL12 receptor ACKR3 in endothelial cells mediates leukocyte infiltration through the vascular endothelium, we first investigated endothelial permeability in mice. The permeability of the endothelium in the vasculature is a critical factor in trafficking of blood-borne elements into the sub-endothelial space. In order to find out if the aEC-ACKR3 can lead to a 'leaky' phenotype of the vascular endothelium in mice, we injected the animals intravenously with Evans Blue (EVB) introducing the dye into the bloodstream of the mice. Injection of the EVB dye allows to observe the amount of a traceable dye that passed through the endothelium of the mice. The dye was traced back in the aortic arch and the aorta of the mice, as well as the lungs. After 30 minutes of incubation, we perfused the mice with saline to remove the blood and eliminate excess EVB from the organs. Next, we measured the amount of EVB that breached through the endothelium and remained in the organs (Figure 12, A). There were no significant differences in EVB quantities that infiltrated in the aortic arches (Figure 12, B-C), aortas (Figure 12, D) or in the lungs (Figure 12, E) of the control and aEC-ACKR3 deficient mice, indicating that aEC-ACKR3 does not affect vascular integrity.

3.1.6 Endothelium-immune cell adhesion analysis

Following the above described findings, we postulated that aEC-ACKR3 may be involved in endothelial adhesion, a crucial step in trans-endothelial migration of the immune cells during atherosclerosis, as well as other diseases. Deficiency of aEC-ACKR3 may be limiting the adhesion of leukocytes to the vascular endothelium and thereby curbing arterial invasion of the immune cells. In support of this notion, ACKR3 was previously shown to impact cell adhesion in endothelial progenitor cells *in-vitro* (Dai et al., 2011). The potential impact of aEC-ACKR3 on endothelial adhesion was first tested via *ex-vivo* perfusion of fluorescently labeled leukocytes through carotid arteries collected from control and aEC-ACKR3 deficient mice (Figure 13, A). Leukocyte adhesion onto aEC-ACKR3 deficient arteries was significantly diminished, suggesting that ACKR3 is indeed involved in the regulation of the endothelial adhesion process (Figure 13, B-C). Next, ACKR3 mediated adhesion was further confirmed *in-vivo* via intravital microscopy (Figure 13, A). The experiment involved testing of three different subsets of leukocytes in order to comprehend the extent of ACKR3 mediated endothelial adhesion: myeloid cells ($CD11b^+$), classical monocytes ($Ly6C^+$) and neutrophils ($Ly6G^+$). Adhesion of all leukocyte subsets onto the carotid arteries was strongly limited in the absence of aEC-ACKR3 regardless of the immune cell type (Figure 13, D-G), suggesting a strong, general effect of aEC-ACKR3 on leukocyte adhesion.

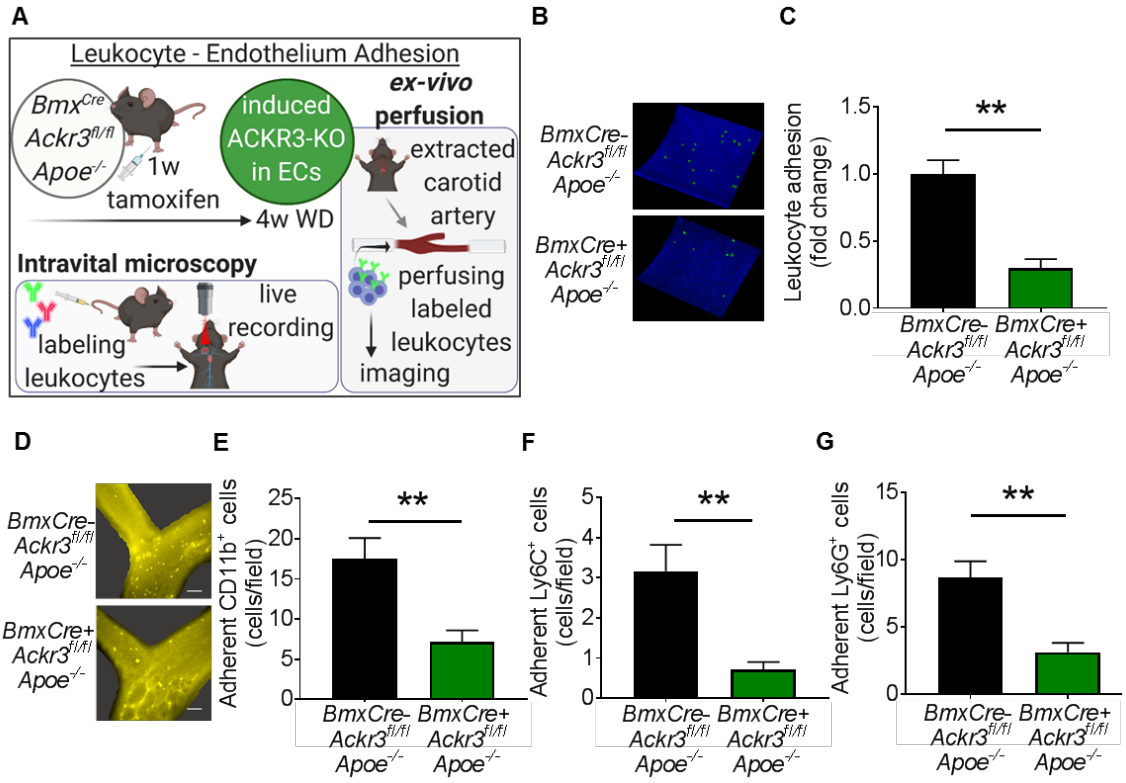

Figure 13: Endothelial ACKR3 regulates endothelium-leukocyte adhesion.

A. Schematic representation of the experimental setup (created with BioRender.com). **B-C.** Representative images (**B**; green= fluorescently labeled CD45+ cells, blue=arterial wall) and fold change (**C**) of adhered leukocytes onto *ex-vivo* perfused carotid arteries (n=5). **D.** Representative images of intravital microscopy (scale bar: 100 µm). Quantification of adherent **E.** CD11b+, **F.** Ly6C+ and **G.** Ly6G+ cells (n=6-8). Bar graphs represent ±SEM. **p<0.01.

3.1.7 Assessment of adhesion molecule expression in mice

During atherosclerosis, endothelial cells in the vasculature are subjected to inflammatory stimuli and therefore upregulate the surface expression of adhesion molecules, such as intracellular adhesion molecule-1 (ICAM-1), vascular adhesion molecule-1 (VCAM-1) and selectins (Gimbrone & García-Cardeña, 2016). This process allows immune cells to adhere to the endothelial cells and transmigrate into the sub-endothelial space to combat the source of inflammation.

In order to elucidate the mechanism behind aEC-ACKR3 mediated adhesion, we examined the presence of ICAM-1+ cells in atherosclerotic lesions of mice via immunofluorescent staining. The analysis revealed a significant decrease in ICAM-1+ cells in the endothelial lining of the aortic root lesions of aEC-ACKR3 deficient mice (Figure 14, A-B). Along with this, macrophage content within the lesions correlated positively and significantly with the amount of ICAM-1+ cells of the lesions (Figure 14, C), indicating a significant link between vascular adhesion and lesional macrophage accumulation. Furthermore, expression of *Ackr3, Icam* and *Vcam* was analyzed in whole aortic arches via ddPCR. The expression of the adhesion molecules correlated positively with *Ackr3* expression in the arches, although a stronger correlation was observed with *Icam* (Figure 14, D).

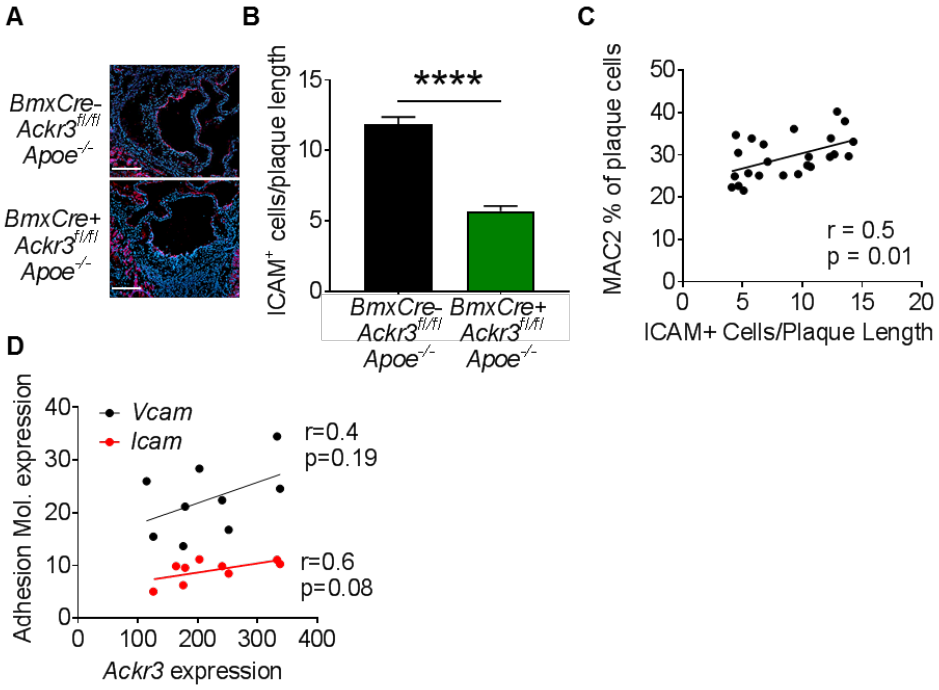

Figure 14: Endothelial ACKR3 deficiency decreases adhesion molecule expression.

A-B. Representative images (**A**; scale bar: 250 µm, red=ICAM) and quantification (**B**) of ICAM+ cells on the endothelial lining of mouse aortic root lesions (n=12-14). **C.** Pearson r correlation of lesional macrophages and ICAM+ endothelial cells in aortic root lesions (r=0.5, p=0.01) (n=24). **D.** Pearson r correlation of *Icam* (r=0.6, p=0.08) and *Vcam* (r=0.4, p=0.19) expression with *Ackr3* expression in whole aortic arches (n=9). Bar graphs represent ±SEM. ***p<0.001.

3.1.8 Adhesion molecule expression in human endothelial cells

In order to better understand and validate the role of ACKR3 in endothelial adhesion, we investigated the impact of ACKR3 on adhesion molecule expression in human coronary artery endothelial cells (HCAECs). To this end, ACKR3 was silenced in inflamed HCAECs, as it would be the case under atherosclerotic conditions (Figure 15, A). Flow cytometry analysis revealed that ACKR3 silenced HCAECs had decreased ICAM, VCAM and E-selectin expression, all of which are known to be upregulated in endothelial cells during atherosclerosis to facilitate immune cell adhesion (Figure 15, B-F). Further strengthening this finding, expression of these adhesion molecules correlated very significantly with ACKR3 expression in the cells (Figure 15, G-H).

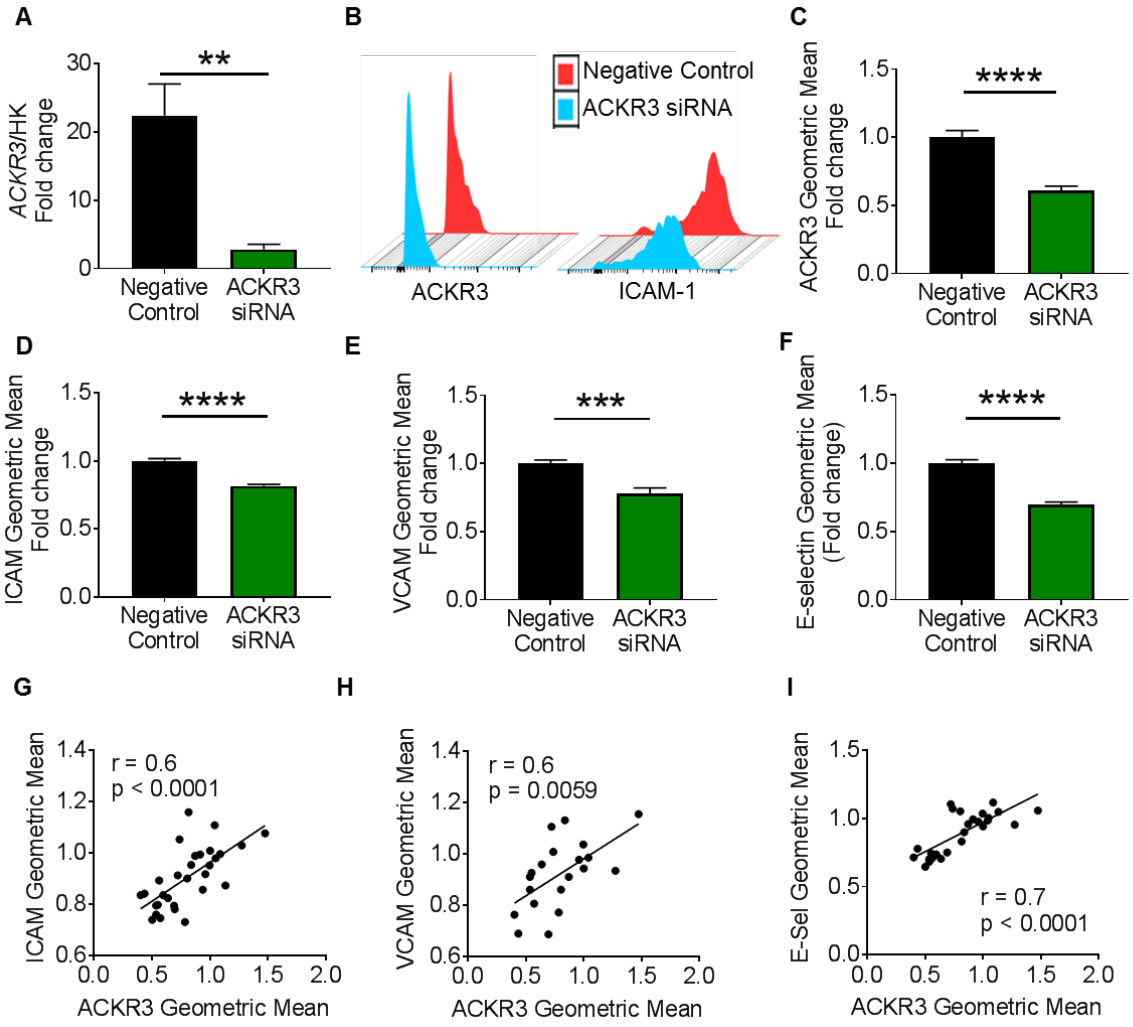

Figure 15: ACKR3 regulates adhesion molecule expression in HCAECs.

A. ddCPR quantified expression of *ACKR3* in control and silences HCAECs stimulated with TNF-α (n=6). **B.** Representative flow cytometry histograms of ACKR3 and ICAM-1. **C-F.** Expression (geometric mean by flow cytometry) of **C.** ACKR3, **D.** ICAM, **E.** VCAM and **F.** E-selectin in control and silenced HCAECs stimulated with TNF-α (n=3 independent batches). Pearson r correlation of **G.** ICAM (n=31-34), **H.** VCAM (n=21-23) and **I.** E-selectin expression with ACKR3 expression in HCAECs stimulated with TNF-α; r=0.6, p=0.00001 and r=0.6, p=0.0059, respectively. Bar graphs represent ±SEM. **p<0.01, ***p<0.001, ****p<0.0001.

3.1.9 Assessment of endothelial ACKR3 signaling

For a long time, ACKR3 was considered a non-signaling, decoy receptor for its main ligand CXCL12 (Boldajipour et al., 2008; Naumann et al., 2010; Wang et al., 2012). In our study however, we showed that CXCL12 levels were not affected in aEC-ACKR3 deficient mice. Furthermore, recent findings unveiled the ability of ACKR3 to signal through β-arrestin and mitogen activated protein kinase (MAPK) pathway, as well as NF-kB (Alampour-Rajabi et al., 2015; Ishizuka et al., 2021; Li et al., 2019; Lin et al., 2014). MAPK and NF-kB signaling are well-known inflammatory pathways that are established to prompt ICAM and VCAM expression in endothelial and other cell types (X. L. Chen et al., 2005; Choi et al., 2010; Zhong et al., 2012). In order to understand whether ACKR3 silencing affected these pathways in inflamed HCAECs, we carried out a MAPK phosphorylation antibody array experiment. ACKR3 silencing led to significant downregulation of the key MAPK pathway mediators, including reduced ERK1/2 phosphorylation (Figure 16, A-B). The decrease in ERK1/2 phosphorylation upon ACKR3 silencing was further confirmed in HCAECs via western blot analysis (Figure 16, C). Moreover, stimulation of ACKR3 with its agonist VUF confirmed an increase in ERK1/2 phosphorylation in the cells (Figure 16, D). Activated Akt and ERK1/2 can phosphorylate the NF-κB inhibitor IκBα kinase (IIK), leading to the activation of NF-κB (Bai et al., 2009; Chen et al., 2016). NF-κB is an upstream promoter of ICAM, VCAM and E-selectin (Ledebur & Parks, 1995; Shu et al., 1993). Quantitative ELISA analysis showed a significant decrease of NF-κB p-65 phosphorylation in ACKR3 silenced HCAECs (Figure 16, E). Western blot analysis confirmed this finding and an increase in NF-κB p-65 phosphorylation was also observed in VUF treated HCAECs (Figure 16, F). To further confirm these findings, we used ACKR3-transfected HEK cells overexpressing ACKR3 compared to control cells (Figure 16, G). Indeed, ACKR3 overexpressing cells showed increased NF-κB p-65 phosphorylation analyzed quantitatively by ELISA (Figure 16, H). Previously, we and others revealed that ACKR3 can control PPAR-γ expression in AT (Gencer, Döring, et al., 2021; Li et al., 2014). PPAR-γ is anti-inflammatory and it is well established to negatively regulate the inflammatory NF-κB (Remels et al., 2009; Scirpo et al., 2015; Sung et al., 2006). In addition, studies also confirmed inhibition of ICAM and VCAM expression upon PPAR-γ activation (Pasceri et al., 2000; Sasaki et al., 2005). Further supporting our findings described above, ACKR3 silenced HCAECs showed a significant decrease in *PPAR-γ* expression, (Figure 16, I), whereas ACKR3-overexpressing HCAECs revealed an increase in *PPAR-γ* expression, although statistically insignificant (Figure 16, J). Following our *in-vitro* findings revealing marked regulation of NF-κB, a significant transcription factor for ICAM and VCAM expression, we sought to assess the levels of phospho-p65 NF-κB in atherosclerotic endothelial cells of aEC-ACKR3 deficient mice. In line with our findings, analyses of immunofluorescently stained endothelial cells (vWF+) on mouse lesions revealed a significant decrease in phospho-p65 NF-κB (red) expression (Figure 16, K-L). Altogether, these findings establish a pro-inflammatory role for aEC-ACKR3, which promotes NF-κB phosphorylation and thereby adhesion molecule expression in endothelial cells.

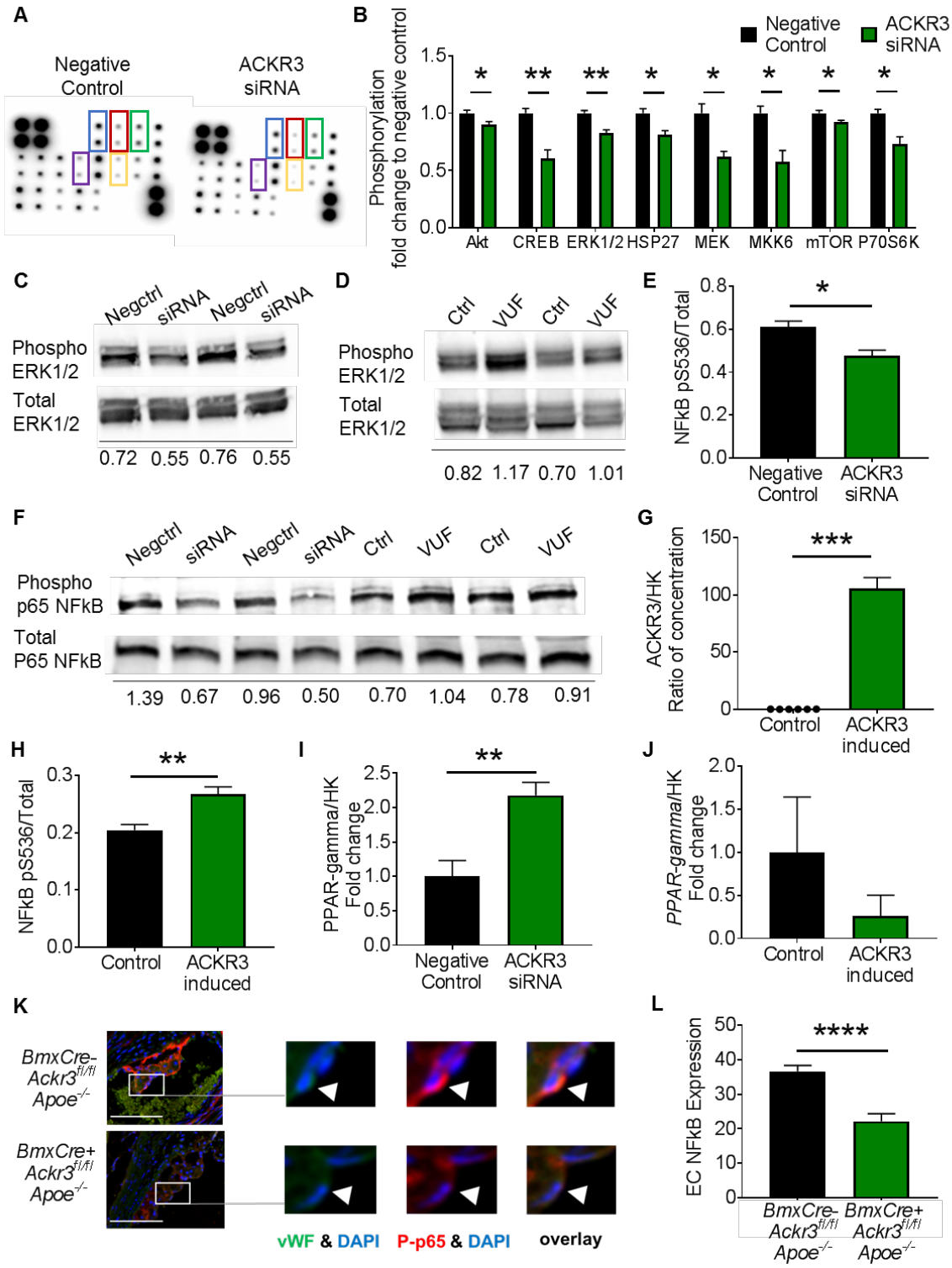

Figure 16: Endothelial ACKR3 signals through MAPK and NF-kB pathways.

A-B. Representative images (**A**; blue=Akt, red=CREB, green=ERK1/2, purple: MEK, yellow: MKK6) and fold change (**B**) of protein phosphorylation in the MAPK pathway (n=4) in control and silenced HCAECs stimulated with TNF-α. **C.** Western blot analysis of ERK1/2 phosphorylation in control and silenced HCAECs stimulated with TNF-α. Numbers below indicate phospho/total signal quantifications. **D.** Western blot analysis of ERK1/2 phosphorylation in control and VUF treated HCAECs stimulated with TNF-α. **E.** Phosphorylation of the NF-kB p-65 subunit quantified by ELISA in control and silenced HCAECs stimulated with TNF-α (n=3). **F.** Western blot analysis of NF-kB p-65 subunit phosphorylation in control and silenced, as well as

control and VUF treated HCAECs stimulated with TNF-α. **G.** Upregulation of *ACKR3* expression in ACKR3-transfected HEK cells quantified by ddPCR (n=6). **H.** Phosphorylation of the NF-kB p-65 subunit quantified by ELISA in control and ACKR3-induced HEK cells stimulated with TNF-α (n=6). Expression of PPAR-γ measured by ddPCR in **I.** control and silenced cells (n=8-9) and in **J.** control and ACKR3-induced HEK cells stimulated with TNF-α (n=6). **K-L.** Representative images (**K**; green=von Willebrand factor, red=ACKR3, blue=DAPI) (scale bar: 100 µm) and quantification (**L**) of phospho-p65 NF-kB expression in aortic root endothelial cells from control and knockout mice (n=3). Bar graphs represent ±SEM. *p<0.05, **p<0.01, ***p<0.001.

3.1.10 Presence of ACKR3 in human atherosclerotic endothelium

ACKR3 in the endothelium of mice revealed significant contribution to atherosclerotic plaque development concomitant with the regulation of arterial immune cell invasion through endothelial adhesion. Further analyses confirmed that human ACKR3 is also involved in adhesion molecule expression in endothelial cells. In order to understand if these findings could indicate a potential relevance of ACKR3 in human atherosclerosis, we sought to establish the presence of human ACKR3 specifically in the endothelium of atherosclerotic lesions. Immunofluorescent staining of ACKR3 together with the endothelial marker vWF confirmed the presence of ACKR3 in human atherosclerotic endothelium (Figure 17), indicating a relevance of aEC-ACKR3 in human atherosclerosis.

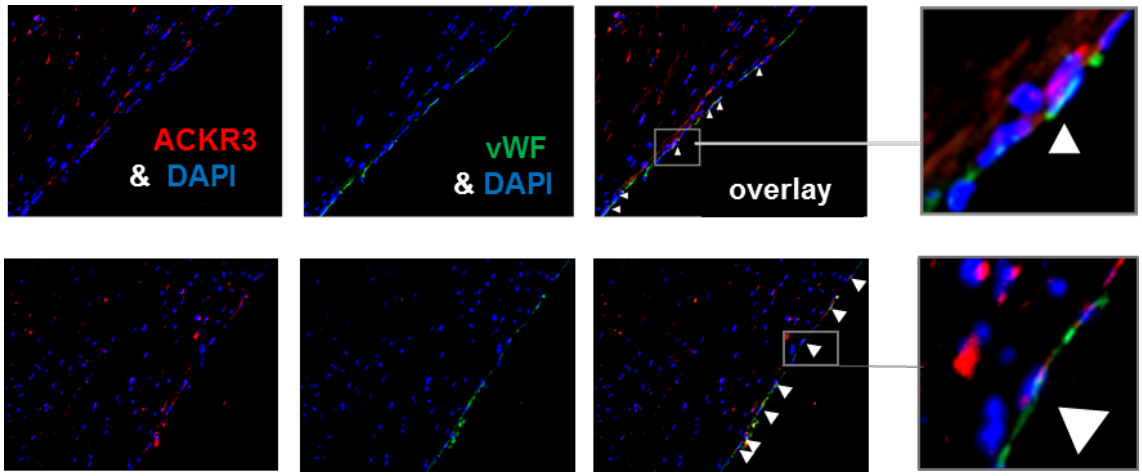

Figure 17: ACKR3 is present in human atherosclerotic endothelium.

Immunofluorescent staining of ACKR3 (red), von Willebrand Factor (green) and nuclei (DAPI, blue).

3.1.11 The impact of aEC-ACKR3 on atherosclerosis

Altogether, our data establish that aEC-ACKR3 contributes to atherosclerotic lesion growth by supporting immune cell adhesion to the arterial wall and thereby regulating infiltration of the cells into atherosclerotic lesions (Figure 18). *In-vitro* analyses in HCAECs disclosed that ACKR3 silencing results in downregulation of adhesion molecules and phosphorylated ERK1/2, Akt and NF-kB p65, which are inflammatory pathways involved in cell adhesion. Meanwhile, PPAR-γ, which negatively regulates NF-kB, is upregulated.

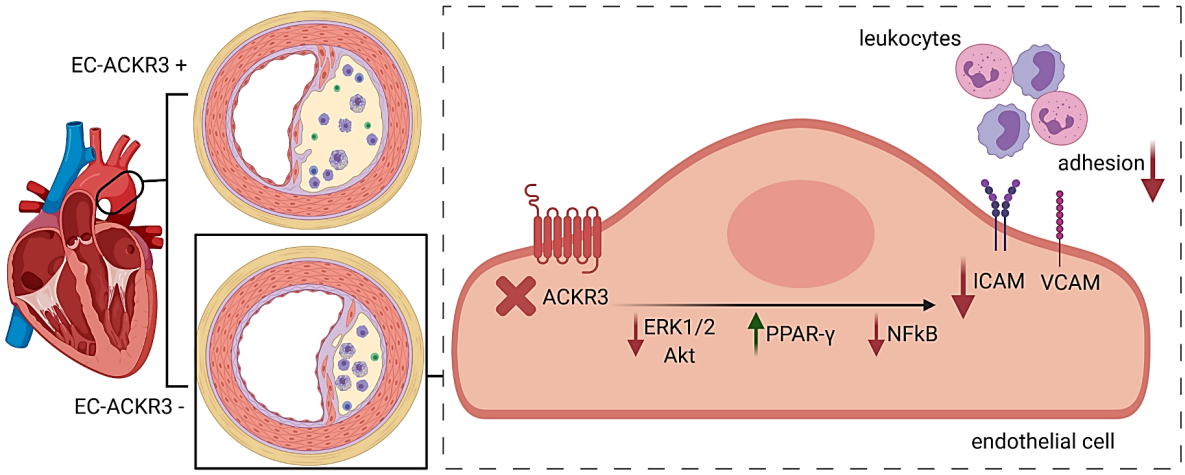

Figure 18: Summary of the roles of aEC-ACKR3 in atherosclerosis.

Graphical representation of aEC-ACKR3 mediated processes in atherosclerotic lesions and endothelial cells (created with BioRender.com).

3.2 The role of smooth muscle cell specific ACKR3 in atherosclerosis

ACKR3 was found to be expressed in SMCs (Berahovich et al., 2014; Neusser et al., 2010), which are apart from endothelial cells an important cell type in the vasculature that is involved in the pathobiology of atherosclerosis. In this chapter, I will focus on the role of SMC specific ACKR3 (SMC-ACKR3) in atherosclerosis.

3.2.1 Atherosclerotic plaque size analysis

Ackr3$^{fl/fl}$*Apoe*$^{-/-}$ and *Smmhc*^{Cre}*Apoe*$^{-/-}$ were crossed to generate *Smmhc*^{Cre}*Ackr3*$^{fl/fl}$*Apoe*$^{-/-}$ mice, which were then treated with tamoxifen and subsequently subjected to 12 weeks of WD feeding (Figure 19, A).

Three regions were selected to analyze lesions in 12-week WD fed mice: the aortic roots, arches and the aortas (Figure 19, B). Lesions in the aortic roots were visualized via H&E staining (Figure 19, C) and the lesion sizes between control and SMC-ACKR3 deficient mice did not differ (Figure 19, D). Similarly, lesions in the aortic arches did not exhibit a significant difference in size between the two groups (Figure 19, E-F). Likewise, lesion size analyses via Oil-Red O staining in the aortas showed no difference upon SMC-ACKR3 deficiency in atherosclerotic mice (Figure 19, G-H). In summary, the findings disclosed that SMC-ACKR3 does not affect atherosclerotic lesion sizes.

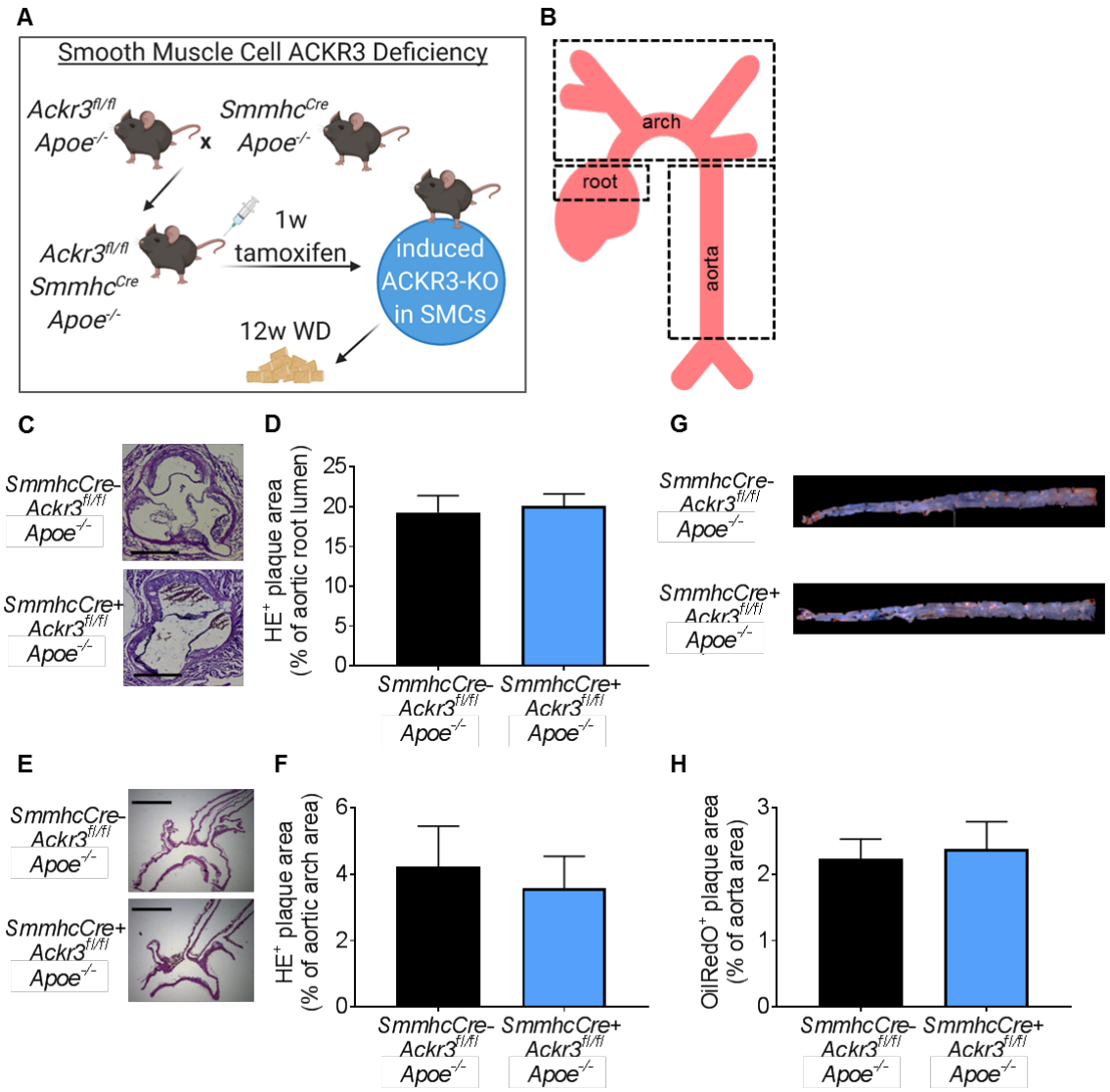

Figure 19: SMC-ACKR3 deficiency does not affect atherosclerotic lesion sizes in Apoe$^{-/-}$ mice.

A. Schematic representation of the experimental setup (created with BioRender.com). **B.** Schematic representation of atherosclerosis prone regions assessed for lesion sizes. **C-D.** Representative images (**C**; scale bar: 500 µm) and quantification (**D)** of atherosclerotic lesion sizes in the aortic roots stained with H&E (n=8-9). **E-F.** Representative images (**E**; scale bar:250 µm) and quantification (**F**) of atherosclerotic lesion sizes in the aortic arches (n=8-9). **G-H.** Representative images (**G**) and quantification (**H**) of atherosclerotic lesion sizes in the abdominal aortas (n=8-9). Bar graphs represent ±SEM.

3.2.2 Examination of plaque composition and stability

Initial analyses did not indicate a role for SMC-ACKR3 in atherosclerotic lesion growth. In order to understand whether SMC-ACKR3 could be involved in further parameters of atherosclerosis, we analyzed the cellular composition of the plaques by quantifying the amount of macrophages and SMCs via immunofluorescent stainings. There were no significant differences in either cell type within the lesions (Figure 20, A-C). Furthermore, plaque stability was examined via Mason Trichrome staining exhibiting the collagen content within lesions. Interestingly, SMC-ACKR3 deficient mice had significantly higher amounts of lesional collagen compared to control mice (Figure 20, D-E), which was not correlated to the amount of SMCs in the lesions (Figure 20, F). These results indicate that SMC-ACKR3 does not play a role in atherosclerosis, other than a potential plaque-stabilizing effect through lesional collagen content.

Another interesting finding in SMC-ACKR3 deficient mice was leukocytosis, similar to aEC-ACKR3 deficient mice (Table 8). Leukocytosis in SMC-ACKR3 deficient mice was attributed to the significant increase in neutrophils and B cells in the circulation (Table 8). Lipid levels in the plasma were not affected (Table 8).

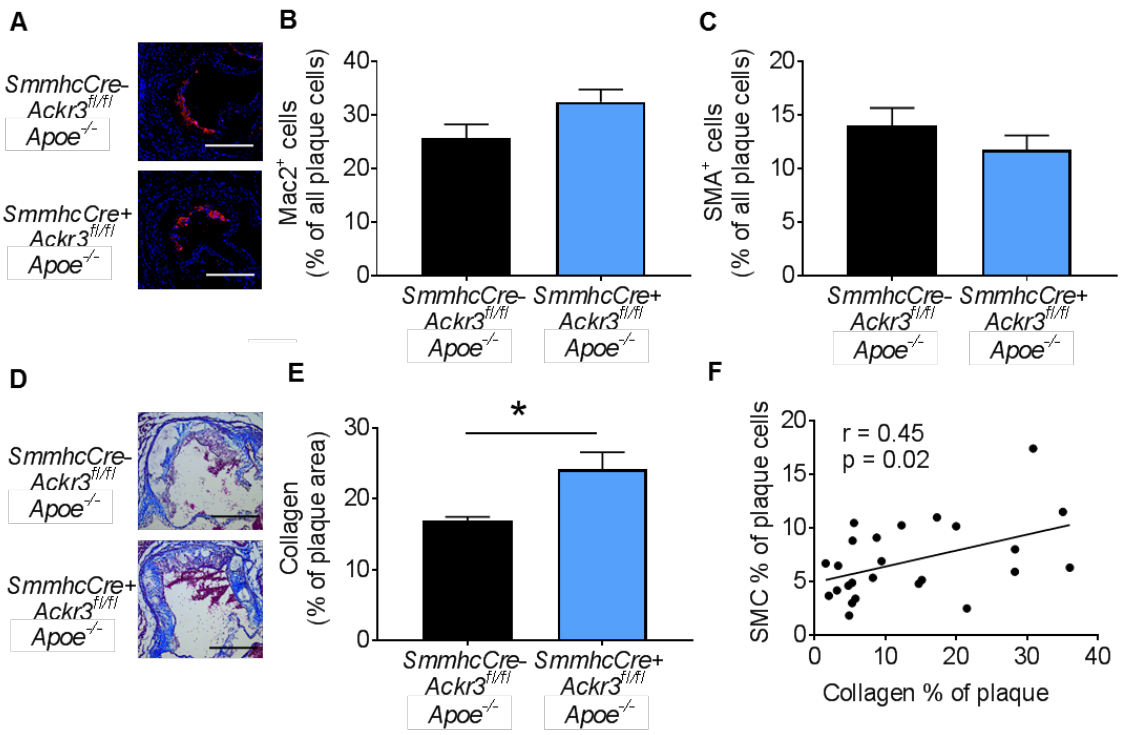

Figure 20: SMC-ACKR3 deficiency does not alter plaque composition but stability in Apoe$^{-/-}$ mice.

A. Representative images (scale bar: 250 µm) and **B.** quantification of macrophage (MAC2+) content in the lesions (n=8-9). **C.** Quantification of SMC (SMA+) content in the aortic roots (n=8-9). **D.** Representative images (scale bar: 250 µm) and **E.** quantification of collagen content in the aortic roots (n=8-9). F. Pearson r correlation between lesional SMC content and lesional collagen content (r=-0.2, p=0.41). Bar graphs represent ±SEM. *p<0.05.

3.3 The role of hematopoietic cell specific ACKR3 in atherosclerosis

ACKR3 in the vascular endothelium disclosed a significant role for the receptor in endothelium-leukocyte adhesion and thereby immune cell accumulation in atherosclerotic lesions. Furthermore, aEC- as well as SMC-specific deficiency of the receptor led to leukocytosis in *Apoe*$^{-/-}$ mice. In order to find out whether ACKR3 found on immune cells plays a role in atherosclerosis, the receptor was knocked out in the hematopoietic compartment of *Apoe*$^{-/-}$ mice (htACKR3). To this end, bone marrow was extracted from *Uni*$^{Cre+}$*Ackr3*$^{fl/fl}$*Apoe*$^{-/-}$ mice (ubiquitous knockout) as well as *Uni*$^{Cre-}$*Ackr3*$^{fl/fl}$*Apoe*$^{-/-}$ mice and transplanted into into irradiated *Apoe*$^{-/-}$ mice. After 4 weeks of recovery time from the irradiation, mice were treated with tamoxifen to induce hematopoietic deletion of *Ackr3* and then mice were placed on a 12-week WD (Figure 21, A).

3.3.1 Atherosclerotic plaque size analysis

In 12-week WD fed mice, the aortic roots, arches and the aortas were analysed for atherosclerotic lesion size assessment (Figure 21, B). Lesion sizes in the aortic roots between control and htACKR3 deficient mice did not differ (Figure 21, C-D). Similarly, lesions in the aortic arches did not show a significant difference in size between the two groups (Figure 21, D-E). Likewise, lesion size analyses in the aortas showed no difference upon htACKR3 deficiency in atherosclerotic mice. These findings indicate that htACKR3 may not be involved in atherosclerosis.

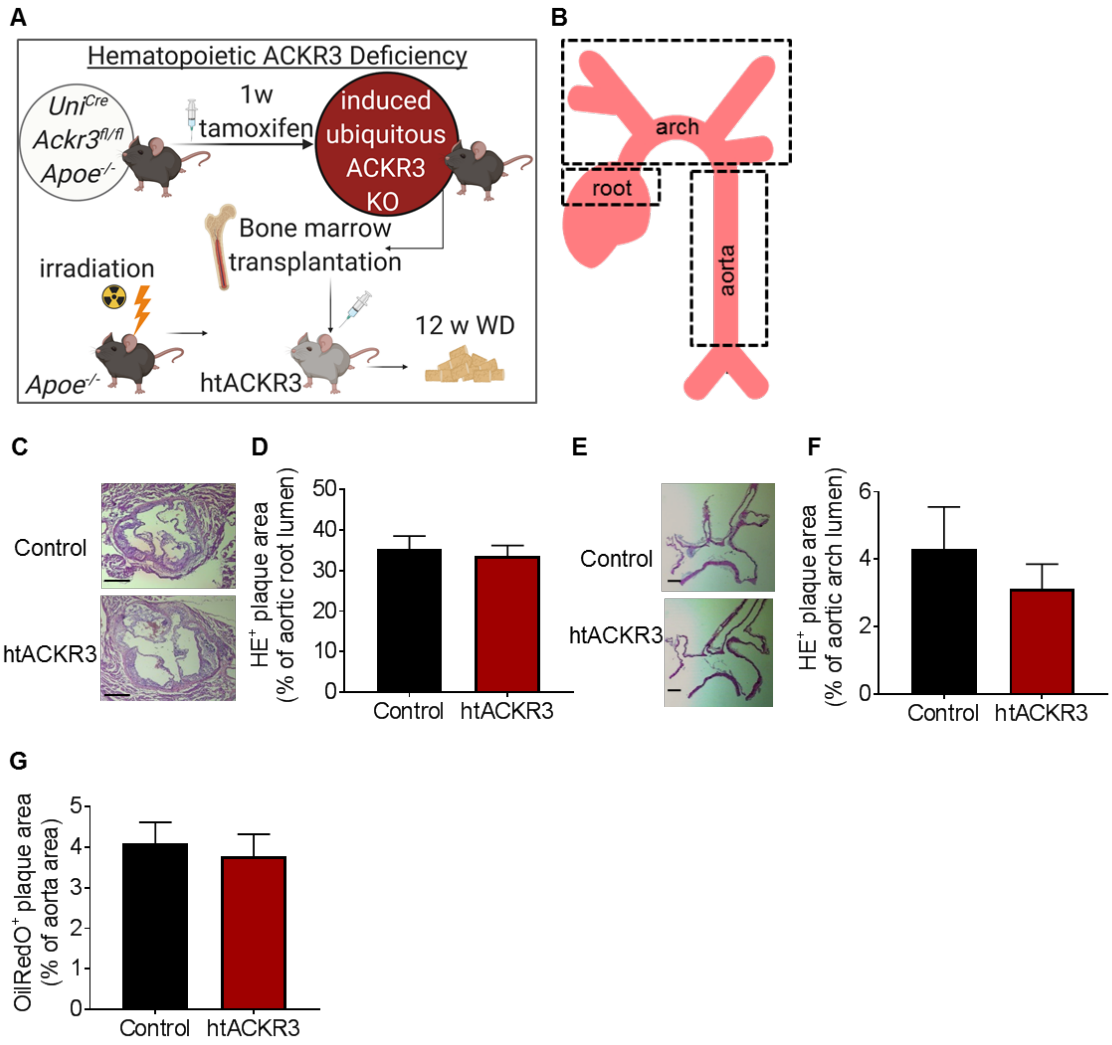

Figure 21: htACKR3 deficiency does not affect atherosclerotic lesion sizes in Apoe$^{-/-}$ mice.

A. Schematic representation of the experimental setup (created with BioRender.com). **B.** Schematic representation of atherosclerosis prone regions assessed for lesion sizes. **C.** Representative images (scale bar: 500 µm) and **D.** quantification of atherosclerotic lesion sizes in the aortic roots (n=14-16). **E.** Representative images (scale bar: 500 µm) and **E.** quantification of atherosclerotic lesion sizes in the aortic arches (n=8-14). **F.** Quantification of atherosclerotic lesion sizes in the abdominal aortas (n=15-16). Bar graphs represent ±SEM.

3.3.2 Assessment of plaque composition and stability

In order to understand whether htACKR3 could be involved in further characteristics of atherosclerotic lesions, we analyzed the cellular composition of the plaques by quantifying the amount of macrophages and SMCs via immunofluorescent stainings. There were no significant differences in either cell type within the lesions (Figure 22, A-C). Furthermore, plaque stability was examined via Mason Trichrome staining exhibiting the collagen content within lesions. Although there was a trend towards a decrease in htACKR3 deficient mice, amounts of lesional collagen did not differ significantly between the two groups (Figure 22, D-E).

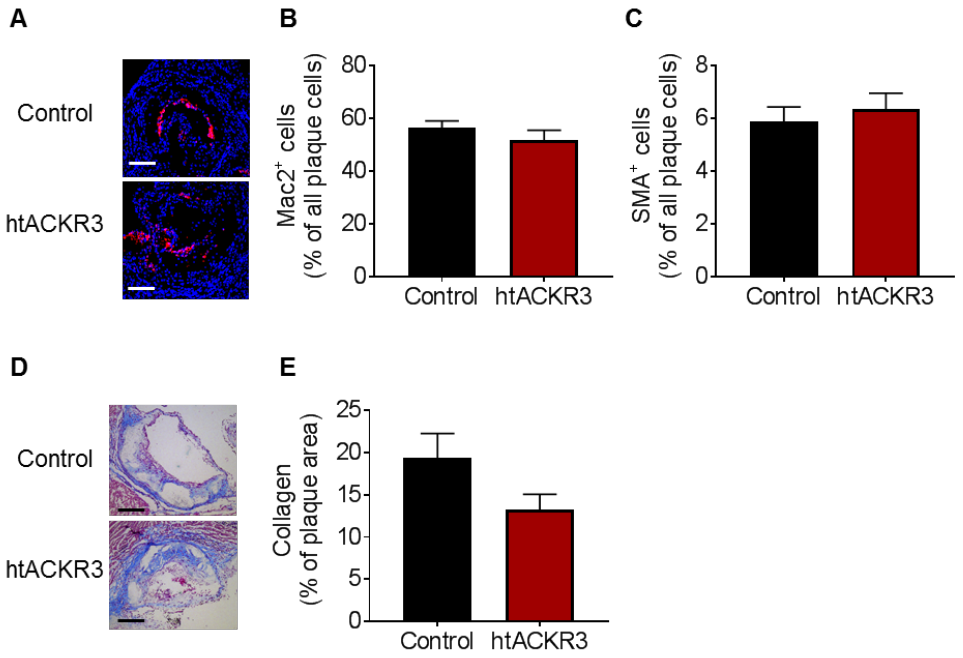

Figure 22: htACKR3 deficiency does not affect atherosclerotic lesion composition or stability in Apoe$^{-/-}$ mice.

A. Representative images (scale bar: 250 µm) and **B.** quantification of macrophage (MAC2+) content in the lesions (n=15). **C.** Quantification of SMC (SMA+) content in the aortic roots (n=15). **D.** Representative images (scale bar: 250 µm) and **E.** quantification of collagen content in the aortic roots (n=15). Bar graphs represent ±SEM.

Moreover, further analyses confirmed that the amount of circulating leukocytes as well as leukocyte subsets, circulating CXCL12 and cholesterol levels did not change between control and htACKR3 deficient mice (Table 9). Altogether, these findings indicate that htACKR3 does not affect atherosclerosis development nor leukocytosis.

3.4 The role of adipocyte and hepatocyte specific ACKR3 in lipid level regulation and atherosclerosis

Few studies focused on the role of ACKR3 in metabolic complications. WD fed mice were reported to upregulate ACKR3 in AT during obesity (Peng et al., 2016), suggesting a role for AT-ACKR3 during hyperlipidemia. Another study revealed that systemic knockout of ACKR3 led to increased cholesterol levels in the sera of *Apoe*$^{-/-}$ mice and the activation of ACKR3 with a synthetic ligand decreased serum lipid levels (Li et al., 2014). These findings were associated with modulated lipid uptake by the AT, suggesting that AT-ACKR3 may be responsible for the regulation of systemic lipid levels. Furthermore, deficiency of ACKR3 in this study was shown to increase neointima formation in atherosclerotic lesions, proposing a beneficial role of ACKR3 dependent lipid level regulation in atherosclerosis. However, the study was performed on a systemic level with regards to ACKR3 manipulation and tissue specific knockout models, such as AT or liver specific studies, have not yet been implemented in order to draw more specific conclusions. AT is a dynamic metabolic tissue that carries out substantial functions, such as lipid storage, glucose and energy balance, as well as thermogenesis (Frayn, 2002). Liver, on the hand, is another important metabolic organ taking part in lipid metabolism in addition to its other important functions, such as aiding metabolism (Kalra et al., 2021). Nonetheless, these organs may become dysfunctional upon excessive build-up of lipids, leading to complications such as metabolic syndrome, which is also associated with atherosclerosis (Benedict & Zhang, 2017; Giorgino, 2009; Liu et al., 2010; Matafome & Seiça, 2017; Oda, 2008; van Greevenbroek et al., 2016; Varghese et al., 2018). Therefore, the role of ACKR3 in terms of lipid accumulation within these organs should be investigated carefully.

In this study, we investigated the impact of adipocyte specific ACKR3 (adACKR3) on atherosclerotic lesions as well as systemic lipid levels. To this end, *Ackr3*$^{fl/fl}$*Apoe*$^{-/-}$ and *Adipoq*^{Cre}*Apoe*$^{-/-}$ were crossed to generate *Adipoq*^{Cre}*Ackr3*$^{fl/fl}$*Apoe*$^{-/-}$ mice, which were then treated with tamoxifen and subsequently subjected to 4 or 12 weeks of WD (Figure 23, A, H).

3.4.1 Assessment of atherosclerosis

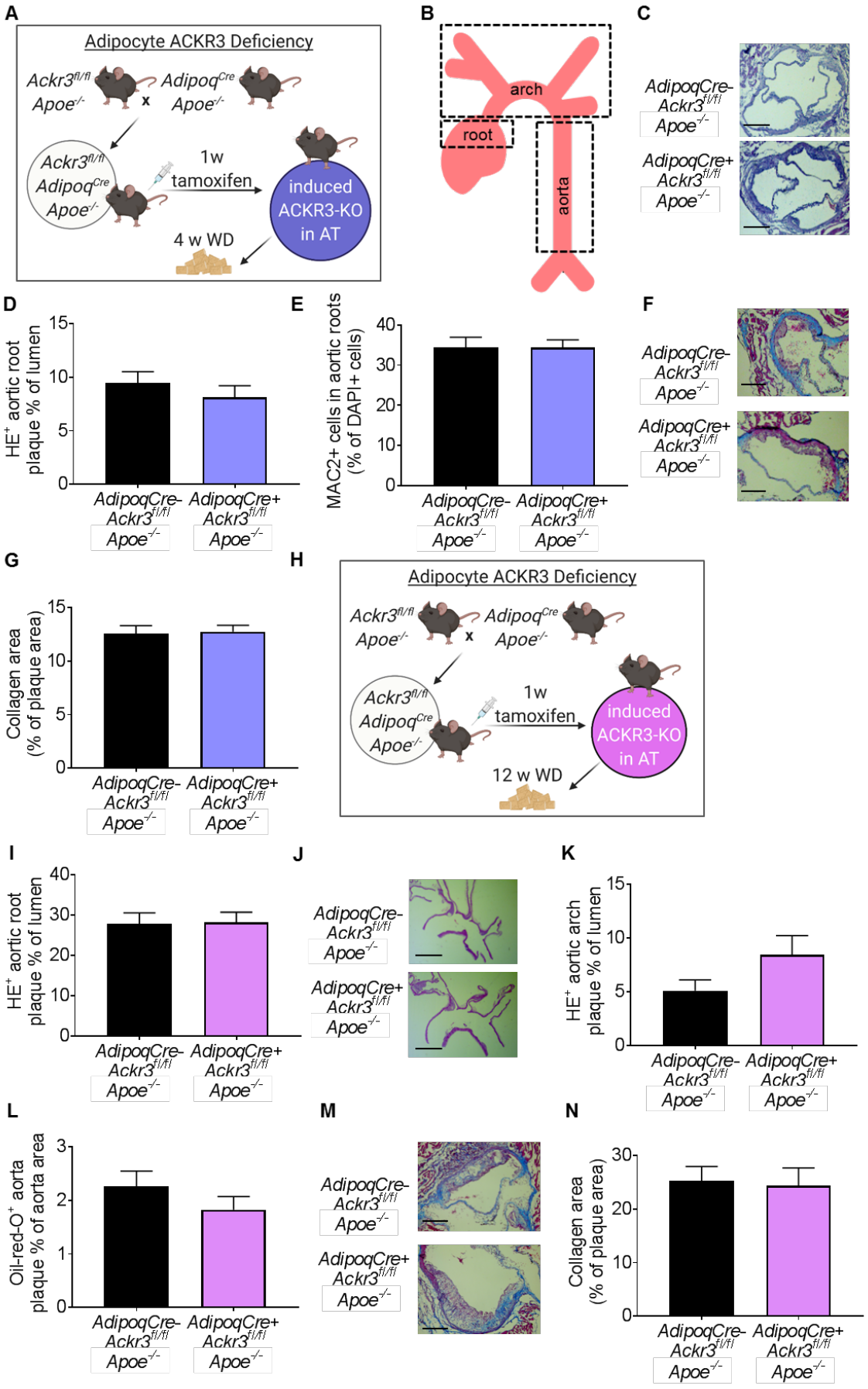

Figure 23: Adipocyte specific ACKR3 does not impact atherosclerotic lesions.

A. Schematic representation of the 4-week experimental setup. **B.** Schematic representation of atherosclerosis prone regions assessed for lesion sizes (created with BioRender.com). **C.** Representative images (scale bar: 500 µm) and **D.** quantification of atherosclerotic lesion sizes in the aortic roots (n=14). **E.** Quantification of macrophage (MAC2+) content in the lesions (n=10). **F.** Representative images (scale bar: 250 µm) and **G.** quantification of collagen content in the aortic roots (n=13-16). **H.** Schematic representation of the 12-week experimental setup (created with BioRender.com). **I.** Quantification of atherosclerotic lesion sizes in the aortic roots (n=14). **J.** Representative images (scale bar: 250 µm) and **K.** quantification of atherosclerotic lesion sizes in the aortic arches (n=14). **L.** Quantification of atherosclerotic lesion sizes in the aortas (n=12-14). **M.** Representative images (scale bar: 250 µm) and **N.** quantification of collagen content in the aortic roots (n=13-14). Bar graphs represent ±SEM.

Mice with adACKR3 deficiency were examined for atherosclerotic lesion sizes in the aortic roots after 4 weeks of WD. H&E stained lesions in the roots did not show a significant difference in size between the control and the adACKR3 deficient mice (Figure 23, C-D). Further analysis of the plaques also did not reveal any differences in the macrophage (Figure 23, E) or collagen content in the lesions (Figure 23, F-G). General characteristics of the mice, such as leukocyte and leukocyte subset counts in circulation, as well as plasma CXCL12 levels were not altered either (Table 10). In order to understand whether a longer WD could unveil a potential impact of adACKR3 on atherosclerotic lesions, mice were fed with 12 weeks of WD. Atherosclerotic lesions in the aortic roots (Figure 23, I), aortic arches (Figure 23, J-K) and aortas (Figure 23, L) did not show any significant changes in size. Furthermore, plaque stability characterization also did not indicate any lesional collagen differences between the control and adACKR3 deficient mice (Figure 23, M-N). Altogether, these findings suggest that adACKR3 is not involved in atherosclerosis development.

3.4.2 Examination of lipid levels

In order to understand whether ACKR3 in adipocytes was involved in regulating lipid levels, as indicated in the literature based on systemic studies, we examined lipid levels in control and adACKR3 deficient mice. Adipocyte deficiency of ACKR3 revealed decreased triglyceride as well as cholesterol levels in the AT of *Apoe*$^{-/-}$ mice (Figure 24, A-B).

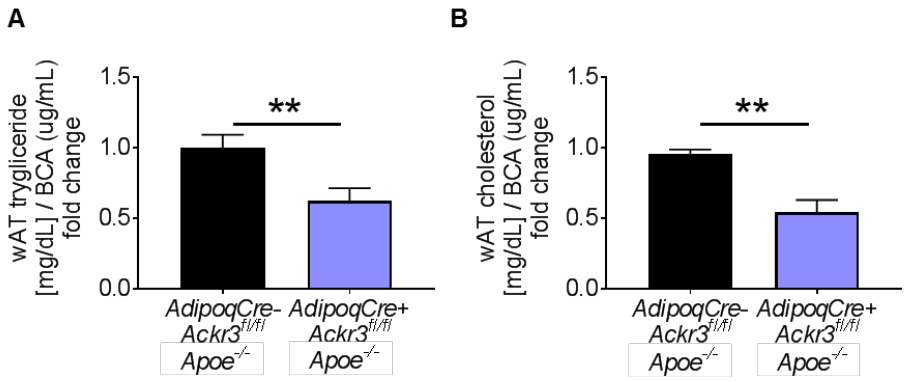

Figure 24: Adipocyte specific ACKR3 deficiency decreases lipid levels in the adipose tissue of Apoe$^{-/-}$ mice.

A. Total triglyceride (n=12-14) and **B.** total cholesterol (n=9-10) levels in visceral white AT samples normalized to total protein levels. Bar graphs represent ±SEM. **p<0.01.

Following these findings, we sought to investigate how the lipid levels were affected in the circulation of the mice. Surprisingly, despite a decrease in the AT lipid levels, there were no differences in triglyceride (Figure 25, A) or in cholesterol levels in plasma samples (Figure 25, B). In order to expose possible changes in the circulating lipoprotein levels, we performed fast-performance liquid chromatography to quantify the levels of lipoprotein fractions in the plasma samples. There were no differences observed in the levels of vLDL (Figure 25, D), LDL (Figure 25, E) or HDL (Figure 25, F) between the two groups.

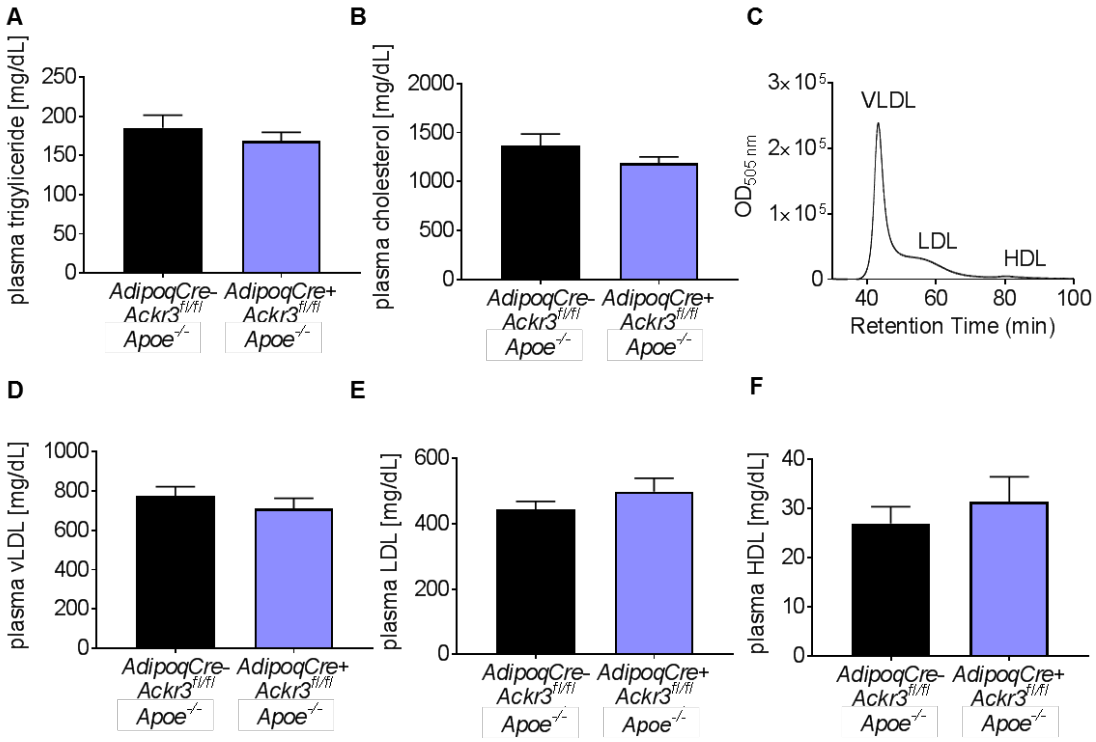

Figure 25: Adipocyte specific ACKR3 deficiency does not impact plasma lipid levels of Apoe$^{-/-}$ mice.

A. Total triglyceride and **B.** total cholesterol levels in the plasma samples (n=13-14). **C.** Representative HPLC chromatogram of plasma lipoprotein fractions (VLDL, LDL and HDL). Plasma levels of **D.** VLDL, **E.** LDL and **F.** HDL levels (n=12-14). Bar graphs represent ±SEM.

In addition, lipid levels were quantified in liver samples to inspect the possible impact of altered AT lipid levels on hepatic lipids. Assessment of liver samples confirmed that adACKR3 deficiency did not impact hepatic lipid levels, characterized by triglyceride (Figure 26, A) and cholesterol (Figure 26, B) levels in the tissue.

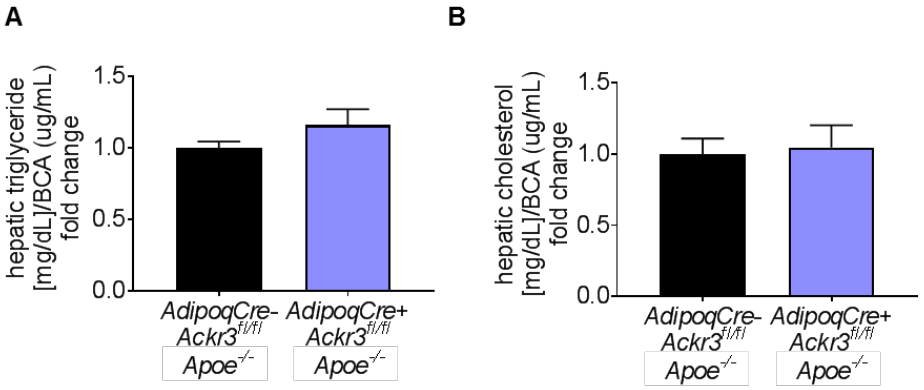

Figure 26: Adipocyte specific ACKR3 deficiency does not impact hepatic lipid levels of Apoe$^{-/-}$ mice.

A. Total triglyceride (n=12-14) and **B.** total cholesterol (n=9-10) levels in the liver samples normalized to total protein levels. Bar graphs represent ±SEM.

3.4.3 Lipid receptor expression in adipose tissue

Analyses in control and adACKR3 deficient mice suggest a local impact of adACKR3 on lipid metabolism as the lipid levels were only affected in the AT of mice. Next, we assessed the expression of lipid receptors in the AT samples in order to understand how adACKR3 deficiency altered AT lipid levels. To do so, RNA was extracted from the AT samples and the expression of well-known receptors involved in lipid metabolism was measured by means of ddPCR analysis.

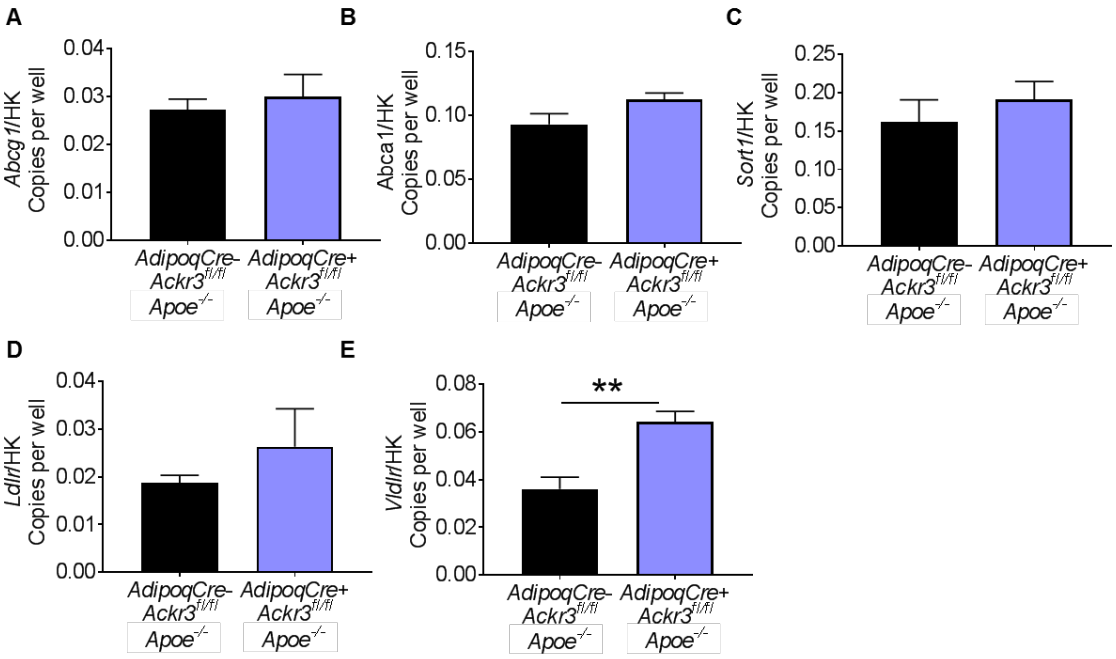

Figure 27: Expression of lipid receptors in AT samples.

Relative gene expression of **A.** *Abcg1,* **B.** *Abca1,* **C** *Sort1*, **D.** *Ldlr* and **D.** *Vldlr* to housekeeping genes (HK) (*Gapdh* or *18S*) analyzed on ddPCR (n=4-7). Bar graphs represent ±SEM. **p<0.01.

No significant differences were observed in the expression of *Abcg1, Abca1, Ldlr* and *Sort1* between the two groups (Figure 27, A-D). Interestingly, *Vldlr* expression was significantly higher in the adACKR3 deficient mice reflecting a possible compensatory mechanism (Figure 27, E).

In order to evaluate further potential mechanisms involved in the regulation of lipid levels in AT samples, the expression of *Angtpl4* and *Ppar-γ* was analyzed via ddPCR. Angptl4 and PPAR-γ are play a key role in triglyceride metabolism as they negatively modulate the activity of lipoprotein lipase (LPL), which is responsible for lipid uptake into the tissue (Ben-Zvi et al., 2015; Sukonina et al., 2006). As a result, Angptl4 and PPAR-γ limit lipid uptake into AT by limiting LPL activity. Expression of both *Angptl4* and *Ppar-γ* was found to be significantly upregulated in the AT of adACKR3 deficient mice compared to control mice (Figure 28, A-B). In line with these findings, PPAR-γ phosphorylation was higher in the AT of adACKR3 deficient mice (Figure 28, C-D). Further advancing these findings, LPL activity in the AT samples correlated significantly with triglyceride levels in the AT (Figure 28, E), indicating that the observed lipid level changes in the AT may be due to the modulation of LPL activity as also suggested by the increase of *Angptl4* and *Ppar-γ* in the tissue.

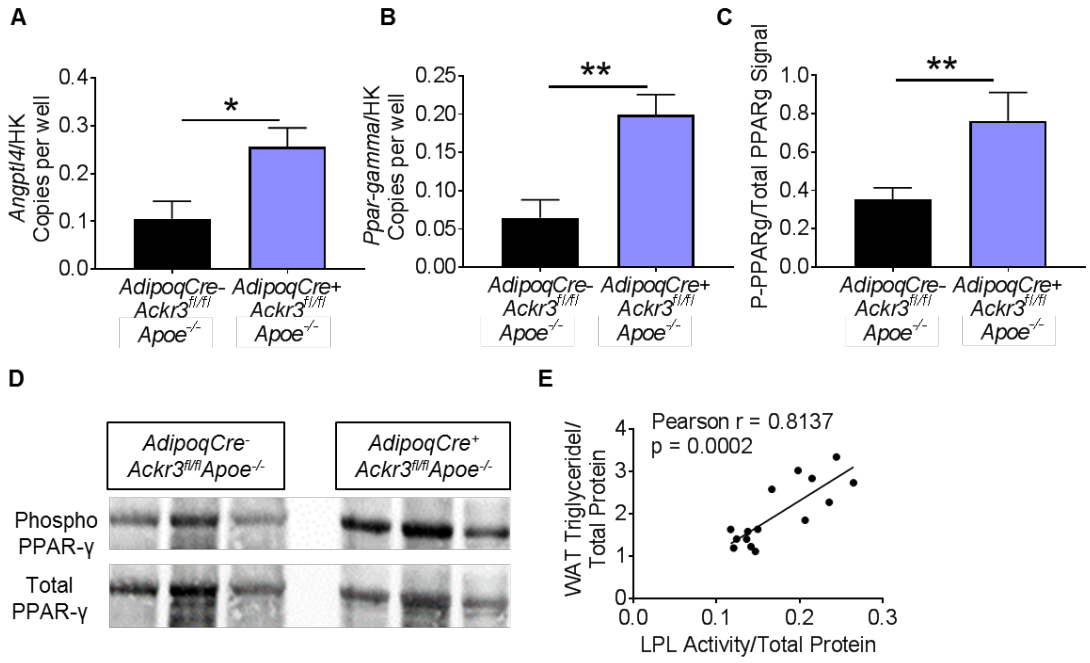

Figure 28: Adipocyte specific ACKR3 modulates AT lipid levels via Angptl4 and PPAR-γ.

Relative gene expression of **A.** *Angptl4* and **B.** *Pparg* to housekeeping genes (HK) (*Gapdh or 18S*) analyzed on ddPCR (all n=4-7). **C.** Quantification of the western blot analysis of phospho-PPAR-γ normalized to total PPAR-γ on Image-J Software (n=4). **D.** Representative western blot images of phospho-PPAR-γ and total PPAR-γ protein expression in AT samples. **E.** Pearson r correlation between AT total triglyceride content and AT LPL activity (r=0.8137, p=0.0002), (n=15). Bar graphs represent ±SEM. *p<0.05, **p<0.01.

3.4.4 The impact of adACKR3 on adipocytes

Altogether, these findings indicate that adACKR3 indeed regulates AT lipid levels by upregulating Angptl4 and PPAR-γ which in return downregulate LPL activity (Figure 29). Nonetheless, adACKR3 deficiency was not enough to alter blood lipid levels in our mouse model and no potential consequent effects on atherosclerosis were observed.

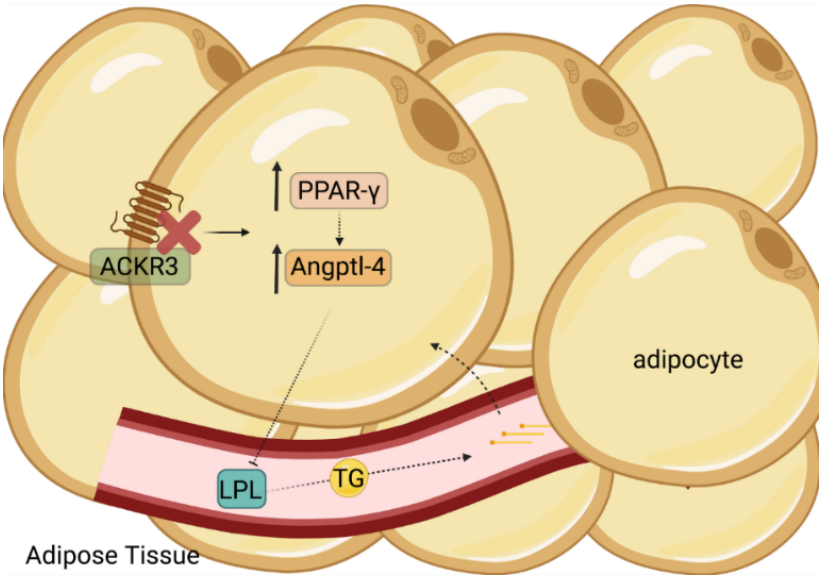

Figure 29: The impact of adACKR3 on adipocytes.

Adipocyte specific ACKR3 decreases AT lipid levels by upregulating Angptl4 and PPAR-γ, which in turn inhibit LPL activity and thereby limit lipid uptake into the adipocytes. Created with BioRender.com.

3.4.5 The role of hepatocyte specific ACKR3

In the ACKR3 study reported by Li et al., lipid uptake by the liver was not affected upon synthetic ligand treatment for ACKR3 (Li et al., 2014). We also did not observe any differences in hepatic lipid levels upon adACKR3 knockout. However, the liver itself is a central organ in lipid metabolism and because adACKR3 exhibited tissue specific, local changes in lipid levels, we investigated whether hepatocyte specific ACKR3 (hACKR3) could impact liver lipid levels. To this end, hepatocyte specific knockout of ACKR3 was induced by adeno-associated virus mediated expression of iCre recombinase under the Albumin promoter in *Ackr3*$^{fl/fl}$*Apoe*$^{-/-}$ mice (Figure 30, A). hACKR3 deficiency did not show any differences in triglyceride or cholesterol levels in the liver samples of *Apoe*$^{-/-}$ mice (Figure 30, B-C). Similarly, lipid levels did not change between the two genotypes in the AT (Figure 30, D-E) and in the plasma samples (Figure 30, F-G). Counts of leukocytes and leukocyte subsets in the blood via flow cytometry analysis also did not reveal any changes upon hACKR3 deficiency in mice (Table 11). Furthermore, aortic root lesion sizes upon 4 weeks WD did not differ between control and hACKR3 deficient mice (Figure 30, H-I), indicating that hACKR3 is not involved in lipid metabolism or in atherosclerosis.

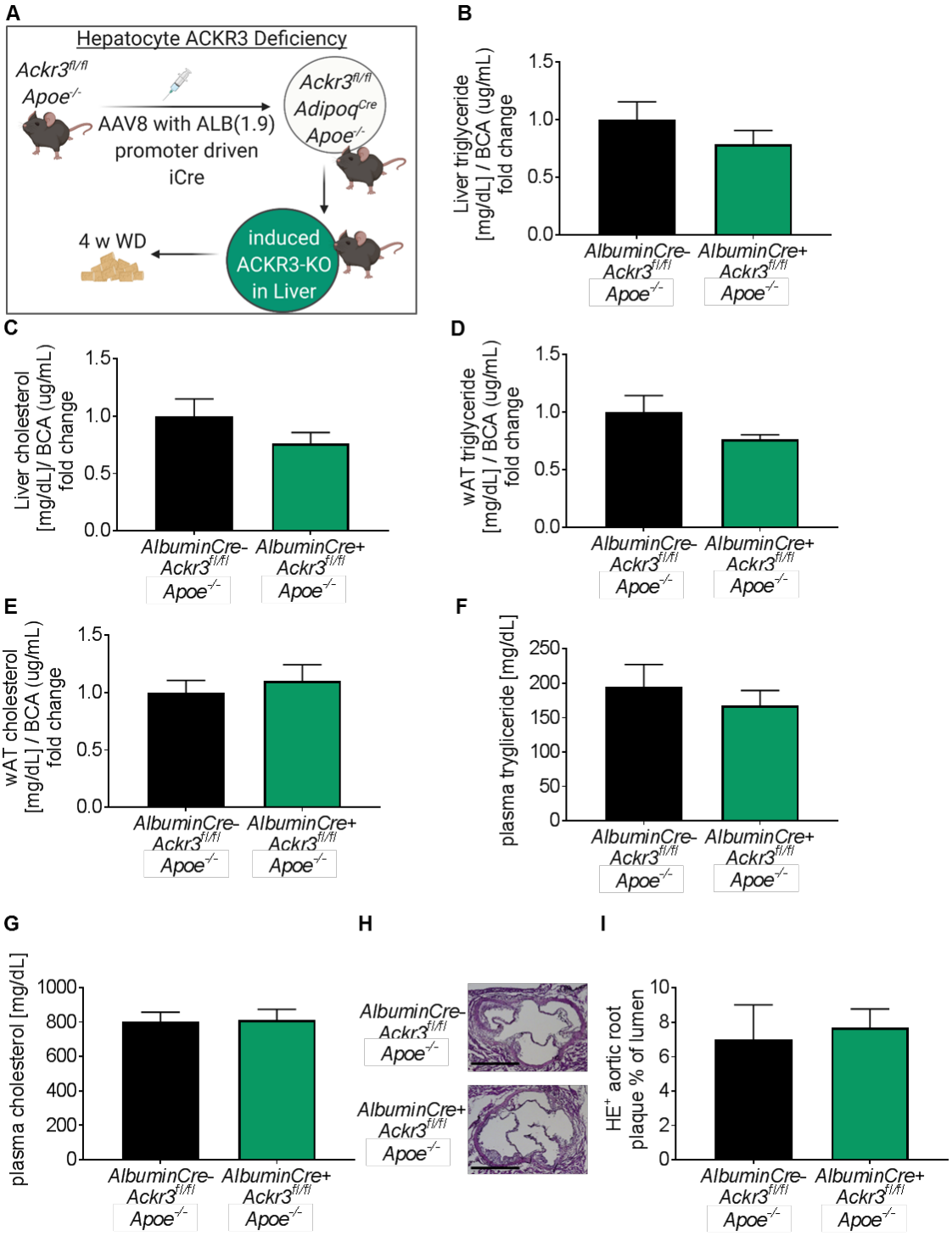

Figure 30: Hepatocyte specific ACKR3 deficiency does not affect lipid levels or atherosclerosis.

A. Schematic representation of the 4-week experimental setup (created with BioRender.com). **B.** Total triglyceride and **C.** total cholesterol levels in the liver samples normalized to total protein levels (n=11-12). **D.** Total triglyceride and **E.** total cholesterol levels in the visceral white AT samples normalized to total protein levels (n=9-10). **F.** Total triglyceride and **G.** total cholesterol levels in the plasma samples (n=10-11). **H.** Representative images (scale bar: 500 µm) and **I.** quantification of atherosclerotic lesion sizes in the aortic roots (n=11-12). Bar graphs represent ±SEM.

4. Summary

Atherosclerosis is the underlying pathology of CVDs which are recognized as the major deadly diseases worldwide. The chemokine system plays various significant roles in the progression of atherosclerosis and therefore establishes a potential therapeutic target for the treatment of atherosclerosis. ACKR3 is the alternative receptor of the atherosclerotic chemokine CXCL12, although there is a significant lack of knowledge in terms of the roles of ACKR3 in atherosclerosis. In this thesis, ACKR3 was studied in atherosclerotic mouse models. In doing so, the impact of ACKR3 was characterized during atherosclerosis with regards to its cell specific roles. To this end, the cre-lox recombination system was utilized to allow cell specific deletion of *Ackr3* in mice developing atherosclerosis in response to a diet rich in lipids. The study investigated ACKR3 in arterial endothelial cells, SMCs, hematopoietic cells, adipocytes and hepatocytes. Intriguingly, endothelial cell deficiency of ACKR3 in arteries protected mice significantly against atherosclerotic lesion development. This was attributed to the role of ACKR3 in endothelial cell adhesion, which plays a significant role in arterial immune cell adhesion followed by transmigration. Surprisingly, the same effect was not observed when ACKR3 was knocked out in the hematopoietic compartment, suggesting an endothelial cell specific role of ACKR3 in cell adhesion. Furthermore, ACKR3 in SMCs did not affect atherosclerosis other than lesional collagen content, pointing towards a role of SMC specific ACKR3 in plaque stabilization. ACKR3 in adipocytes controlled AT lipid levels, however this did not affect circulating lipid levels and therefore did not have an impact on atherosclerosis. Hepatic ACKR3 was not involved in atherosclerosis. In summary, this study provides detailed analysis of the impact of ACKR3 in certain cell types during atherosclerosis and establishes that ACKR3 expressed in arterial endothelium is heavily involved in diet induced atherosclerosis.

5. Discussion

The aim of this study was to elucidate cell specific roles of ACKR3 in atherosclerosis. To this end, atherosclerotic mouse models were used in order to conditionally knock the receptor out in specific cell types. Below, the findings of this research will be discussed in three chapters; vascular, hematopoietic and organ specific ACKR3 in atherosclerosis.

5.1 The role of vascular ACKR3 in atherosclerosis

The role of ACKR3 in the vascular compartment during atherosclerosis was studied in two main arterial cell types, ECs and SMCs in addition to the hematopoietic compartment.

5.1.1 Arterial endothelial ACKR3 is a novel driver of atherosclerosis

The findings of this study established that the deficiency of aEC in hyperlipidemic mice partially protected against atherosclerosis. The protective role of aEC ACKR3 in atherosclerosis was characterized by attenuated plaque sizes and reduced macrophage accumulation within plaques. In addition, plaque stability was increased, as evident by a decrease in necrotic core content and an increase in collagen content within the lesions. Altogether, these data reveal a pro-atherosclerotic role of endothelial ACKR3.

A key event driving plaque growth during atherosclerosis is the entry of circulating immune cells into the arterial intima through the inflamed endothelium (Blankenberg et al., 2003; Gerhardt & Ley, 2015; Maguire et al., 2019). This phenomenon stimulates accumulation of macrophage foam cells in the sub-endothelial space of arteries, which then exacerbates fatty streak formation (Libby et al., 1996; Maguire et al., 2019; Schwartz et al., 1991). Interfering with this key step can offer a therapeutic potential in the treatment and management of atherosclerosis. As aEC-ACKR3 deficiency diminished macrophage content within the lesions, we sought to investigate its role in leukocyte infiltration into atherosclerotic lesions. Previous studies of other disease models established a role for ACKR3 in immune cell infiltration. For example, knockdown of ACKR3 in the lungs of mice with an allergic airway inflammation reduced immune cell infiltration into the lungs (Chang et al., 2018). Furthermore, another study employing a multiple sclerosis mouse model revealed that endothelial ACKR3 expression was augmented at the CNS vasculature under inflammatory conditions and the blockade of ACKR3 with an antagonist attenuated leukocyte infiltration into the CNS parenchyma (Cruz-Orengo et al., 2011). In line with these findings, our study also revealed that aEC-ACKR3 regulates entry of blood borne leukocytes into atherosclerotic lesions, confirming that ACKR3 plays a significant role in immune cell extravasation.

Next, we sought to understand how aEC-ACKR3 regulates the trans-endothelial entry of leukocytes. The vascular wall is made up of an endothelial lining and its integrity is a crucial factor that maintains the barrier between the arterial intima and the peripheral blood (Mazurek et al., 2017). Loss of endothelial integrity can lead to the formation of gaps between the endothelial cells (inter-endothelial gaps) and thereby allow leakage of peripheral substances (Ochoa & Stevens, 2012).

For example, in the case of atherosclerosis, a leaky phenotype of the arterial endothelium can permit increased entry of immune cells into the lesions. Chemokines and chemokine receptors have been shown to be involved in regulating endothelial permeability. Previously, our research group established that the chemokine receptor CXCR4 expressed by the arterial endothelium was responsible for regulating the endothelial barrier function in mouse vessels (Döring et al., 2017). Furthermore, the chemokine CCL2 and its receptor CCR2 were shown to participate in the blood brain barrier permeability *in vitro* using a co-culture of astrocytes and brain endothelial cells (Dimitrijevic et al., 2006). We speculated that the modification of the arterial endothelial cells through an endothelial receptor knockout (ACKR3) may have played a role in the permeability of the arterial endothelium. However, surprisingly the EVB assay revealed that aEC-ACKR3 did not play a role in the maintenance of the vascular integrity. Another key mechanism that could be altered through aEC-ACKR3 knockout is the adhesive properties of the endothelial cells. Adhesion of immune cells onto the vascular wall is a critical step during transmigration of the immune cells into the sub-endothelial space (Blankenberg et al., 2003; Desideri & Ferri, 2005). Previous *in vitro* studies using endothelial progenitor cells (EPCs) and cancer cells established that ACKR3 plays a significant role in cell adhesion (Dai et al., 2011; Gentilini et al., 2019; Ma et al., 2016). An *in vitro* study using EPCs established that anti-ACKR3 antibody treatment interfered with EPC adhesion onto extracellular matrix components as well as human umbilical vein endothelial cell (HUVEC) monolayer (Dai et al., 2011). This was again confirmed in another study, in which ACKR3 transfected activated endothelial cells (via TNF-α and IL-1ß stimulation) adhered markedly less to a HUVEC monolayer compared to control activated endothelial cells (Burns et al., 2006). However, the role of ACKR3 in cell adhesion has never been confirmed in *in-vivo* disease models before, especially in the context of atherosclerosis. Evident by the *ex-vivo* perfusion assay, as well as the intravital microscopy; adhesion of the mouse immune cells onto aEC-ACKR3 deficient arteries was very significantly reduced. This finding confirms that ACKR3 indeed regulates endothelial adhesion. Intravital microscopy allowed testing of three different subsets of immune cells; myeloid cells ($CD11b^+$), classical monocytes ($Ly6C^+$) and neutrophils($Ly6G^+$). Adhesion of all three immune cell types decreased very significantly and showed no cell type dependent difference. These findings are therefore novel and robustly confirm that aEC-ACKR3 is a strong regulator of endothelial adhesion. In conjunction with the previous findings, it is safe to conclude that the elimination of aEC-ACKR3 allows protection against atherosclerotic lesion development by curbing immune cell adhesion and thereby infiltration into the arteries. Thus, targeting ACKR3 in the arterial endothelial cells holds great value and potential for further investigation of therapeutic approaches; not only in the treatment of atherosclerosis but also of other disease models, in which immune cell adhesion and infiltration can be a key target. Nevertheless, there are some aspects that need to be addressed first. For example, aEC-ACKR3 deficiency mediated leukocytosis is not yet understood. This could be due to a number of reasons, such as regulation of haematopoiesis or rise in chemotactic ligand gradients as a result of loss of ACKR3 mediated scavenging activity. Although, the latter seems rather unlikely due to the fact that the circulating and bone marrow levels of CXCL12 did not change in the aEC-ACKR3 knockout. This suggests that aEC-ACKR3 might not scavenge and form CXCL12 gradients. Another possibility is that the

arterial ACKR3 is involved in the homing and recruitment of the immune cells and given its role in cell adhesion it may be possible that this is a functional role of ACKR3 in the arteries. Furthermore, there is a possibility that the immune cells may have accumulated in the circulation due to the restriction of trans-endothelial migration mediated by the loss of aEC-ACKR3. The exact mechanism behind leucocytosis driven by loss of aEC-ACKR3 needs to be elucidated in further studies.

Additional analyses to expand the understanding of ACKR3 driven endothelial adhesion revealed that ACKR3 deficiency decreases the expression of crucial adhesion molecules, such as ICAM, VCAM and E-Selectin, in inflamed endothelial cells. This impact of ACKR3 was observed concomitant with a downregulation of the key mediators of the MAPK pathway, such as Akt and ERK1/2, as well as NF-kB. MAPK and NF-kB pathways are well described inflammatory pathways implicated in various disease settings (X. L. Chen et al., 2005; Choi et al., 2010; Dragoni et al., 2017; Lin et al., 2014; Tamanini et al., 2003). ERK/NF-kB signaling was reported to activate ICAM and VCAM expression in endothelial cells and NF-kB is a well-known transcription factor of endothelial adhesion molecules (Liu et al., 2017; Zhong et al., 2012). These observations were accompanied by the upregulation of PPAR-γ, which negatively regulates and suppresses NF-kB (Remels et al., 2009; Scirpo et al., 2015; Sung et al., 2006). These findings were in line with previous studies that disclosed the ability of ACKR3 to signal through ß-arrestin 2 mediated MAPK pathway, including Akt and ERK1/2 (Alampour-Rajabi et al., 2015; Chatterjee et al., 2014; Ishizuka et al., 2021; Lefkowitz & Shenoy, 2005; Li et al., 2019; Rafiei et al., 2019). Former studies investigating inflammatory disease models in mice, such as acute pulmonary and acute peritoneal inflammation, also reported that ACKR3 inhibition reduced NF-kB phosphorylation (Ngamsri et al., 2020; Ngamsri et al., 2017). Apart from suppressing NF-kB, PPAR-γ was also shown to suppress ICAM and VCAM expression in endothelial cells, which are downstream targets of NF-kB (Pasceri et al., 2000; Sasaki et al., 2005). Thus, ACKR3 silencing dependent downregulation of MAPK and NF-kB and upregulation of PPAR-γ are in line with the observations of downregulated adhesion molecule expression. In addition, we and others previously also showed that ACKR3 deficiency can upregulate PPAR-γ in the AT of mice (Gencer, Döring, et al., 2021; Li et al., 2014). The fact that this observation is also true in endothelial cells indicates a general effect of ACKR3 on PPAR-γ, although the mechanism is not yet understood. Remarkably, however, PPAR-γ and NF-kB were also revealed to affect ACKR3 expression in turn, implying a potential feedback mechanism between these molecules (Shi et al., 2020; Tarnowski et al., 2010; Zhao et al., 2015). For example, a study revealed that pioglitazone (an anti-diabetic medication) treatment lead to suppression of ACKR3 expression in differentiated macrophages via the activation of PPAR-γ (Zhao et al., 2015). Even more interestingly, the study further looked into the effects of pioglitazone treatment in patients who underwent surgical carotid endarterectomy. After 2 months of treatment, patients who received pioglitazone had significantly less ACKR3 as well as ACKR3 ligand (CXCL11 and CXCL12) expression in their atherosclerotic lesions compared to that of patients without pioglitazone treatment. PPAR-γ expression, on the other hand, was increased significantly in pioglitazone treated patients. Furthermore, the authors did not observe any differences in CXCR4 or CXCR3 expression (Zhao et al., 2015). This is an intriguing finding because

PPAR-γ activation via agonist treatments, such as rosiglitazone and GW7845, was shown to restrict atherosclerosis development in mice (Levi et al., 2003; Li et al., 2000). Taking these findings, as well as our findings into account, activation of PPAR-γ and inhibition of ACKR3 may offer therapeutic potential in atherosclerosis treatment. Therefore, the relationship and mechanism between PPAR-γ and ACKR3 as well as the effects of PPAR-γ agonists on ACKR3 need to be elucidated. Since pioglitazone treatment did not affect CXCR4 or CXCR3 expression in the study by Zhao et al. (Zhao et al., 2015), the effect of PPAR-γ agonists may have the potential to be specific to ACKR3, which would then also overcome the problem of the complex interaction between ACKR3 and the alternative receptors of ACKR3 ligands.

Interestingly, aEC-ACKR3 deficiency did not change the levels of the main ACKR3 ligand, CXCL12, in the circulation or in the bone marrow of *Apoe*$^{-/-}$ mice. ACKR3 was previously considered as a non-signaling, decoy receptor for its ligands CXCL11 and CXCL12 (Boldajipour et al., 2008; Naumann et al., 2010). This characterization of ACKR3 may be true depending on the animal model and disease model. In our study, however, ACKR3 did not act as a scavenger receptor, on the contrary, it proved to be a functional, signalling receptor. A limitation of our study is the fact that C57BL/6 (B6) mice do not express the other ACKR3 ligand, CXCL11 (Sierro et al., 2007). Therefore, our observations in mice cannot account for possible roles of CXCL11 in atherosclerosis. The *in vivo* effects of ACKR3 in the presence of CXCL11 can be studied using other mouse models expressing CXCL11, such as Swiss Webster mice (Widney et al., 2000). It is important to understand how the presence of CXCL11 might affect the signalling behaviour of ACKR3 *in vivo* and how ACKR3 may in turn affect the CXCL11-CXCR3 axis. CXCR3 was suggested to promote atherosclerosis in hyperlipidemic mice, as its antagonism restricted infiltration of CXCR3+ effector cells into atherosclerotic lesions (van Wanrooij et al., 2008). Furthermore, MIF is also reported to bind ACKR3 (Wang et al., 2018). MIF is a pro-inflammatory ligand and it was reported to enhance adhesion molecule expression in endothelial cells, which increased leukocyte adhesion onto endothelium (Cheng et al., 2010). Of note, plasma MIF levels in aEC-ACKR3 deficient mice exhibited a tendency towards a decrease, however, there were no statistically significant changes. Although this decrease was insignificant, the possibility that MIF may be involved in the observed ACKR3 dependent adhesion effects on the endothelial cells cannot be ruled out. Moreover, ligands of ACKR3 are reported to bind other receptors, for example CXCL12 is also a ligand for CXCR4 and MIF is also a ligand for CXCR4, CD74 as well as CXCR2 (Wang et al., 2018). These receptors and ligands also play various roles in the context of atherosclerosis, especially with regards to their cell-specific roles. For example, arterial endothelial CXCR4 was shown to play an atheroprotective role by sustaining the barrier function of the arterial endothelium (Döring et al., 2017). The atheroprotective role of CXCR4 was also revealed in B cells, which coincided with a significant decrease in immunoglobulin M levels in the plasma samples of mice (Doring et al., 2020). On the other hand, MIF is established to be a highly inflammatory atypical chemokine with pro-atherosclerotic roles (Bernhagen et al., 2007; Döring et al., 2014; Wu et al., 2017). CXCR2, an alternative receptor of MIF, also mediates atherogenic signaling via MIF in addition to its pro-atherosclerotic immune cell recruitment roles via its other ligand CXCL1 (Gencer, Evans, et al., 2021; Krammer et al., 2021). As a result, these receptor-ligand interactions

are very complex, and it is difficult to de-couple their effects. Ligand interactions of ACKR3 remain to be studied in further detail. Despite no significant changes in terms of amount, we noticed that the CXCL12 levels in the plasma correlated significantly with atherosclerotic lesion sizes in our control mice, implying that circulating CXCL12 may be associated with lesion development. This observation is in line with our recent publication revealing that circulating CXCL12 released by endothelial cells drives atherosclerosis in hyperlipidemic mice (Döring et al., 2019). It is important to note, that this conclusion was based on an endothelial knockout of the chemokine CXCL12, which decreased the levels of circulating CXCL12 in mice and lead to a decrease in atherosclerotic lesion sizes (Döring et al., 2019). This study, on the other hand, investigates the endothelial knockout of the receptor ACKR3. Remarkably, the correlation between circulating CXCL12 levels and the lesion sizes observed in our control mice was lost in aEC-ACKR3 deficient mice, suggesting that the interaction between circulating CXCL12 and endothelial receptor ACKR3 may be driving atherosclerosis. Although, the study by Döring et al. (Döring et al., 2019) suggests that the endothelial knockout of CXCL12 significantly decreases circulating levels of CXCL12, in our study we cannot state whether or not the circulating CXCL12 is mainly derived from the endothelial cells. Previously, our research group also established that the alternate receptor of CXCL12, CXCR4, plays an atheroprotective role in endothelial cells (Döring et al., 2017). Although the results do not overlap fully, significant contrasting effects between endothelial ACKR3 and endothelial CXCR4 were observed. Most importantly, in sharp contrast to ACKR3, CXCR4 deficiency in arterial endothelial cells of the atherosclerotic mice revealed increased ICAM+ cells in the atherosclerotic endothelium and accordingly, leukocyte adhesion onto the CXCR4 deficient endothelium was increased. These findings may be indicating that there might be changes of the signaling behavior of CXCL12 depending on the availability of the receptors. In support of this notion, it is important to note that the affinity between ACKR3 and CXCL12 is reported to be higher than that of CXCR4 and CXCL12 (Balabanian et al., 2005). One possibility is that CXCL12 signaling may be skewed towards ACKR3 when the receptor is present and this signaling preference might shift to CXCR4 in the absence of ACKR3, which may not be reflected in the quantities of CXCL12. It is not clear whether or not this may have happened in our study as the signaling activity of CXCL12/CXCR4 *in vivo* cannot be solely assessed by the expression levels of the receptor or the abundance of the ligand. One approach to evaluate whether or not the observed atheroprotective impact of aEC-ACKR3 deficiency in our study could be a result of CXCL12/CXCR4 signaling may be to treat aEC-ACKR3 deficient mice with CXCR4 inhibitors. If CXCR4 inhibition during aEC-ACKR3 deficiency reveals significant differences to aEC-ACKR3 deficient mice in terms of atheroprotection, then the involvement of CXCR4 in the absence of ACKR3 may be considered. These theories need to be studied in detail in further studies in order to draw more robust conclusions with regards to the ACKR3-CXCL12-CXCR4 axis.

5.1.2 Smooth muscle cell specific ACKR3 in atherosclerosis

Apart from ECs, SMCs make up another main cell type in the vascular system and are important in the onset and development of atherosclerotic disease of the arteries (Bennett et al., 2016; Rafieian-Kopaei et al., 2014; Schwartz et al., 1991). Deficiency of ACKR3 in the SMCs of hyperlipidemic mice did not reveal any impact on atherosclerotic lesion sizes. Further characterization of the plaques also did not show any changes in the cell composition of the lesions. Interestingly, however, lesional collagen content was significantly increased in SMC-ACKR3 mice compared to control mice. These results indicate that SMC specific ACKR3 does not significantly affect atherosclerosis, although its deficiency may play a role in the mechanical stabilization of the plaques through increased collagen content. This type of mechanical stabilization may protect the plaques from rupture. Nonetheless, plaque rupture is not a common feature in *Apoe*$^{-/-}$ mice and extremely long fat feeding, such as 37 to 59 weeks according to Johnson and Jackson would be necessary to induce plaque rupture (Johnson & Jackson, 2001). Therefore, studying the impact of increased collagen content in SMC-ACKR3 deficient mice with regards to the stabilization of the plaques was out of scope of this study. Moreover, collagen increase within lesions may not always be atheroprotective. While decreased collagen within lesions may result in the susceptibility of the plaque to rupture, too much collagen may support atherosclerotic lesion advancement by allowing deposition of more lipoproteins and growth factors (Rekhter, 1999). Furthermore, a study reported that collagen can stimulate monocyte differentiation into macrophages and promote accumulation of intracellular lipid in macrophages, resembling the characteristic of pro-atherosclerotic events (Wesley et al., 1998). Hence, SMC-ACKR3 driven increase in collagen content is inconclusive with regards to its effects in atherosclerosis.

SMCs within the lesions are a primary source of collagen synthesis (Nadkarni et al., 2009). Nevertheless, the amount of collagen within the plaques of mice was not correlated to the quantity of the SMCs in our study. Lesional SMC count was not significantly altered between the two genotypes, suggesting that SMC-ACKR3 might not have impacted SMC proliferation or migration within the lesions. It is also interesting to note that the role SMC-ACKR3 deficiency in mice did not sharply contrast the results of SMC-CXCR4 deficiency, as in the case of aEC specific roles of the two receptors. Döring et al. studied CXCR4 in SMCs via two promoters; *Tagln* and *Smmhc* (Döring et al., 2017). Although *Tagln* is a widely used promoter for cre dependent deletion of flanked genes in SMCs, it is also known to be expressed by non-SMC cell types, such as cardiac myocytes, megakaryocytes, spleen, myeloid cells and platelets (Chakraborty et al., 2019). The Smmhc promoter, on the other hand, is known to be expressed in vascular and non-vascular SMCs, therefore potentially offering more specificity in comparison to Tagln promoter when studying SMCs (Xin et al., 2002). The *Tagln*^{Cre} model allowed Döring et al. to study the constitutive deletion of CXCR4 presumably in SMCs, whereas the *Smmhc*^{Cre} model was a conditional knockout of CXCR4 in SMCs. *Tagln*^{Cre} mediated deletion of CXCR4 in SMCs revealed increased lesion sizes in the aortas and aortic roots of hyperlipidemic mice, which was observed with a decrease in lesional SMC content (Döring et al., 2017). Interestingly, *Smmhc*^{Cre} mediated conditional deletion of CXCR4 in SMCs increased lesion sizes in the aortic roots and arches of hyperlipidemic

mice, however, lesional SMC content did not change between the two genotypes. The collagen levels were not reported. Although the effects of both receptors on lesional collagen cannot be compared, it is clear that SMC-CXCR4 is involved in atherosclerosis, whereas SMC-ACKR3 does not seem to be under conditional knockout conditions. Further studies including constitutive deletion of ACKR3 specifically in SMCs can be done in mice in order to draw stronger conclusions. Of note, in order to ensure consistency and comparability, this study only involved conditional knockout mouse models as constitutive lack of ACKR3 ubiquitously as well as in endothelial cells was previously established to be lethal in mice (Sierro et al., 2007).

5.2 ACKR3 in the hematopoietic compartment

Hematopoietic cells are important components of the circulatory system and their role in atherosclerosis is of utmost prominence. Although ACKR3 was previously thought to be absent in leukocytes (Berahovich et al., 2010), recent studies revealed its expression in several subsets of immune cells, such as B cells, T cells, monocytes, macrophages and neutrophils (Koenen et al., 2019). An *in-vitro* study previously suggested that monocytic ACKR3 might contribute to atherosclerosis, due to the observation that ACKR3 was upregulated during monocyte to macrophage differentiation, which also increased the phagocytic activity of the macrophages (Ma et al., 2013). These findings may suggest a role of immune cell ACKR3 in lesional macrophage accumulation. In order to find out whether immune cell specific ACKR3 contributes to atherosclerosis, we studied the impact of hematopoietic ACKR3 in *Apoe*$^{-/-}$ mice. Our analyses revealed that the absence of ACKR3 in bone marrow derived cells did not affect atherosclerosis by any means. Lesion sizes as well as characteristics, such as lesional macrophage content, remained the same between the two genotypes, ruling out the contribution of ht-ACKR3 to atherosclerotic disease. Of note, a limitation of this study is that potential effects of ACKR3 in immune cells were investigated by means of a general knockout of the receptor in the whole hematopoietic compartment. This was mainly to understand whether or not the lesional macrophage accumulation would be affected similarly to the endothelial knockout model. Future studies could be aimed at dissecting the role of ACKR3 in specific immune cell types, such as myeloid cell specific deletion of ACKR3 via the *CD11b*^{Cre} or *LysM*^{Cre} mouse models or mononuclear phagocyte cell specific deletion via the *CX3CR1*^{Cre} mouse model. Interestingly, as opposed to the aEC and SMC specific ACKR3 deletion models, ht-ACKR3 deficiency did not impact circulating immune cell numbers, at all. This may be suggesting that the ACKR3 expressed in the arteries might be responsible for the homing and recruitment of the immune cells. This could also imply that a certain ACKR3 ligand expressed by the immune cells may be responsible for their response to arterial ACKR3. The fact that ht-ACKR3 did not have an impact of immune cell quantities in the circulation may also suggest that ACKR3 might not be involved in haematopoiesis.

5.3 The role of AT and liver specific ACKR3 in atherosclerosis

The role of organ specific ACKR3 during atherosclerosis was studied in two main metabolic organs; AT and liver.

5.3.1 Adipocyte & hepatocyte specific ACKR3 in atherosclerosis

The study by Li and colleagues suggested that ACKR3 in AT was responsible for regulating blood lipid levels (Li et al., 2014). The authors studied this role of ACKR3 with a systemic knockout of *Ackr3*, as well as ACKR3 agonist injections into mice. CCX771, produced by Chemocentryx (commercially unavailable) was used as an ACKR3 agonist in the study of Li et al. Of note, studies reported contradicting effects of CCX771; for example several researchers used CCX771 as an antagonist of ACKR3 (Luo et al., 2018; Qian et al., 2018; Sartina et al., 2012; Yamada et al., 2015), whereas others reported using CCX771 as an agonist of ACKR3 (Li et al., 2014; Zabel et al., 2009). Li and colleagues reported that activating ACKR3 reduced the expression of *Angptl4* and *Ppar-γ* in the AT and thereby increased the activity of LPL, which resulted in greater lipid uptake into the AT of mice. Meanwhile, mice with ubiquitous ablation of *Ackr3* developed monocytosis, which the authors attributed to increased blood lipid levels. Nonetheless, considering our tissue specific mouse models, increase in circulating immune cell subsets could be due to the action of arterial ACKR3. Furthermore, the reported monocytosis was observed concomitant with increased macrophage accumulation within plaques which were induced via wire injury (Li et al., 2014). Nevertheless, the authors drew these conclusions based on a systemic genetic knockout of *Ackr3*, as well as systemic administrations of CCX771 in mice. As a result, it is not clear whether or not these observations are causative and or coupled. In order to de-couple the ACKR3 driven effects in these studies, tissue / cell specific examinations should be implemented.

The aim of this study was to elucidate precisely the role of adipocyte specific ACKR3 in atherosclerosis. Our study revealed that AT-ACKR3 deficiency did not impact atherosclerotic lesions in mice in early or in advanced stages. On the other hand, in line with some of the findings from Li et al. AT-ACKR3 deficiency decreased lipid levels in the AT of mice, indeed confirming that adipocyte specific ACKR3 regulates AT lipid levels. Further confirming the findings of Li et al. our results also revealed that AT-ACKR3 regulates tissue lipid levels by altering LPL activity through the modulation of *Angptl4* and *Ppar-γ.* As already discussed above, this impact of ACKR3 on *Ppar-γ* was also evident in endothelial cells.

Surprisingly, however, lipid altering effect of ACKR3 in the AT was not reflected on the systemic lipid levels of mice; plasma triglyceride and cholesterol levels did not change between control and AT-ACKR3 deficient mice. In order to rule out potential changes in lipoprotein levels that may have been masked in general lipid level measurements, we quantified the amounts of vLDL, LDL and HDL in plasma samples, however no differences were observed. Further analyses disclosed that the hepatic lipid levels were also unaltered. Along with this, unlike in our EC and SMC specific ACKR3 deficiency mouse models, AT-ACKR3 deficiency did not impact blood leukocyte or leukocyte subset counts. Altogether, these findings establish that ACKR3 exerts local effects in terms

of lipid level regulation. The finding that the blood lipid levels and the circulating leukocyte levels did not change in our mouse model may explain why we did not observe any differences in atherosclerotic lesions. These findings also suggest that another cell type may be responsible for the effects that were observed in addition to the AT specific effects of ACKR3 in the study of Li et al., such as monocytosis and altered serum lipid levels. Both their and our study ruled out the potential impact of liver specific ACKR3. Hepatocyte specific deficiency of ACKR3 did not alter any lipid levels in the liver, circulation or in the AT of the mice. Moreover, atherosclerotic lesion sizes were unchanged between the two genotypes, indicating that hACKR3 does not play a role in the regulation of lipid levels or in atherosclerosis. This also implies that the lipid regulating effect of ACKR3 may be tissue specific. Considering this theory, further organs involved in lipid metabolism, such as the intestines, heart and skeletal muscle, should also be studied separately. Perhaps one aspect that may be easily overlooked in this field despite its highly significant role in the management of systemic metabolism and the lipid homeostasis is the nervous system. CNS is reported to communicate with the liver in a bidirectional manner and modulate liver lipid metabolism and VLDL production (Taher et al., 2017). Furthermore, the sympathetic nervous system (SNS) has also been shown to modulate the triglyceride storage in the AT and triglyceride production in the liver (Geerling et al., 2014). There is a possibility that the systemic manipulation of ACKR3 may have heavily involved the nervous system. This idea is more intriguing by the fact that the ACKR3 is extensively present in the brain (Banisadr et al., 2016; Ehrlich et al., 2021; Puchert et al., 2017; Quinn et al., 2018).

It is also important to note that our findings are specific to hyperlipidemic conditions and these observations may not be reproducible under normolipidemic conditions. For example, lipid lowering effects of soy protein in hemodialysis patients were shown to be effective in hyperlipidemic patients, but not in normolipidemic patients (S. T. Chen et al., 2005). Furthermore, our studies investigating the impact of organ specific ACKR3 on lipid level regulation did not include fasting or feeding approaches, which may also reveal potential effects that may otherwise be overshadowed. Another important factor to consider is the potential role of ACKR3 in the muscle tissues. Clearly, systemic knockout of ACKR3 reveals far more effects than those observed upon single tissue specific effects. There is a possibility that ACKR3 may also impact muscle tissue specific LPL activity, as LPL is also abundantly present in the muscle tissues beside AT. Interestingly, the activity of LPL was reported to be contrasting between the AT and muscle tissue in starvation and refeeding experiments (Bonnet et al., 2000; Zechner et al., 2000). Further studies with tissue specific approaches are required in order to dissect the role of ACKR3 in lipid level regulation. The observation that ACKR3 deficiency can limit lipid accumulation in the AT may provide insight into the research of lipotoxicity induced diseases as well as obesity and metabolic syndrome research.

5.4 The therapeutic potential of ACKR3

This study revealed that aEC-ACKR3 holds great potential in the treatment of atherosclerosis. The principles of the actions of aEC-ACKR3 also highlight it as a candidate for other disease models, in which interfering with immune cell adhesion onto the endothelium could be a therapeutic target, such as multiple sclerosis. Nevertheless, these observations are based on genetic ablation of ACKR3 under certain circumstances, such as diet induced atherosclerosis in *Apoe*$^{-/-}$ mice. These findings need to be further investigated via ACKR3 inhibitor treatments in order to observe whether the genetic knockout effects could be reproduced via pharmacological inhibition of the receptor.

Moreover, the desired 'inhibition' of ACKR3 needs to be specified; ACKR3 has several ligands and the 'inhibition' technique can either mean interference with one or several ACKR3 ligands, interference with the internalization of the receptor or interference with the inhibition of its signaling abilities, such as ß-arrestin recruitment. Studying the pharmacological inhibition of ACKR3 has been a challenging endeavor over the past couple of years as there is a lack of commercially available, well-described chemical tools to do so. Nonetheless, there have been some publications very recently reporting the discovery of candidates for ACKR3 inhibition. In May 2020, a group of researchers proposed diphenylacetamides as ACKR3 inhibitors, showing that they can inhibit ß-arrestin *in vitro* (Menhaji-Klotz et al., 2020). This is a great tool, as antagonism of ACKR3 recruited ß-arrestin would in theory interfere with the downstream MAPK signaling. Moreover, at the end of 2020, an ACKR3 antagonist was discovered and named ACT-1004-1239 (Richard-Bildstein et al., 2020). The antagonist is reported to interfere with the scavenging activity of ACKR3, as treated mice showed an increase in circulating CXCL12 levels, according to the study. This antagonist was then tested in humans with regards to its safety. The study reported that ACT-1004-1239 treatment in humans was well tolerated and it increased CXCL12 levels in the plasma, whereas CXCL11 levels were not affected (Huynh et al., 2021). This is contrasting our study with genetic manipulation of ACKR3 and it implies that there may be mechanistic differences during pharmacological inhibition of ACKR3. The study did not investigate the impact of increased circulating CXCL12 concentrations in the patients on parameters such as leukocyte counts or lipid levels. This would be highly important in the interpretation of systemic ACKR3 antagonism in humans. Of note, previously our research group established that CXCL12 drives atherosclerosis (Döring et al., 2019) and in addition, GWAS study also reported a strong association of the *Cxcl12* locus and CVDs (Farouk et al., 2010). While inhibition of ACKR3 may offer therapeutic potentials, such as interfering with ACKR3 driven immune cell accumulation in the parenchyma during inflammatory demyelinating diseases as reasoned in the study (Huynh et al., 2021), elevating CXCL12 may be detrimental in other disease aspects, such as atherosclerosis. Therefore, the effects of pharmacological inhibition of ACKR3 need to be studied in detail. As eluded to before, the effect of ACKR3 in the nervous system needs to be scrutinized and further evaluated. Without understanding the impact of ACKR3 in various compartments of the body, it would remain as a premature target. Especially given the discrepancies between genetic and

pharmacological targeting of ACKR3, its mechanism needs to be understood better before proceeding to ubiquitous anti-ACKR3 treatments. A safer option to approach therapeutics based on ACKR3 mediated processes could be cell specific targeting of ACKR3 activity. Endothelium is the primary site of atherosclerosis initiation and a concept of endothelial specific drug delivery could offer a breakthrough treatment strategy avoiding the drug reaching other cells types with potential adverse outcomes as well as avoiding the rapid elimination of the circulating drug by the kidneys and the liver (Moghimi & Szebeni, 2003). For this purpose, drug cargoes that are specifically designed to bind the endothelium via specific markers, such as ICAM and platelet endothelial cell adhesion molecule (PECAM), may be utilized (Simone et al., 2009). In order to do so, drugs can be coated in carriers, such as phospholipid based liposomes, and to ensure the delivery of this cargo to the endothelium, molecules such as ICAM and PECAM can be used as affinity moieties and the cargo can be conjugated with targeting peptides (Simone et al., 2009).

6. Concluding Remarks and future perspectives

The chemokine and chemokine receptor system is highly complex and the actions of these molecules vary significantly based on cell type, disease model, types of stimuli, etc. Furthermore, there is a great interplay between the ligands and their respective receptors; several different ligands can bind to several different receptors and both the ligands and the receptors may form homo- or heterodimers, making the interpretation of their actions and effects very difficult. It is therefore very important to study the members of the chemokine & chemokine receptor system with regards to their cell-specific effects in the context of certain disease models. This is especially beneficial in understanding possible outcomes and side effects when a stimulatory or an inhibitory approach of a certain candidate is considered for therapeutic purposes. Another coat of complexity is presented by the fact that the observed cell specific effects of chemokines or chemokine receptors may alter when a systemic treatment approach is taken. Despite these difficulties, due to their wide ranging and substantial effects, targeting the chemokine & receptor system is highly promising in the treatment of inflammatory diseases, especially atherosclerosis.

So far, limited success with chemokine / chemokine receptor treatment based clinical trials is reported in the field of atherosclerosis. Two clinical trials targeting the chemokine receptors CCR5 (ClinicalTrials.gov identifier: NCT03402815) and CCR2 (ClinicalTrials.gov identifier: NCT00715169) can be highlighted in terms of preliminary promising results. CCR5 antagonism with the molecule maraviroc in human immunodeficiency virus patients showed improvements in cardiovascular risk factors, such as arterial stiffness and endothelial dysfunction (Francisci et al., 2019). Furthermore, blocking CCR2 with the humanized monoclonal antibody MLN1202 in patients with atherosclerosis risk significantly decreased serum levels of C-reactive protein, a well-known inflammatory marker linked to coronary artery disease (Gilbert et al., 2011). Nonetheless, these studies are based on systemic treatments and local treatment options targeting the chemokine system are not yet in place. Considering the highly complex interactions within the chemokine system and the intricate roles based on cell and disease specificity, enabling local targeting of the chemokines & chemokine receptors may aid in eliminating some limitations in this field. Henceforth, tissue or cell specific delivery of drugs is a highly exciting concept, especially in scheming treatments with minimal off target effects and high therapeutic efficiency (Zhao et al., 2020). For this purpose, drug cargoes with cell specific markers can be utilized in order to deliver molecules to specific cells. Such drug cargoes are already being explored in the field of cancer, for example nanoparticles of organic (liposomes, polymers), synthetic (carbon nanotubes) and hybrid (liposome-silica hybrid) origins are being studied in the treatment of certain cancer types (Yao et al., 2020). Such strategies can also be adapted and developed for cell specific treatments targeting specific chemokines or chemokine receptors in the context of atherosclerosis.

This study identifies endothelial ACKR3 as a novel and prominent target to be studied further in the context of atherosclerosis. This may also apply to other disease models in which inhibiting endothelial translocation of the immune cells may be targeted as a therapeutic approach, such as multiple sclerosis. This potential of ACKR3 was also previously addressed in another study with an experimental autoimmune encephalomyelitis study in mice (Cruz-Orengo et al., 2011)

Moreover, adipocyte specific ACKR3 may have the potential to be studied further in the context of adipose tissue lipid accumulation and associated disease models, such as obesity and adipose tissue inflammation.

Bibliography

Alampour-Rajabi, S., El Bounkari, O., Rot, A., Müller-Newen, G., Bachelerie, F., Gawaz, M., Weber, C., Schober, A., & Bernhagen, J. (2015, Nov). MIF interacts with CXCR7 to promote receptor internalization, ERK1/2 and ZAP-70 signaling, and lymphocyte chemotaxis. *Faseb j, 29*(11), 4497-4511. https://doi.org/10.1096/fj.15-273904

An, Z., Li, J., Yu, J., Wang, X., Gao, H., Zhang, W., Wei, Z., Zhang, J., Zhang, Y., Zhao, J., & Liang, X. (2019, 2019/11/02). Neutrophil extracellular traps induced by IL-8 aggravate atherosclerosis via activation NF-κB signaling in macrophages. *Cell Cycle, 18*(21), 2928-2938. https://doi.org/10.1080/15384101.2019.1662678

Andrew, D. P., Ruffing, N., Kim, C. H., Miao, W., Heath, H., Li, Y., Murphy, K., Campbell, J. J., Butcher, E. C., & Wu, L. (2001, Jan 1). C-C chemokine receptor 4 expression defines a major subset of circulating nonintestinal memory T cells of both Th1 and Th2 potential. *J Immunol, 166*(1), 103-111. https://doi.org/10.4049/jimmunol.166.1.103

Bachelerie, F., Ben-Baruch, A., Burkhardt, A. M., Combadiere, C., Farber, J. M., Graham, G. J., Horuk, R., Sparre-Ulrich, A. H., Locati, M., Luster, A. D., Mantovani, A., Matsushima, K., Murphy, P. M., Nibbs, R., Nomiyama, H., Power, C. A., Proudfoot, A. E., Rosenkilde, M. M., Rot, A., Sozzani, S., Thelen, M., Yoshie, O., & Zlotnik, A. (2014). International Union of Basic and Clinical Pharmacology. [corrected]. LXXXIX. Update on the extended family of chemokine receptors and introducing a new nomenclature for atypical chemokine receptors. *Pharmacol Rev, 66*(1), 1-79. https://doi.org/10.1124/pr.113.007724

Bachelerie, F., Graham, G. J., Locati, M., Mantovani, A., Murphy, P. M., Nibbs, R., Rot, A., Sozzani, S., & Thelen, M. (2014, Mar). New nomenclature for atypical chemokine receptors. *Nat Immunol, 15*(3), 207-208. https://doi.org/10.1038/ni.2812

Baggiolini, M., Dewald, B., & Moser, B. (1997, 1997/04/01). Human Chemokines: An Update. *Annual Review of Immunology, 15*(1), 675-705. https://doi.org/10.1146/annurev.immunol.15.1.675

Bai, D., Ueno, L., & Vogt, P. K. (2009). Akt-mediated regulation of NFkappaB and the essentialness of NFkappaB for the oncogenicity of PI3K and Akt. *International journal of cancer, 125*(12), 2863-2870. https://doi.org/10.1002/ijc.24748

Balabanian, K., Lagane, B., Infantino, S., Chow, K. Y., Harriague, J., Moepps, B., Arenzana-Seisdedos, F., Thelen, M., & Bachelerie, F. (2005, Oct 21). The chemokine SDF-1/CXCL12 binds to and signals through the orphan receptor RDC1 in T lymphocytes. *J Biol Chem, 280*(42), 35760-35766. https://doi.org/10.1074/jbc.M508234200

Balaji, S., Watson, C. L., Ranjan, R., King, A., Bollyky, P. L., & Keswani, S. G. (2015, 2015/11//). Chemokine Involvement in Fetal and Adult Wound Healing. *Advances in wound care, 4*(11), 660-672. https://doi.org/10.1089/wound.2014.0564

Banisadr, G., Podojil, J. R., Miller, S. D., & Miller, R. J. (2016, Mar). Pattern of CXCR7 Gene Expression in Mouse Brain Under Normal and Inflammatory Conditions. *J Neuroimmune Pharmacol, 11*(1), 26-35. https://doi.org/10.1007/s11481-015-9616-y

Ben-Zvi, D., Barrandon, O., Hadley, S., Blum, B., Peterson, Q. P., & Melton, D. A. (2015). Angptl4 links α-cell proliferation following glucagon receptor inhibition with adipose tissue triglyceride metabolism. *Proceedings of the National Academy of Sciences of the United States of America, 112*(50), 15498-15503. https://doi.org/10.1073/pnas.1513872112

Benedict, M., & Zhang, X. (2017). Non-alcoholic fatty liver disease: An expanded review. *World journal of hepatology, 9*(16), 715-732. https://doi.org/10.4254/wjh.v9.i16.715

Bennett, M. R., Sinha, S., & Owens, G. K. (2016). Vascular Smooth Muscle Cells in Atherosclerosis. *Circulation Research, 118*(4), 692-702. https://doi.org/10.1161/CIRCRESAHA.115.306361

Berahovich, R. D., Zabel, B. A., Lewén, S., Walters, M. J., Ebsworth, K., Wang, Y., Jaen, J. C., & Schall, T. J. (2014). Endothelial expression of CXCR7 and the regulation of systemic CXCL12 levels. *Immunology, 141*(1), 111-122. https://doi.org/10.1111/imm.12176

Berahovich, R. D., Zabel, B. A., Penfold, M. E. T., Lewén, S., Wang, Y., Miao, Z., Gan, L., Pereda, J., Dias, J., Slukvin, I. I., McGrath, K. E., Jaen, J. C., & Schall, T. J. (2010). CXCR7 Protein Is Not Expressed on Human or Mouse Leukocytes. *The Journal of Immunology, 185*(9), 5130. https://doi.org/10.4049/jimmunol.1001660

Bernhagen, J., Krohn, R., Lue, H., Gregory, J. L., Zernecke, A., Koenen, R. R., Dewor, M., Georgiev, I., Schober, A., Leng, L., Kooistra, T., Fingerle-Rowson, G., Ghezzi, P., Kleemann, R., McColl, S. R., Bucala, R., Hickey, M. J., & Weber, C. (2007, May). MIF is a noncognate ligand of CXC chemokine receptors in inflammatory and atherogenic cell recruitment. *Nat Med, 13*(5), 587-596. https://doi.org/10.1038/nm1567

Blankenberg, S., Barbaux, S., & Tiret, L. (2003, 2003/10/01/). Adhesion molecules and atherosclerosis. *Atherosclerosis, 170*(2), 191-203. https://doi.org/https://doi.org/10.1016/S0021-9150(03)00097-2

Bobryshev, Y. V. (2006). Monocyte recruitment and foam cell formation in atherosclerosis. *Micron, 37*(3), 208-222. https://doi.org/10.1016/j.micron.2005.10.007

Boersma, C. J., Pool, C. W., Van Heerikhuize, J. J., & Van Leeuwen, F. W. (1994, Feb). Characterization of opioid binding sites in the neural and intermediate lobe of the rat pituitary gland by quantitative receptor autoradiography. *J Neuroendocrinol, 6*(1), 47-56. https://doi.org/10.1111/j.1365-2826.1994.tb00554.x

Boisvert, W. A., Rose, D. M., Johnson, K. A., Fuentes, M. E., Lira, S. A., Curtiss, L. K., & Terkeltaub, R. A. (2006, 2006/04/01/). Up-Regulated Expression of the CXCR2 Ligand KC/GRO-α in Atherosclerotic Lesions Plays a Central Role in Macrophage Accumulation and Lesion Progression. *The American journal of pathology, 168*(4), 1385-1395. https://doi.org/https://doi.org/10.2353/ajpath.2006.040748

Boldajipour, B., Mahabaleshwar, H., Kardash, E., Reichman-Fried, M., Blaser, H., Minina, S., Wilson, D., Xu, Q., & Raz, E. (2008, Feb 8). Control of chemokine-guided cell migration by ligand sequestration. *Cell, 132*(3), 463-473. https://doi.org/10.1016/j.cell.2007.12.034

Bonnet, M., Leroux, C., Faulconnier, Y., Hocquette, J.-F. o., Bocquier, F. o., Martin, P., & Chilliard, Y. (2000). Lipoprotein Lipase Activity and mRNA Are Up-Regulated by Refeeding in Adipose Tissue and Cardiac Muscle of Sheep. *The Journal of Nutrition, 130*(4), 749-756. https://doi.org/10.1093/jn/130.4.749

Boring, L., Gosling, J., Cleary, M., & Charo, I. F. (1998, Aug 27). Decreased lesion formation in CCR2-/- mice reveals a role for chemokines in the initiation of atherosclerosis. *Nature, 394*(6696), 894-897. https://doi.org/10.1038/29788

Brocard, J., Warot, X., Wendling, O., Messaddeq, N., Vonesch, J. L., Chambon, P., & Metzger, D. (1997, Dec 23). Spatio-temporally controlled site-specific somatic mutagenesis in the mouse. *Proc Natl Acad Sci U S A, 94*(26), 14559-14563. https://doi.org/10.1073/pnas.94.26.14559

Burns, J. M., Summers, B. C., Wang, Y., Melikian, A., Berahovich, R., Miao, Z., Penfold, M. E., Sunshine, M. J., Littman, D. R., Kuo, C. J., Wei, K., McMaster, B. E., Wright, K., Howard, M. C., & Schall, T. J. (2006, Sep 4). A novel chemokine receptor for SDF-1 and I-TAC involved in cell survival, cell adhesion, and tumor development. *The Journal of experimental medicine, 203*(9), 2201-2213. https://doi.org/10.1084/jem.20052144

Busillo, J. M., & Benovic, J. L. (2007). Regulation of CXCR4 signaling. *Biochimica et biophysica acta, 1768*(4), 952-963. https://doi.org/10.1016/j.bbamem.2006.11.002

Caron, K. M., & Smithies, O. (2001, Jan 16). Extreme hydrops fetalis and cardiovascular abnormalities in mice lacking a functional Adrenomedullin gene. *Proc Natl Acad Sci U S A, 98*(2), 615-619. https://doi.org/10.1073/pnas.021548898

Chakraborty, R., Saddouk, F. Z., Carrao, A. C., Krause, D. S., Greif, D. M., & Martin, K. A. (2019, 2019/04/01). Promoters to Study Vascular Smooth Muscle. *Arteriosclerosis, Thrombosis, and Vascular Biology, 39*(4), 603-612. https://doi.org/10.1161/ATVBAHA.119.312449

Chang, H.-C., Huang, P.-H., Syu, F.-S., Hsieh, C.-H., Chang, S. L.-Y., Lu, J., & Chen, H.-C. (2018). Critical involvement of atypical chemokine receptor CXCR7 in allergic airway inflammation. *Immunology, 154*(2), 274-284. https://doi.org/10.1111/imm.12881

Chatterjee, M., Borst, O., Walker, B., Fotinos, A., Vogel, S., Seizer, P., Mack, A., Alampour-Rajabi, S., Rath, D., Geisler, T., Lang, F., Langer, H. F., Bernhagen, J., & Gawaz, M. (2014). Macrophage Migration Inhibitory Factor Limits Activation-Induced Apoptosis of Platelets via CXCR7-Dependent Akt Signaling. *Circulation Research, 115*(11), 939-949. https://doi.org/doi:10.1161/CIRCRESAHA.115.305171

Chen, B., Liu, J., Ho, T. T., Ding, X., & Mo, Y. Y. (2016, 2016/12/01). ERK-mediated NF-κB activation through ASIC1 in response to acidosis. *Oncogenesis, 5*(12), e279-e279. https://doi.org/10.1038/oncsis.2016.81

Chen, S. T., Ferng, S. H., Yang, C. S., Peng, S. J., Lee, H. R., & Chen, J. R. (2005, Dec). Variable effects of soy protein on plasma lipids in hyperlipidemic and normolipidemic hemodialysis patients. *Am J Kidney Dis, 46*(6), 1099-1106. https://doi.org/10.1053/j.ajkd.2005.08.031

Chen, X. L., Xia, Z. F., Wei, D., Ben, D. F., Wang, Y. J., & Deng, N. Q. (2005, Dec). [Activation of p38 MAPK signal transduction pathway by burn serum and the expression of VCAM-1 in HUVECs induced by NF-kappaB]. *Zhonghua Shao Shang Za Zhi, 21*(6), 426-429.

Chen, Z., Sakuma, M., Zago, A. C., Zhang, X., Shi, C., Leng, L., Mizue, Y., Bucala, R., & Simon, D. I. (2004, 2004/04/01). Evidence for a Role of Macrophage Migration Inhibitory Factor in Vascular Disease. *Arteriosclerosis, Thrombosis, and Vascular Biology, 24*(4), 709-714. https://doi.org/10.1161/01.ATV.0000119356.35748.9e

Cheng, Q., McKeown, S. J., Santos, L., Santiago, F. S., Khachigian, L. M., Morand, E. F., & Hickey, M. J. (2010, Jul 15). Macrophage migration inhibitory factor increases leukocyte-endothelial interactions in human endothelial cells via promotion of expression of adhesion molecules. *J Immunol, 185*(2), 1238-1247. https://doi.org/10.4049/jimmunol.0904104

Chistiakov, D. A., Bobryshev, Y. V., & Orekhov, A. N. (2016). Macrophage-mediated cholesterol handling in atherosclerosis. *Journal of cellular and molecular medicine, 20*(1), 17-28. https://doi.org/10.1111/jcmm.12689

Choi, K. W., Park, H. J., Jung, D. H., Kim, T. W., Park, Y. M., Kim, B. O., Sohn, E. H., Moon, E. Y., Um, S. H., Rhee, D. K., & Pyo, S. (2010, Nov-Dec). Inhibition of TNF-α-induced adhesion molecule expression by diosgenin in mouse vascular smooth muscle cells via downregulation of the MAPK, Akt and NF-κB signaling pathways. *Vascul Pharmacol, 53*(5-6), 273-280. https://doi.org/10.1016/j.vph.2010.09.007

Clore, G. M., Appella, E., Yamada, M., Matsushima, K., & Gronenborn, A. M. (1990, Feb 20). Three-dimensional structure of interleukin 8 in solution. *Biochemistry, 29*(7), 1689-1696. https://doi.org/10.1021/bi00459a004

Cruz-Orengo, L., Holman, D. W., Dorsey, D., Zhou, L., Zhang, P., Wright, M., McCandless, E. E., Patel, J. R., Luker, G. D., Littman, D. R., Russell, J. H., & Klein, R. S. (2011). CXCR7 influences leukocyte entry into the CNS parenchyma by controlling abluminal CXCL12 abundance during autoimmunity. *The Journal of experimental medicine, 208*(2), 327-339. https://doi.org/10.1084/jem.20102010

Cuesta-Gomez, N., Graham, G. J., & Campbell, J. D. M. (2021, 2021/04/17). Chemokines and their receptors: predictors of the therapeutic potential of mesenchymal stromal cells. *Journal of translational medicine, 19*(1), 156. https://doi.org/10.1186/s12967-021-02822-5

D'Alterio, C., Consales, C., Polimeno, M., Franco, R., Cindolo, L., Portella, L., Cioffi, M., Calemma, R., Marra, L., Claudio, L., Perdonà, S., Pignata, S., Facchini, G., Cartenì, G., Longo, N., Pucci, L., Ottaiano, A., Costantini, S., Castello, G., & Scala, S. (2010, Nov). Concomitant CXCR4 and CXCR7 expression predicts poor prognosis in renal cancer. *Curr Cancer Drug Targets, 10*(7), 772-781. https://doi.org/10.2174/156800910793605839

Dai, X., Tan, Y., Cai, S., Xiong, X., Wang, L., Ye, Q., Yan, X., Ma, K., & Cai, L. (2011, Jun). The role of CXCR7 on the adhesion, proliferation and angiogenesis of endothelial progenitor cells. *J Cell Mol Med, 15*(6), 1299-1309. https://doi.org/10.1111/j.1582-4934.2011.01301.x

Davies, P. F. (2009). Hemodynamic shear stress and the endothelium in cardiovascular pathophysiology. *Nature clinical practice. Cardiovascular medicine, 6*(1), 16-26. https://doi.org/10.1038/ncpcardio1397

de Jager, S. C. A., Bot, I., Kraaijeveld, A. O., Korporaal, S. J. A., Bot, M., van Santbrink, P. J., van Berkel, T. J. C., Kuiper, J., & Biessen, E. A. L. (2013, 2013/03/01). Leukocyte-Specific CCL3 Deficiency Inhibits Atherosclerotic Lesion Development by Affecting Neutrophil Accumulation. *Arteriosclerosis, Thrombosis, and Vascular Biology, 33*(3), e75-e83. https://doi.org/10.1161/ATVBAHA.112.300857

Décaillot, F. M., Kazmi, M. A., Lin, Y., Ray-Saha, S., Sakmar, T. P., & Sachdev, P. (2011, Sep 16). CXCR7/CXCR4 heterodimer constitutively recruits beta-arrestin to enhance cell migration. *J Biol Chem, 286*(37), 32188-32197. https://doi.org/10.1074/jbc.M111.277038

Desideri, G., & Ferri, C. (2005). Endothelial activation. Sliding door to atherosclerosis. *Curr Pharm Des, 11*(17), 2163-2175. https://doi.org/10.2174/1381612054367382

Dimitrijevic, O. B., Stamatovic, S. M., Keep, R. F., & Andjelkovic, A. V. (2006, Jun). Effects of the chemokine CCL2 on blood-brain barrier permeability during ischemia-reperfusion injury. *J Cereb Blood Flow Metab, 26*(6), 797-810. https://doi.org/10.1038/sj.jcbfm.9600229

Doring, Y., Jansen, Y., Cimen, I., Aslani, M., Gencer, S., Peters, L. J. F., Duchene, J., Weber, C., & van der Vorst, E. P. C. (2020, Mar 13). B-Cell-Specific CXCR4 Protects Against Atherosclerosis Development and Increases Plasma IgM Levels. *Circ Res, 126*(6), 787-788. https://doi.org/10.1161/CIRCRESAHA.119.316142

Döring, Y., Noels, H., van der Vorst, E. P. C., Neideck, C., Egea, V., Drechsler, M., Mandl, M., Pawig, L., Jansen, Y., Schröder, K., Bidzhekov, K., Megens, R. T. A., Theelen, W., Klinkhammer, B. M., Boor, P., Schurgers, L., van Gorp, R., Ries, C., Kusters, P. J. H., van der Wal, A., Hackeng, T. M., Gäbel, G., Brandes, R. P., Soehnlein, O., Lutgens, E., Vestweber, D., Teupser, D., Holdt, L. M., Rader, D. J., Saleheen, D., & Weber, C. (2017). Vascular CXCR4 Limits Atherosclerosis by Maintaining Arterial Integrity: Evidence From Mouse and Human Studies. *Circulation, 136*(4), 388-403. https://doi.org/10.1161/CIRCULATIONAHA.117.027646

Döring, Y., Pawig, L., Weber, C., & Noels, H. (2014). The CXCL12/CXCR4 chemokine ligand/receptor axis in cardiovascular disease. *Front Physiol, 5*, 212. https://doi.org/10.3389/fphys.2014.00212

Doring, Y., van der Vorst, E. P. C., Duchene, J., Jansen, Y., Gencer, S., Bidzhekov, K., Atzler, D., Santovito, D., Rader, D. J., Saleheen, D., & Weber, C. (2019, Mar 5). CXCL12 Derived From Endothelial Cells Promotes Atherosclerosis to Drive Coronary Artery Disease. *Circulation, 139*(10), 1338-1340. https://doi.org/10.1161/CIRCULATIONAHA.118.037953

Döring, Y., van der Vorst, E. P. C., Duchene, J., Jansen, Y., Gencer, S., Bidzhekov, K., Atzler, D., Santovito, D., Rader, D. J., Saleheen, D., & Weber, C. (2019, Mar 5). CXCL12 Derived From Endothelial Cells Promotes Atherosclerosis to Drive Coronary Artery Disease. *Circulation, 139*(10), 1338-1340. https://doi.org/10.1161/circulationaha.118.037953

Dragoni, S., Hudson, N., Kenny, B.-A., Burgoyne, T., McKenzie, J. A., Gill, Y., Blaber, R., Futter, C. E., Adamson, P., Greenwood, J., & Turowski, P. (2017). Endothelial MAPKs Direct ICAM-1 Signaling to Divergent Inflammatory Functions. *Journal of immunology (Baltimore, Md. : 1950), 198*(10), 4074-4085. https://doi.org/10.4049/jimmunol.1600823

Edward Zhou, X., Melcher, K., & Eric Xu, H. (2019, Mar). Structural biology of G protein-coupled receptor signaling complexes. *Protein Sci, 28*(3), 487-501. https://doi.org/10.1002/pro.3526

Ehrlich, A. T., Semache, M., Couvineau, P., Wojcik, S., Kobayashi, H., Thelen, M., Gross, F., Hogue, M., Le Gouill, C., Darcq, E., Bouvier, M., & Kieffer, B. L. (2021, 2021/09/28). Ackr3-Venus knock-in mouse lights up brain vasculature. *Molecular Brain, 14*(1), 151. https://doi.org/10.1186/s13041-021-00862-y

Eisenberg, S. (1983, Feb 1). Lipoproteins and lipoprotein metabolism. A dynamic evaluation of the plasma fat transport system. *Klin Wochenschr, 61*(3), 119-132. https://doi.org/10.1007/bf01486366

Farouk, S. S., Rader, D. J., Reilly, M. P., & Mehta, N. N. (2010). CXCL12: a new player in coronary disease identified through human genetics. *Trends in cardiovascular medicine, 20*(6), 204-209. https://doi.org/10.1016/j.tcm.2011.08.002

Flora, G. D., & Nayak, M. K. (2019). A Brief Review of Cardiovascular Diseases, Associated Risk Factors and Current Treatment Regimes. *Curr Pharm Des, 25*(38), 4063-4084. https://doi.org/10.2174/1381612825666190925163827

Fra, A. M., Locati, M., Otero, K., Sironi, M., Signorelli, P., Massardi, M. L., Gobbi, M., Vecchi, A., Sozzani, S., & Mantovani, A. (2003, Mar 1). Cutting edge: scavenging of inflammatory CC chemokines by the promiscuous putatively silent chemokine receptor D6. *J Immunol, 170*(5), 2279-2282. https://doi.org/10.4049/jimmunol.170.5.2279

Francisci, D., Pirro, M., Schiaroli, E., Mannarino, M. R., Cipriani, S., Bianconi, V., Alunno, A., Bagaglia, F., Bistoni, O., Falcinelli, E., Bury, L., Gerli, R., Mannarino, E., De Caterina, R., & Baldelli, F. (2019). Maraviroc Intensification Modulates Atherosclerotic Progression in HIV-Suppressed Patients at High Cardiovascular Risk. A Randomized, Crossover Pilot Study. *Open forum infectious diseases, 6*(4), ofz112-ofz112. https://doi.org/10.1093/ofid/ofz112

Frayn, K. (2002). Adipose tissue as a buffer for daily lipid flux. *Diabetologia, 45*, 1201-1210.

Frostegård, J. (2013). Immunity, atherosclerosis and cardiovascular disease. *BMC medicine, 11*, 117-117. https://doi.org/10.1186/1741-7015-11-117

Galliera, E., Jala, V. R., Trent, J. O., Bonecchi, R., Signorelli, P., Lefkowitz, R. J., Mantovani, A., Locati, M., & Haribabu, B. (2004, Jun 11). beta-Arrestin-dependent constitutive internalization of the human chemokine decoy receptor D6. *J Biol Chem, 279*(24), 25590-25597. https://doi.org/10.1074/jbc.M400363200

Gatto, L., & Prati, F. (2020). Subclinical atherosclerosis: how and when to treat it? *European Heart Journal Supplements, 22*(Supplement_E), E87-E90. https://doi.org/10.1093/eurheartj/suaa068

Gebauer, F., Tachezy, M., Effenberger, K., von Loga, K., Zander, H., Marx, A., Kaifi, J. T., Sauter, G., Izbicki, J. R., & Bockhorn, M. (2011, Aug 1). Prognostic impact of CXCR4 and CXCR7 expression in pancreatic adenocarcinoma. *J Surg Oncol, 104*(2), 140-145. https://doi.org/10.1002/jso.21957

Geerling, J. J., Boon, M. R., Kooijman, S., Parlevliet, E. T., Havekes, L. M., Romijn, J. A., Meurs, I. M., & Rensen, P. C. (2014, Feb). Sympathetic nervous system control of triglyceride metabolism: novel concepts derived from recent studies. *J Lipid Res, 55*(2), 180-189. https://doi.org/10.1194/jlr.R045013

Gencer, S., Döring, Y., Jansen, Y., Bayasgalan, S., Schengel, O., Müller, M., Peters, L. J. F., Weber, C., & van der Vorst, E. P. C. (2021). Adipocyte-Specific ACKR3 Regulates Lipid Levels in Adipose Tissue. *Biomedicines, 9*(4), 394. https://www.mdpi.com/2227-9059/9/4/394

Gencer, S., Evans, B. R., van der Vorst, E. P. C., Döring, Y., & Weber, C. (2021, Jan 25). Inflammatory Chemokines in Atherosclerosis. *Cells, 10*(2). https://doi.org/10.3390/cells10020226

Gencer, S., van der Vorst, E. P. C., Aslani, M., Weber, C., Döring, Y., & Duchene, J. (2019, Apr). Atypical Chemokine Receptors in Cardiovascular Disease. *Thromb Haemost, 119*(4), 534-541. https://doi.org/10.1055/s-0038-1676988

Gentilini, A., Caligiuri, A., Raggi, C., Rombouts, K., Pinzani, M., Lori, G., Correnti, M., Invernizzi, P., Rovida, E., Navari, N., Di Matteo, S., Alvaro, D., Banales, J. M., Rodrigues, P., Raschioni, C., Donadon, M., Di Tommaso, L., & Marra, F. (2019, Sep 1). CXCR7 contributes to the aggressive phenotype of cholangiocarcinoma cells. *Biochim Biophys Acta Mol Basis Dis, 1865*(9), 2246-2256. https://doi.org/10.1016/j.bbadis.2019.04.020

Gerhardt, T., & Ley, K. (2015). Monocyte trafficking across the vessel wall. *Cardiovascular Research, 107*(3), 321-330. https://doi.org/10.1093/cvr/cvv147

Gerrits, H., van Ingen Schenau, D. S., Bakker, N. E., van Disseldorp, A. J., Strik, A., Hermens, L. S., Koenen, T. B., Krajnc-Franken, M. A., & Gossen, J. A. (2008, May). Early postnatal lethality and cardiovascular defects in CXCR7-deficient mice. *Genesis, 46*(5), 235-245. https://doi.org/10.1002/dvg.20387

Gilbert, J., Lekstrom-Himes, J., Donaldson, D., Lee, Y., Hu, M., Xu, J., Wyant, T., & Davidson, M. (2011, Mar 15). Effect of CC chemokine receptor 2 CCR2 blockade on serum C-reactive protein in individuals at atherosclerotic risk and with a single nucleotide polymorphism of the monocyte chemoattractant protein-1 promoter region. *Am J Cardiol, 107*(6), 906-911. https://doi.org/10.1016/j.amjcard.2010.11.005

Gimbrone, M. A., & García-Cardeña, G. (2016). Endothelial Cell Dysfunction and the Pathobiology of Atherosclerosis. *Circulation Research, 118*(4), 620-636. https://doi.org/doi:10.1161/CIRCRESAHA.115.306301

Giorgino, F. (2009, Nov). Adipose tissue function and dysfunction: organ cross talk and metabolic risk. *Am J Physiol Endocrinol Metab, 297*(5), E975-976. https://doi.org/10.1152/ajpendo.00488.2009

Graham, G. J., Locati, M., Mantovani, A., Rot, A., & Thelen, M. (2012, Jul 30). The biochemistry and biology of the atypical chemokine receptors. *Immunol Lett, 145*(1-2), 30-38. https://doi.org/10.1016/j.imlet.2012.04.004

Gravel, S., Malouf, C., Boulais, P. E., Berchiche, Y. A., Oishi, S., Fujii, N., Leduc, R., Sinnett, D., & Heveker, N. (2010, Dec 3). The peptidomimetic CXCR4 antagonist TC14012 recruits beta-arrestin to CXCR7: roles of receptor domains. *J Biol Chem, 285*(49), 37939-37943. https://doi.org/10.1074/jbc.C110.147470

Grieb, G., Kim, B. S., Simons, D., Bernhagen, J., & Pallua, N. (2014). MIF and CD74 - suitability as clinical biomarkers. *Mini Rev Med Chem, 14*(14), 1125-1131. https://doi.org/10.2174/1389557515666150203143317

Gurevich, V. V., & Gurevich, E. V. (2019, 2019-February-19). GPCR Signaling Regulation: The Role of GRKs and Arrestins [Review]. *Frontiers in Pharmacology, 10*(125). https://doi.org/10.3389/fphar.2019.00125

Hanlon, C. D., & Andrew, D. J. (2015). Outside-in signaling--a brief review of GPCR signaling with a focus on the Drosophila GPCR family. *Journal of cell science, 128*(19), 3533-3542. https://doi.org/10.1242/jcs.175158

Hao, H., Hu, S., Chen, H., Bu, D., Zhu, L., Xu, C., Chu, F., Huo, X., Tang, Y., Sun, X., Ding, B.-S., Liu, D.-P., Hu, S., & Wang, M. (2017). Loss of Endothelial CXCR7 Impairs Vascular Homeostasis and Cardiac Remodeling After Myocardial Infarction. *Circulation, 135*(13), 1253-1264. https://doi.org/doi:10.1161/CIRCULATIONAHA.116.023027

Hao, W., & Friedman, A. (2014). The LDL-HDL profile determines the risk of atherosclerosis: a mathematical model. *PLoS One, 9*(3), e90497-e90497. https://doi.org/10.1371/journal.pone.0090497

Harrington, J. R. (2000). The role of MCP-1 in atherosclerosis. *Stem Cells, 18*(1), 65-66. https://doi.org/10.1634/stemcells.18-1-65

Hattermann, K., Held-Feindt, J., Lucius, R., Müerköster, S. S., Penfold, M. E., Schall, T. J., & Mentlein, R. (2010, Apr 15). The chemokine receptor CXCR7 is highly expressed in human glioma cells and mediates antiapoptotic effects. *Cancer Res, 70*(8), 3299-3308. https://doi.org/10.1158/0008-5472.Can-09-3642

Herrington, W., Lacey, B., Sherliker, P., Armitage, J., & Lewington, S. (2016, 2016/02/19). Epidemiology of Atherosclerosis and the Potential to Reduce the Global Burden of Atherothrombotic Disease. *Circulation Research, 118*(4), 535-546. https://doi.org/10.1161/CIRCRESAHA.115.307611

Hughes, C. E., & Nibbs, R. J. B. (2018, Aug). A guide to chemokines and their receptors. *Febs j, 285*(16), 2944-2971. https://doi.org/10.1111/febs.14466

Huo, Y., Weber, C., Forlow, S. B., Sperandio, M., Thatte, J., Mack, M., Jung, S., Littman, D. R., & Ley, K. (2001, 11/01/). The chemokine KC, but not monocyte chemoattractant protein-1, triggers monocyte arrest on early atherosclerotic endothelium. *The Journal of Clinical Investigation, 108*(9), 1307-1314. https://doi.org/10.1172/JCI12877

Huynh, C., Henrich, A., Strasser, D. S., Boof, M.-L., Al-Ibrahim, M., Meyer Zu Schwabedissen, H. E., Dingemanse, J., & Ufer, M. (2021, 2021/06/01). A Multipurpose First-in-Human Study With the Novel CXCR7 Antagonist ACT-1004-1239 Using CXCL12 Plasma Concentrations as Target Engagement Biomarker [https://doi.org/10.1002/cpt.2154]. *Clinical Pharmacology & Therapeutics, 109*(6), 1648-1659. https://doi.org/https://doi.org/10.1002/cpt.2154

Ikeda, Y., Kumagai, H., Skach, A., Sato, M., & Yanagisawa, M. (2013). Modulation of circadian glucocorticoid oscillation via adrenal opioid-CXCR7 signaling alters emotional behavior. *Cell, 155*(6), 1323-1336. https://doi.org/10.1016/j.cell.2013.10.052

Indra, A. K., Warot, X., Brocard, J., Bornert, J. M., Xiao, J. H., Chambon, P., & Metzger, D. (1999, Nov 15). Temporally-controlled site-specific mutagenesis in the basal layer of the epidermis: comparison of the recombinase activity of the tamoxifen-inducible Cre-ER(T) and Cre-ER(T2) recombinases. *Nucleic Acids Res, 27*(22), 4324-4327. https://doi.org/10.1093/nar/27.22.4324

Ishizuka, M., Harada, M., Nomura, S., Ko, T., Ikeda, Y., Guo, J., Bujo, S., Yanagisawa-Murakami, H., Satoh, M., Yamada, S., Kumagai, H., Motozawa, Y., Hara, H., Fujiwara, T., Sato, T., Takeda, N., Takeda, N., Otsu, K., Morita, H., Toko, H., & Komuro, I. (2021, Feb 9). CXCR7 ameliorates myocardial infarction as a β-arrestin-biased receptor. *Sci Rep, 11*(1), 3426. https://doi.org/10.1038/s41598-021-83022-5

Jiang, C., Li, R., Ma, X., Hu, H., Wei, L., & Zhao, J. (2020, Oct). Plerixafor stimulates adhesive activity and endothelial regeneration of endothelial progenitor cells via elevating CXCR7 expression. *J Diabetes Complications, 34*(10), 107654. https://doi.org/10.1016/j.jdiacomp.2020.107654

Kalra, A., Yetiskul, E., Wehrle, C. J., & Tuma, F. (2021). Physiology, Liver. In *StatPearls*. StatPearls Publishing

Copyright © 2021, StatPearls Publishing LLC.

Kapas, S., & Clark, A. J. (1995, Dec 26). Identification of an orphan receptor gene as a type 1 calcitonin gene-related peptide receptor. *Biochem Biophys Res Commun, 217*(3), 832-838. https://doi.org/10.1006/bbrc.1995.2847

Karin, N. (2010, Sep). The multiple faces of CXCL12 (SDF-1alpha) in the regulation of immunity during health and disease. *J Leukoc Biol, 88*(3), 463-473. https://doi.org/10.1189/jlb.0909602

Khatana, C., Saini, N. K., Chakrabarti, S., Saini, V., Sharma, A., Saini, R. V., & Saini, A. K. (2020). Mechanistic Insights into the Oxidized Low-Density Lipoprotein-Induced Atherosclerosis. *Oxid Med Cell Longev, 2020*, 5245308. https://doi.org/10.1155/2020/5245308

Kim, H., Kim, M., Im, S.-K., & Fang, S. (2018). Mouse Cre-LoxP system: general principles to determine tissue-specific roles of target genes. *Laboratory animal research, 34*(4), 147-159. https://doi.org/10.5625/lar.2018.34.4.147

Kitamura, K., Kangawa, K., Kawamoto, M., Ichiki, Y., Nakamura, S., Matsuo, H., & Eto, T. (1993, Apr 30). Adrenomedullin: a novel hypotensive peptide isolated from human pheochromocytoma. *Biochem Biophys Res Commun, 192*(2), 553-560. https://doi.org/10.1006/bbrc.1993.1451

Klein, K. R., Karpinich, N. O., Espenschied, S. T., Willcockson, H. H., Dunworth, W. P., Hoopes, S. L., Kushner, E. J., Bautch, V. L., & Caron, K. M. (2014, Sep 8). Decoy receptor CXCR7 modulates adrenomedullin-mediated cardiac and lymphatic vascular development. *Dev Cell, 30*(5), 528-540. https://doi.org/10.1016/j.devcel.2014.07.012

Koenen, J., Bachelerie, F., Balabanian, K., Schlecht-Louf, G., & Gallego, C. (2019). Atypical Chemokine Receptor 3 (ACKR3): A Comprehensive Overview of its Expression and Potential Roles in the Immune System. *Molecular Pharmacology, 96*(6), 809. https://doi.org/10.1124/mol.118.115329

Kojima, Y., Weissman, I. L., & Leeper, N. J. (2017, Jan 31). The Role of Efferocytosis in Atherosclerosis. *Circulation, 135*(5), 476-489. https://doi.org/10.1161/circulationaha.116.025684

Krammer, C., Kontos, C., Dewor, M., Hille, K., Dalla Volta, B., El Bounkari, O., Taş, K., Sinitski, D., Brandhofer, M., Megens, R. T. A., Weber, C., Schultz, J. R., Bernhagen, J., & Kapurniotu, A. (2021, Mar 16). A MIF-Derived Cyclopeptide that Inhibits MIF Binding and Atherogenic Signaling via the Chemokine Receptor CXCR2. *Chembiochem, 22*(6), 1012-1019. https://doi.org/10.1002/cbic.202000574

Lapidot, T., & Kollet, O. (2002, 2002/10/01). The essential roles of the chemokine SDF-1 and its receptor CXCR4 in human stem cell homing and repopulation of transplanted immune-deficient NOD/SCID and NOD/SCID/B2mnull mice. *Leukemia, 16*(10), 1992-2003. https://doi.org/10.1038/sj.leu.2402684

Ledebur, H. C., & Parks, T. P. (1995, Jan 13). Transcriptional regulation of the intercellular adhesion molecule-1 gene by inflammatory cytokines in human endothelial cells. Essential roles of a variant NF-kappa B site and p65 homodimers. *J Biol Chem, 270*(2), 933-943. https://doi.org/10.1074/jbc.270.2.933

Lefkowitz, R. J., & Shenoy, S. K. (2005, Apr 22). Transduction of receptor signals by beta-arrestins. *Science, 308*(5721), 512-517. https://doi.org/10.1126/science.1109237

Lestavel, S., & Fruchart, J. C. (1994, Jun). Lipoprotein receptors. *Cell Mol Biol (Noisy-le-grand), 40*(4), 461-481.

Levi, Z., Shaish, A., Yacov, N., Levkovitz, H., Trestman, S., Gerber, Y., Cohen, H., Dvir, A., Rhachmani, R., Ravid, M., & Harats, D. (2003, Jan). Rosiglitazone (PPARgamma-agonist) attenuates atherogenesis with no effect on hyperglycaemia in a combined diabetes-atherosclerosis mouse model. *Diabetes Obes Metab, 5*(1), 45-50. https://doi.org/10.1046/j.1463-1326.2003.00240.x

Levoye, A., Balabanian, K., Baleux, F., Bachelerie, F., & Lagane, B. (2009, Jun 11). CXCR7 heterodimerizes with CXCR4 and regulates CXCL12-mediated G protein signaling. *Blood, 113*(24), 6085-6093. https://doi.org/10.1182/blood-2008-12-196618

Ley, K., Miller, Y. I., & Hedrick, C. C. (2011). Monocyte and macrophage dynamics during atherogenesis. *Arteriosclerosis, Thrombosis, and Vascular Biology, 31*(7), 1506-1516. https://doi.org/10.1161/ATVBAHA.110.221127

Li, A. C., Brown, K. K., Silvestre, M. J., Willson, T. M., Palinski, W., & Glass, C. K. (2000, Aug). Peroxisome proliferator-activated receptor gamma ligands inhibit development of atherosclerosis in LDL receptor-deficient mice. *J Clin Invest, 106*(4), 523-531. https://doi.org/10.1172/jci10370

Li, M., & Ransohoff, R. M. (2009, Apr). The roles of chemokine CXCL12 in embryonic and brain tumor angiogenesis. *Semin Cancer Biol, 19*(2), 111-115. https://doi.org/10.1016/j.semcancer.2008.11.001

Li, S., Fong, K. W., Gritsina, G., Zhang, A., Zhao, J. C., Kim, J., Sharp, A., Yuan, W., Aversa, C., Yang, X. J., Nelson, P. S., Feng, F. Y., Chinnaiyan, A. M., de Bono, J. S., Morrissey, C., Rettig, M. B., & Yu, J. (2019, May 15). Activation of MAPK Signaling by CXCR7 Leads to Enzalutamide Resistance in Prostate Cancer. *Cancer Res, 79*(10), 2580-2592. https://doi.org/10.1158/0008-5472.Can-18-2812

Li, X., Zhu, M., Penfold, M. E., Koenen, R. R., Thiemann, A., Heyll, K., Akhtar, S., Koyadan, S., Wu, Z., Gremse, F., Kiessling, F., van Zandvoort, M., Schall, T. J., Weber, C., & Schober, A. (2014, Mar 18). Activation of CXCR7 limits atherosclerosis and improves hyperlipidemia by increasing cholesterol uptake in adipose tissue. *Circulation, 129*(11), 1244-1253. https://doi.org/10.1161/circulationaha.113.006840

Libby, P., Geng, Y. J., Aikawa, M., Schoenbeck, U., Mach, F., Clinton, S. K., Sukhova, G. K., & Lee, R. T. (1996, Oct). Macrophages and atherosclerotic plaque stability. *Curr Opin Lipidol, 7*(5), 330-335. https://doi.org/10.1097/00041433-199610000-00012

Lin, L., Han, M. M., Wang, F., Xu, L. L., Yu, H. X., & Yang, P. Y. (2014, 2014/10/01). CXCR7 stimulates MAPK signaling to regulate hepatocellular carcinoma progression. *Cell Death & Disease, 5*(10), e1488-e1488. https://doi.org/10.1038/cddis.2014.392

Liu, Q., Bengmark, S., & Qu, S. (2010, 2010/04/28). The role of hepatic fat accumulation in pathogenesis of non-alcoholic fatty liver disease (NAFLD). *Lipids in Health and Disease, 9*(1), 42. https://doi.org/10.1186/1476-511X-9-42

Liu, T., Zhang, L., Joo, D., & Sun, S.-C. (2017). NF-κB signaling in inflammation. *Signal transduction and targeted therapy, 2*, 17023. https://doi.org/10.1038/sigtrans.2017.23

Lo Sasso, G., Schlage, W. K., Boué, S., Veljkovic, E., Peitsch, M. C., & Hoeng, J. (2016). The Apoe(-/-) mouse model: a suitable model to study cardiovascular and respiratory diseases in the context of cigarette smoke exposure and harm reduction. *Journal of translational medicine, 14*(1), 146-146. https://doi.org/10.1186/s12967-016-0901-1

Lue, H., Kleemann, R., Calandra, T., Roger, T., & Bernhagen, J. (2002, Apr). Macrophage migration inhibitory factor (MIF): mechanisms of action and role in disease. *Microbes Infect, 4*(4), 449-460. https://doi.org/10.1016/s1286-4579(02)01560-5

Luker, K. E., Lewin, S. A., Mihalko, L. A., Schmidt, B. T., Winkler, J. S., Coggins, N. L., Thomas, D. G., & Luker, G. D. (2012, Nov 8). Scavenging of CXCL12 by CXCR7 promotes tumor growth and metastasis of CXCR4-positive breast cancer cells. *Oncogene, 31*(45), 4750-4758. https://doi.org/10.1038/onc.2011.633

Luo, Y., Azad, A. K., Karanika, S., Basourakos, S. P., Zuo, X., Wang, J., Yang, L., Yang, G., Korentzelos, D., Yin, J., Park, S., Zhang, P., Campbell, J. J., Schall, T. J., Cao, G., Li, L., & Thompson, T. C. (2018, May 15). Enzalutamide and CXCR7 inhibitor combination treatment suppresses cell growth and angiogenic signaling in castration-resistant prostate cancer models. *Int J Cancer, 142*(10), 2163-2174. https://doi.org/10.1002/ijc.31237

Ma, D. M., Luo, D. X., & Zhang, J. (2016, Oct 6). SDF-1/CXCR7 axis regulates the proliferation, invasion, adhesion, and angiogenesis of gastric cancer cells. *World J Surg Oncol, 14*(1), 256. https://doi.org/10.1186/s12957-016-1009-z

Ma, Q., Jones, D., Borghesani, P. R., Segal, R. A., Nagasawa, T., Kishimoto, T., Bronson, R. T., & Springer, T. A. (1998, Aug 4). Impaired B-lymphopoiesis, myelopoiesis, and derailed cerebellar neuron migration in CXCR4- and SDF-1-deficient mice. *Proc Natl Acad Sci U S A, 95*(16), 9448-9453. https://doi.org/10.1073/pnas.95.16.9448

Ma, W., Liu, Y., Ellison, N., & Shen, J. (2013, May 31). Induction of C-X-C chemokine receptor type 7 (CXCR7) switches stromal cell-derived factor-1 (SDF-1) signaling and phagocytic activity in macrophages linked to atherosclerosis. *J Biol Chem, 288*(22), 15481-15494. https://doi.org/10.1074/jbc.M112.445510

Maguire, E. M., Pearce, S. W. A., & Xiao, Q. (2019, Jan). Foam cell formation: A new target for fighting atherosclerosis and cardiovascular disease. *Vascul Pharmacol, 112*, 54-71. https://doi.org/10.1016/j.vph.2018.08.002

Mahley, R. W., Innerarity, T. L., Rall, S. C., Jr., & Weisgraber, K. H. (1984, Dec 1). Plasma lipoproteins: apolipoprotein structure and function. *J Lipid Res, 25*(12), 1277-1294.

Malekmohammad, K., Bezsonov, E. E., & Rafieian-Kopaei, M. (2021). Role of Lipid Accumulation and Inflammation in Atherosclerosis: Focus on Molecular and Cellular Mechanisms. *Front Cardiovasc Med, 8*, 707529. https://doi.org/10.3389/fcvm.2021.707529

Mansbach, C. M., & Siddiqi, S. A. (2010). The biogenesis of chylomicrons. *Annual review of physiology, 72*, 315-333. https://doi.org/10.1146/annurev-physiol-021909-135801

Marinissen, M. J., & Gutkind, J. S. (2001, Jul). G-protein-coupled receptors and signaling networks: emerging paradigms. *Trends Pharmacol Sci, 22*(7), 368-376. https://doi.org/10.1016/s0165-6147(00)01678-3

Matafome, P., & Seiça, R. (2017). Function and Dysfunction of Adipose Tissue. *Adv Neurobiol, 19*, 3-31. https://doi.org/10.1007/978-3-319-63260-5_1

Mazurek, R., Dave, J. M., Chandran, R. R., Misra, A., Sheikh, A. Q., & Greif, D. M. (2017). Vascular Cells in Blood Vessel Wall Development and Disease. *Advances in pharmacology (San Diego, Calif.), 78*, 323-350. https://doi.org/10.1016/bs.apha.2016.08.001

Menhaji-Klotz, E., Ward, J., Brown, J. A., Loria, P. M., Tan, C., Hesp, K. D., Riccardi, K. A., Litchfield, J., & Boehm, M. (2020, 2020/06/11). Discovery of Diphenylacetamides as CXCR7 Inhibitors with Novel β-Arrestin Antagonist Activity. *ACS Medicinal Chemistry Letters, 11*(6), 1330-1334. https://doi.org/10.1021/acsmedchemlett.0c00163

Metzemaekers, M., Vanheule, V., Janssens, R., Struyf, S., & Proost, P. (2018, 2018-January-15). Overview of the Mechanisms that May Contribute to the Non-Redundant Activities of Interferon-Inducible CXC Chemokine Receptor 3 Ligands [Review]. *Frontiers in Immunology, 8*(1970). https://doi.org/10.3389/fimmu.2017.01970

Metzger, D., & Chambon, P. (2001, May). Site- and time-specific gene targeting in the mouse. *Methods, 24*(1), 71-80. https://doi.org/10.1006/meth.2001.1159

Meyrath, M., Szpakowska, M., Zeiner, J., Massotte, L., Merz, M. P., Benkel, T., Simon, K., Ohnmacht, J., Turner, J. D., Krüger, R., Seutin, V., Ollert, M., Kostenis, E., & Chevigné, A. (2020, 2020/06/19). The atypical chemokine receptor ACKR3/CXCR7 is a broad-spectrum scavenger for opioid peptides. *Nature Communications, 11*(1), 3033. https://doi.org/10.1038/s41467-020-16664-0

Miao, Z., Luker, K. E., Summers, B. C., Berahovich, R., Bhojani, M. S., Rehemtulla, A., Kleer, C. G., Essner, J. J., Nasevicius, A., Luker, G. D., Howard, M. C., & Schall, T. J. (2007). CXCR7 (RDC1) promotes breast and lung tumor growth in vivo and is expressed on tumor-associated vasculature. *Proceedings of the National Academy of Sciences, 104*(40), 15735. https://doi.org/10.1073/pnas.0610444104

Moghimi, S. M., & Szebeni, J. (2003, Nov). Stealth liposomes and long circulating nanoparticles: critical issues in pharmacokinetics, opsonization and protein-binding properties. *Prog Lipid Res, 42*(6), 463-478. https://doi.org/10.1016/s0163-7827(03)00033-x

Nadkarni, S. K., Bouma, B. E., de Boer, J., & Tearney, G. J. (2009). Evaluation of collagen in atherosclerotic plaques: the use of two coherent laser-based imaging methods. *Lasers in medical science, 24*(3), 439-445. https://doi.org/10.1007/s10103-007-0535-x

Nagasawa, T. (2007). The chemokine CXCL12 and regulation of HSC and B lymphocyte development in the bone marrow niche. *Adv Exp Med Biol, 602*, 69-75. https://doi.org/10.1007/978-0-387-72009-8_9

Naghavi, M., Libby, P., Falk, E., Casscells, S. W., Litovsky, S., Rumberger, J., Badimon, J. J., Stefanadis, C., Moreno, P., Pasterkamp, G., Fayad, Z., Stone, P. H., Waxman, S., Raggi, P., Madjid, M., Zarrabi, A., Burke, A., Yuan, C., Fitzgerald, P. J., Siscovick, D. S., de Korte, C. L., Aikawa, M., Juhani Airaksinen, K. E., Assmann, G., Becker, C. R., Chesebro, J. H., Farb, A., Galis, Z. S., Jackson, C., Jang, I. K., Koenig, W., Lodder, R. A., March, K., Demirovic, J., Navab, M., Priori, S. G., Rekhter, M. D., Bahr, R., Grundy, S. M., Mehran, R., Colombo, A., Boerwinkle, E., Ballantyne, C., Insull, W., Jr., Schwartz, R. S., Vogel, R., Serruys, P. W., Hansson, G. K., Faxon, D. P., Kaul, S., Drexler, H., Greenland, P., Muller, J. E., Virmani, R., Ridker, P. M., Zipes, D. P., Shah, P. K., & Willerson, J. T.

(2003, Oct 7). From vulnerable plaque to vulnerable patient: a call for new definitions and risk assessment strategies: Part I. *Circulation, 108*(14), 1664-1672. https://doi.org/10.1161/01.Cir.0000087480.94275.97

Naumann, U., Cameroni, E., Pruenster, M., Mahabaleshwar, H., Raz, E., Zerwes, H. G., Rot, A., & Thelen, M. (2010, Feb 11). CXCR7 functions as a scavenger for CXCL12 and CXCL11. *PLoS One, 5*(2), e9175. https://doi.org/10.1371/journal.pone.0009175

Nelson, R. H. (2013). Hyperlipidemia as a risk factor for cardiovascular disease. *Primary care, 40*(1), 195-211. https://doi.org/10.1016/j.pop.2012.11.003

Neusser, M. A., Kraus, A. K., Regele, H., Cohen, C. D., Fehr, T., Kerjaschki, D., Wüthrich, R. P., Penfold, M. E. T., Schall, T., & Segerer, S. (2010, 2010/05/01/). The chemokine receptor CXCR7 is expressed on lymphatic endothelial cells during renal allograft rejection. *Kidney International, 77*(9), 801-808. https://doi.org/https://doi.org/10.1038/ki.2010.6

Ngamsri, K.-C., Jans, C., Putri, R. A., Schindler, K., Gamper-Tsigaras, J., Eggstein, C., Köhler, D., & Konrad, F. M. (2020, 2020-March-10). Inhibition of CXCR4 and CXCR7 Is Protective in Acute Peritoneal Inflammation [Original Research]. *Frontiers in Immunology, 11*(407). https://doi.org/10.3389/fimmu.2020.00407

Ngamsri, K.-C., Müller, A., Bösmüller, H., Gamper-Tsigaras, J., Reutershan, J., & Konrad, F. M. (2017). The Pivotal Role of CXCR7 in Stabilization of the Pulmonary Epithelial Barrier in Acute Pulmonary Inflammation. *The Journal of Immunology, 198*(6), 2403-2413. https://doi.org/10.4049/jimmunol.1601682

Nguyen, H. T., Reyes-Alcaraz, A., Yong, H. J., Nguyen, L. P., Park, H. K., Inoue, A., Lee, C. S., Seong, J. Y., & Hwang, J. I. (2020, Nov 23). CXCR7: a β-arrestin-biased receptor that potentiates cell migration and recruits β-arrestin2 exclusively through Gβγ subunits and GRK2. *Cell Biosci, 10*(1), 134. https://doi.org/10.1186/s13578-020-00497-x

Ochoa, C. D., & Stevens, T. (2012, Feb 1). Studies on the cell biology of interendothelial cell gaps. *Am J Physiol Lung Cell Mol Physiol, 302*(3), L275-286. https://doi.org/10.1152/ajplung.00215.2011

Oda, E. (2008, 2008/07/01). The Metabolic Syndrome as a Concept of Adipose Tissue Disease. *Hypertension Research, 31*(7), 1283-1291. https://doi.org/10.1291/hypres.31.1283

Odemis, V., Lipfert, J., Kraft, R., Hajek, P., Abraham, G., Hattermann, K., Mentlein, R., & Engele, J. (2012, Mar). The presumed atypical chemokine receptor CXCR7 signals through G(i/o) proteins in primary rodent astrocytes and human glioma cells. *Glia, 60*(3), 372-381. https://doi.org/10.1002/glia.22271

Olson, R. E. (1998, Feb). Discovery of the lipoproteins, their role in fat transport and their significance as risk factors. *J Nutr, 128*(2 Suppl), 439s-443s. https://doi.org/10.1093/jn/128.2.439S

Pan, J.-H., Sukhova, G. K., Yang, J.-T., Wang, B., Xie, T., Fu, H., Zhang, Y., Satoskar, A. R., David, J. R., Metz, C. N., Bucala, R., Fang, K., Simon, D. I., Chapman, H. A., Libby, P., & Shi, G.-P. (2004, 2004/06/29). Macrophage Migration Inhibitory Factor Deficiency

Impairs Atherosclerosis in Low-Density Lipoprotein Receptor-Deficient Mice. *Circulation, 109*(25), 3149-3153. https://doi.org/10.1161/01.CIR.0000134704.84454.D2

Pasceri, V., Wu, H. D., Willerson, J. T., & Yeh, E. T. H. (2000). Modulation of Vascular Inflammation In Vitro and In Vivo by Peroxisome Proliferator–Activated Receptor-γ Activators. *Circulation, 101*(3), 235-238. https://doi.org/doi:10.1161/01.CIR.101.3.235

Peng, H., Zhang, H., & Zhu, H. (2016, Oct 28). Blocking CXCR7-mediated adipose tissue macrophages chemotaxis attenuates insulin resistance and inflammation in obesity. *Biochem Biophys Res Commun, 479*(4), 649-655. https://doi.org/10.1016/j.bbrc.2016.09.158

Pirillo, A., Norata, G. D., & Catapano, A. L. (2013). LOX-1, OxLDL, and atherosclerosis. *Mediators of inflammation, 2013*, 152786-152786. https://doi.org/10.1155/2013/152786

Pittius, C. W., Seizinger, B. R., Pasi, A., Mehraein, P., & Herz, A. (1984, Jun 18). Distribution and characterization of opioid peptides derived from proenkephalin A in human and rat central nervous system. *Brain Res, 304*(1), 127-136. https://doi.org/10.1016/0006-8993(84)90868-0

Pruenster, M., Mudde, L., Bombosi, P., Dimitrova, S., Zsak, M., Middleton, J., Richmond, A., Graham, G. J., Segerer, S., Nibbs, R. J., & Rot, A. (2009, Jan). The Duffy antigen receptor for chemokines transports chemokines and supports their promigratory activity. *Nat Immunol, 10*(1), 101-108. https://doi.org/10.1038/ni.1675

Puchert, M., Obst, J., Koch, C., Zieger, K., & Engele, J. (2020, 2020/01/01/). CXCL11 promotes tumor progression by the biased use of the chemokine receptors CXCR3 and CXCR7. *Cytokine, 125*, 154809. https://doi.org/https://doi.org/10.1016/j.cyto.2019.154809

Puchert, M., Pelkner, F., Stein, G., Angelov, D. N., Boltze, J., Wagner, D. C., Odoardi, F., Flügel, A., Streit, W. J., & Engele, J. (2017, Dec). Astrocytic expression of the CXCL12 receptor, CXCR7/ACKR3 is a hallmark of the diseased, but not developing CNS. *Mol Cell Neurosci, 85*, 105-118. https://doi.org/10.1016/j.mcn.2017.09.001

Qian, T., Liu, Y., Dong, Y., Zhang, L., Dong, Y., Sun, Y., & Sun, D. (2018, Mar). CXCR7 regulates breast tumor metastasis and angiogenesis in vivo and in vitro. *Mol Med Rep, 17*(3), 3633-3639. https://doi.org/10.3892/mmr.2017.8286

Quinn, K. E., Mackie, D. I., & Caron, K. M. (2018). Emerging roles of atypical chemokine receptor 3 (ACKR3) in normal development and physiology. *Cytokine, 109*, 17-23. https://doi.org/10.1016/j.cyto.2018.02.024

Rafiei, S., Gui, B., Wu, J., Liu, X. S., Kibel, A. S., & Jia, L. (2019). Targeting the MIF/CXCR7/AKT Signaling Pathway in Castration-Resistant Prostate Cancer. *Molecular cancer research : MCR, 17*(1), 263-276. https://doi.org/10.1158/1541-7786.MCR-18-0412

Rafieian-Kopaei, M., Setorki, M., Doudi, M., Baradaran, A., & Nasri, H. (2014). Atherosclerosis: process, indicators, risk factors and new hopes. *International journal of preventive medicine, 5*(8), 927-946. https://pubmed.ncbi.nlm.nih.gov/25489440

Rajagopal, S., Kim, J., Ahn, S., Craig, S., Lam, C. M., Gerard, N. P., Gerard, C., & Lefkowitz, R. J. (2010, Jan 12). Beta-arrestin- but not G protein-mediated signaling by the "decoy" receptor CXCR7. *Proc Natl Acad Sci U S A, 107*(2), 628-632. https://doi.org/10.1073/pnas.0912852107

Raman, D., Sobolik-Delmaire, T., & Richmond, A. (2011). Chemokines in health and disease. *Experimental cell research, 317*(5), 575-589. https://doi.org/10.1016/j.yexcr.2011.01.005

Randolph, G. J. (2009). The fate of monocytes in atherosclerosis. *Journal of thrombosis and haemostasis : JTH, 7 Suppl 1*(Suppl 1), 28-30. https://doi.org/10.1111/j.1538-7836.2009.03423.x

Rekhter, M. D. (1999). Collagen synthesis in atherosclerosis: too much and not enough. *Cardiovascular Research, 41*(2), 376-384. https://doi.org/10.1016/s0008-6363(98)00321-6

Remels, A. H., Langen, R. C., Gosker, H. R., Russell, A. P., Spaapen, F., Voncken, J. W., Schrauwen, P., & Schols, A. M. (2009, Jul). PPARgamma inhibits NF-kappaB-dependent transcriptional activation in skeletal muscle. *Am J Physiol Endocrinol Metab, 297*(1), E174-183. https://doi.org/10.1152/ajpendo.90632.2008

Richard-Bildstein, S., Aissaoui, H., Pothier, J., Schäfer, G., Gnerre, C., Lindenberg, E., Lehembre, F., Pouzol, L., & Guerry, P. (2020, Dec 24). Discovery of the Potent, Selective, Orally Available CXCR7 Antagonist ACT-1004-1239. *J Med Chem, 63*(24), 15864-15882. https://doi.org/10.1021/acs.jmedchem.0c01588

Ridker, P. M., Everett, B. M., Thuren, T., MacFadyen, J. G., Chang, W. H., Ballantyne, C., Fonseca, F., Nicolau, J., Koenig, W., Anker, S. D., Kastelein, J. J. P., Cornel, J. H., Pais, P., Pella, D., Genest, J., Cifkova, R., Lorenzatti, A., Forster, T., Kobalava, Z., Vida-Simiti, L., Flather, M., Shimokawa, H., Ogawa, H., Dellborg, M., Rossi, P. R. F., Troquay, R. P. T., Libby, P., & Glynn, R. J. (2017). Antiinflammatory Therapy with Canakinumab for Atherosclerotic Disease. *New England Journal of Medicine, 377*(12), 1119-1131. https://doi.org/10.1056/NEJMoa1707914

Samani, N. J., Erdmann, J., Hall, A. S., Hengstenberg, C., Mangino, M., Mayer, B., Dixon, R. J., Meitinger, T., Braund, P., Wichmann, H. E., Barrett, J. H., König, I. R., Stevens, S. E., Szymczak, S., Tregouet, D. A., Iles, M. M., Pahlke, F., Pollard, H., Lieb, W., Cambien, F., Fischer, M., Ouwehand, W., Blankenberg, S., Balmforth, A. J., Baessler, A., Ball, S. G., Strom, T. M., Braenne, I., Gieger, C., Deloukas, P., Tobin, M. D., Ziegler, A., Thompson, J. R., & Schunkert, H. (2007, Aug 2). Genomewide association analysis of coronary artery disease. *N Engl J Med, 357*(5), 443-453. https://doi.org/10.1056/NEJMoa072366

Sánchez-Martín, L., Sánchez-Mateos, P., & Cabañas, C. (2013, Jan). CXCR7 impact on CXCL12 biology and disease. *Trends Mol Med, 19*(1), 12-22. https://doi.org/10.1016/j.molmed.2012.10.004

Sartina, E., Suguihara, C., Ramchandran, S., Nwajei, P., Rodriguez, M., Torres, E., Hehre, D., Devia, C., Walters, M. J., Penfold, M. E., & Young, K. C. (2012, Jun). Antagonism of CXCR7 attenuates chronic hypoxia-induced pulmonary hypertension. *Pediatr Res, 71*(6), 682-688. https://doi.org/10.1038/pr.2012.30

Sasaki, M., Jordan, P., Welbourne, T., Minagar, A., Joh, T., Itoh, M., Elrod, J. W., & Alexander, J. S. (2005, 2005/02/06). Troglitazone, a PPAR-γ activator prevents endothelial cell adhesion molecule expression and lymphocyte adhesion mediated by TNF-α. *BMC Physiology, 5*(1), 3. https://doi.org/10.1186/1472-6793-5-3

Schober, A., Bernhagen, J., Thiele, M., Zeiffer, U., Knarren, S., Roller, M., Bucala, R., & Weber, C. (2004, 2004/01/27). Stabilization of Atherosclerotic Plaques by Blockade of Macrophage Migration Inhibitory Factor After Vascular Injury in Apolipoprotein E–Deficient Mice. *Circulation, 109*(3), 380-385. https://doi.org/10.1161/01.CIR.0000109201.72441.09

Schober, A., Bernhagen, J., & Weber, C. (2008, Jul). Chemokine-like functions of MIF in atherosclerosis. *Journal of molecular medicine (Berlin, Germany), 86*(7), 761-770. https://doi.org/10.1007/s00109-008-0334-2

Schober, A., Manka, D., von Hundelshausen, P., Huo, Y., Hanrath, P., Sarembock, I. J., Ley, K., & Weber, C. (2002, 2002/09/17). Deposition of Platelet RANTES Triggering Monocyte Recruitment Requires P-Selectin and Is Involved in Neointima Formation After Arterial Injury. *Circulation, 106*(12), 1523-1529. https://doi.org/10.1161/01.CIR.0000028590.02477.6F

Schrevel, M., Karim, R., ter Haar, N. T., van der Burg, S. H., Trimbos, J. B., Fleuren, G. J., Gorter, A., & Jordanova, E. S. (2012, Apr 24). CXCR7 expression is associated with disease-free and disease-specific survival in cervical cancer patients. *Br J Cancer, 106*(9), 1520-1525. https://doi.org/10.1038/bjc.2012.110

Schwartz, C. J., Valente, A. J., Sprague, E. A., Kelley, J. L., & Nerem, R. M. (1991, Feb). The pathogenesis of atherosclerosis: an overview. *Clin Cardiol, 14*(2 Suppl 1), I1-16. https://doi.org/10.1002/clc.4960141302

Scirpo, R., Fiorotto, R., Villani, A., Amenduni, M., Spirli, C., & Strazzabosco, M. (2015). Stimulation of nuclear receptor peroxisome proliferator-activated receptor-γ limits NF-κB-dependent inflammation in mouse cystic fibrosis biliary epithelium. *Hepatology (Baltimore, Md.), 62*(5), 1551-1562. https://doi.org/10.1002/hep.28000

Seimon, T., & Tabas, I. (2009). Mechanisms and consequences of macrophage apoptosis in atherosclerosis. *Journal of lipid research, 50 Suppl*(Suppl), S382-S387. https://doi.org/10.1194/jlr.R800032-JLR200

Seneviratne, A., Hulsmans, M., Holvoet, P., & Monaco, C. (2013). Biomechanical factors and macrophages in plaque stability. *Cardiovascular Research, 99*(2), 284-293. https://doi.org/10.1093/cvr/cvt097

Shi, S., Yu, G., Huang, B., Mi, Y., Kang, Y., & Simon, J. P. (2020, 2020/06/01). PPARG Could Work as a Valid Therapeutic Strategy for the Treatment of Lung Squamous Cell Carcinoma. *PPAR Research, 2020*, 2510951. https://doi.org/10.1155/2020/2510951

Shimizu, N., Soda, Y., Kanbe, K., Liu, H.-y., Mukai, R., Kitamura, T., & Hoshino, H. (2000, 2000/01/15). A Putative G Protein-Coupled Receptor, RDC1, Is a Novel Coreceptor for

Human and Simian Immunodeficiency Viruses. *Journal of Virology, 74*(2), 619-626. https://doi.org/10.1128/JVI.74.2.619-626.2000

Shimizu, S., Brown, M., Sengupta, R., Penfold, M. E., & Meucci, O. (2011). CXCR7 protein expression in human adult brain and differentiated neurons. *PLoS One, 6*(5), e20680. https://doi.org/10.1371/journal.pone.0020680

Shu, H. B., Agranoff, A. B., Nabel, E. G., Leung, K., Duckett, C. S., Neish, A. S., Collins, T., & Nabel, G. J. (1993, 1993/10//). Differential regulation of vascular cell adhesion molecule 1 gene expression by specific NF-kappa B subunits in endothelial and epithelial cells. *Molecular and cellular biology, 13*(10), 6283-6289. https://doi.org/10.1128/mcb.13.10.6283-6289.1993

Sierro, F., Biben, C., Martínez-Muñoz, L., Mellado, M., Ransohoff, R. M., Li, M., Woehl, B., Leung, H., Groom, J., Batten, M., Harvey, R. P., Martínez, A. C., Mackay, C. R., & Mackay, F. (2007, Sep 11). Disrupted cardiac development but normal hematopoiesis in mice deficient in the second CXCL12/SDF-1 receptor, CXCR7. *Proc Natl Acad Sci U S A, 104*(37), 14759-14764. https://doi.org/10.1073/pnas.0702229104

Simone, E., Ding, B.-S., & Muzykantov, V. (2009). Targeted delivery of therapeutics to endothelium. *Cell and tissue research, 335*(1), 283-300. https://doi.org/10.1007/s00441-008-0676-7

Sinitski, D., Kontos, C., Krammer, C., Asare, Y., Kapurniotu, A., & Bernhagen, J. (2019, Apr). Macrophage Migration Inhibitory Factor (MIF)-Based Therapeutic Concepts in Atherosclerosis and Inflammation. *Thromb Haemost, 119*(4), 553-566. https://doi.org/10.1055/s-0039-1677803

Sluiter, T. J., van Buul, J. D., Huveneers, S., Quax, P. H. A., & de Vries, M. R. (2021, Mar 24). Endothelial Barrier Function and Leukocyte Transmigration in Atherosclerosis. *Biomedicines, 9*(4). https://doi.org/10.3390/biomedicines9040328

Smit, M. J., Schlecht-Louf, G., Neves, M., van den Bor, J., Penela, P., Siderius, M., Bachelerie, F., & Mayor, F. (2021, 2021/01/06). The CXCL12/CXCR4/ACKR3 Axis in the Tumor Microenvironment: Signaling, Crosstalk, and Therapeutic Targeting. *Annual Review of Pharmacology and Toxicology, 61*(1), 541-563. https://doi.org/10.1146/annurev-pharmtox-010919-023340

Soehnlein, O., Drechsler, M., Döring, Y., Lievens, D., Hartwig, H., Kemmerich, K., Ortega-Gómez, A., Mandl, M., Vijayan, S., Projahn, D., Garlichs, C. D., Koenen, R. R., Hristov, M., Lutgens, E., Zernecke, A., & Weber, C. (2013, 2013/03/01). Distinct functions of chemokine receptor axes in the atherogenic mobilization and recruitment of classical monocytes [https://doi.org/10.1002/emmm.201201717]. *EMBO Molecular Medicine, 5*(3), 471-481. https://doi.org/https://doi.org/10.1002/emmm.201201717

Soran, H., Adam, S., Mohammad, J. B., Ho, J. H., Schofield, J. D., Kwok, S., Siahmansur, T., Liu, Y., Syed, A. A., Dhage, S. S., Stefanutti, C., Donn, R., Malik, R. A., Banach, M., & Durrington, P. N. (2018). Hypercholesterolaemia - practical information for non-specialists. *Archives of medical science : AMS, 14*(1), 1-21. https://doi.org/10.5114/aoms.2018.72238

Stary, H. C., Chandler, A. B., Glagov, S., Guyton, J. R., Insull, W., Jr., Rosenfeld, M. E., Schaffer, S. A., Schwartz, C. J., Wagner, W. D., & Wissler, R. W. (1994, May). A definition of initial, fatty streak, and intermediate lesions of atherosclerosis. A report from the Committee on Vascular Lesions of the Council on Arteriosclerosis, American Heart Association. *Circulation, 89*(5), 2462-2478. https://doi.org/10.1161/01.cir.89.5.2462

Steinl, D. C., & Kaufmann, B. A. (2015). Ultrasound Imaging for Risk Assessment in Atherosclerosis. *International journal of molecular sciences, 16*(5), 9749-9769. https://www.mdpi.com/1422-0067/16/5/9749

Subbotin, V. M. (2016, 2016/10/01/). Excessive intimal hyperplasia in human coronary arteries before intimal lipid depositions is the initiation of coronary atherosclerosis and constitutes a therapeutic target. *Drug Discovery Today, 21*(10), 1578-1595. https://doi.org/https://doi.org/10.1016/j.drudis.2016.05.017

Sukonina, V., Lookene, A., Olivecrona, T., & Olivecrona, G. (2006, Nov 14). Angiopoietin-like protein 4 converts lipoprotein lipase to inactive monomers and modulates lipase activity in adipose tissue. *Proc Natl Acad Sci U S A, 103*(46), 17450-17455. https://doi.org/10.1073/pnas.0604026103

Sung, B., Park, S., Yu, B. P., & Chung, H. Y. (2006, Jun). Amelioration of age-related inflammation and oxidative stress by PPARgamma activator: suppression of NF-kappaB by 2,4-thiazolidinedione. *Exp Gerontol, 41*(6), 590-599. https://doi.org/10.1016/j.exger.2006.04.005

Tachibana, K., Hirota, S., Iizasa, H., Yoshida, H., Kawabata, K., Kataoka, Y., Kitamura, Y., Matsushima, K., Yoshida, N., Nishikawa, S., Kishimoto, T., & Nagasawa, T. (1998, Jun 11). The chemokine receptor CXCR4 is essential for vascularization of the gastrointestinal tract. *Nature, 393*(6685), 591-594. https://doi.org/10.1038/31261

Taher, J., Farr, S., & Adeli, K. (2017, Feb). Central nervous system regulation of hepatic lipid and lipoprotein metabolism. *Curr Opin Lipidol, 28*(1), 32-38. https://doi.org/10.1097/mol.0000000000000373

Tall, A. R. (1998, Feb). An overview of reverse cholesterol transport. *Eur Heart J, 19 Suppl A*, A31-35.

Tamanini, A., Rolfini, R., Nicolis, E., Melotti, P., & Cabrini, G. (2003, 2003/03/15/). MAP kinases and NF-κB collaborate to induce ICAM-1 gene expression in the early phase of adenovirus infection. *Virology, 307*(2), 228-242. https://doi.org/https://doi.org/10.1016/S0042-6822(02)00078-8

Tarnowski, M., Grymula, K., Reca, R., Jankowski, K., Maksym, R., Tarnowska, J., Przybylski, G., Barr, F. G., Kucia, M., & Ratajczak, M. Z. (2010). Regulation of Expression of Stromal-Derived Factor-1 Receptors: CXCR4 and CXCR7 in Human Rhabdomyosarcomas. *Molecular Cancer Research, 8*(1), 1-14. https://doi.org/10.1158/1541-7786.Mcr-09-0259

Tokunaga, R., Zhang, W., Naseem, M., Puccini, A., Berger, M. D., Soni, S., McSkane, M., Baba, H., & Lenz, H. J. (2018, Feb). CXCL9, CXCL10, CXCL11/CXCR3 axis for immune activation - A target for novel cancer therapy. *Cancer Treat Rev, 63*, 40-47. https://doi.org/10.1016/j.ctrv.2017.11.007

Torraca, V., Cui, C., Boland, R., Bebelman, J. P., van der Sar, A. M., Smit, M. J., Siderius, M., Spaink, H. P., & Meijer, A. H. (2015, Mar). The CXCR3-CXCL11 signaling axis mediates macrophage recruitment and dissemination of mycobacterial infection. *Dis Model Mech, 8*(3), 253-269. https://doi.org/10.1242/dmm.017756

Toth, P. P. (2008). Subclinical atherosclerosis: what it is, what it means and what we can do about it. *International journal of clinical practice, 62*(8), 1246-1254. https://doi.org/10.1111/j.1742-1241.2008.01804.x

Tripathi, D. K., & Poluri, K. M. (2020, Mar 1). Molecular insights into kinase mediated signaling pathways of chemokines and their cognate G protein coupled receptors. *Front Biosci (Landmark Ed), 25*, 1361-1385. https://doi.org/10.2741/4860

Ulvmar, M. H., Hub, E., & Rot, A. (2011). Atypical chemokine receptors. *Experimental cell research, 317*(5), 556-568. https://doi.org/10.1016/j.yexcr.2011.01.012

van der Vorst, E. P. C., Döring, Y., & Weber, C. (2015, 2015-July-21). MIF and CXCL12 in Cardiovascular Diseases: Functional Differences and Similarities [Review]. *Frontiers in Immunology, 6*(373). https://doi.org/10.3389/fimmu.2015.00373

van der Vorst, E. P. C., Maas, S. L., Ortega-Gomez, A., Hameleers, J. M. M., Bianchini, M., Asare, Y., Soehnlein, O., Döring, Y., Weber, C., & Megens, R. T. A. (2017). Functional ex-vivo Imaging of Arterial Cellular Recruitment and Lipid Extravasation. *Bio-protocol, 7*(12), 2344. https://doi.org/10.21769/BioProtoc.2344

van der Vorst, E. P. C., Peters, L. J. F., Muller, M., Gencer, S., Yan, Y., Weber, C., & Doring, Y. (2019). G-Protein Coupled Receptor Targeting on Myeloid Cells in Atherosclerosis. *Front Pharmacol, 10*, 531. https://doi.org/10.3389/fphar.2019.00531

van Greevenbroek, M. M. J., Schalkwijk, C. G., & Stehouwer, C. D. A. (2016). Dysfunctional adipose tissue and low-grade inflammation in the management of the metabolic syndrome: current practices and future advances. *F1000Research, 5*, F1000 Faculty Rev-2515. https://doi.org/10.12688/f1000research.8971.1

Van Raemdonck, K., Van den Steen, P. E., Liekens, S., Van Damme, J., & Struyf, S. (2015, Jun). CXCR3 ligands in disease and therapy. *Cytokine Growth Factor Rev, 26*(3), 311-327. https://doi.org/10.1016/j.cytogfr.2014.11.009

van Wanrooij, E. J. A., de Jager, S. C. A., van Es, T., de Vos, P., Birch, H. L., Owen, D. A., Watson, R. J., Biessen, E. A. L., Chapman, G. A., van Berkel, T. J. C., & Kuiper, J. (2008, 2008/02/01). CXCR3 Antagonist NBI-74330 Attenuates Atherosclerotic Plaque Formation in LDL Receptor–Deficient Mice. *Arteriosclerosis, Thrombosis, and Vascular Biology, 28*(2), 251-257. https://doi.org/10.1161/ATVBAHA.107.147827

Varghese, J. F., Patel, R., & Yadav, U. C. S. (2018, Mar 14). Novel Insights in the Metabolic Syndrome-induced Oxidative Stress and Inflammation-mediated Atherosclerosis. *Curr Cardiol Rev, 14*(1), 4-14. https://doi.org/10.2174/1573403x13666171009112250

Veillard, N. R., Steffens, S., Pelli, G., Lu, B., Kwak, B. R., Gerard, C., Charo, I. F., & Mach, F. (2005, 2005/08/09). Differential Influence of Chemokine Receptors CCR2 and CXCR3 in Development of Atherosclerosis In Vivo. *Circulation, 112*(6), 870-878. https://doi.org/10.1161/CIRCULATIONAHA.104.520718

von Hundelshausen, P., Weber, K. S. C., Huo, Y., Proudfoot, A. E. I., Nelson, P. J., Ley, K., & Weber, C. (2001, 2001/04/03). RANTES Deposition by Platelets Triggers Monocyte Arrest on Inflamed and Atherosclerotic Endothelium. *Circulation, 103*(13), 1772-1777. https://doi.org/10.1161/01.CIR.103.13.1772

Wang, C., Chen, W., & Shen, J. (2018, 2018-June-21). CXCR7 Targeting and Its Major Disease Relevance [Review]. *Frontiers in Pharmacology, 9*(641). https://doi.org/10.3389/fphar.2018.00641

Wang, H., Beaty, N., Chen, S., Qi, C. F., Masiuk, M., Shin, D. M., & Morse, H. C., 3rd. (2012, Jan 12). The CXCR7 chemokine receptor promotes B-cell retention in the splenic marginal zone and serves as a sink for CXCL12. *Blood, 119*(2), 465-468. https://doi.org/10.1182/blood-2011-03-343608

Watanabe, K., Penfold, M. E., Matsuda, A., Ohyanagi, N., Kaneko, K., Miyabe, Y., Matsumoto, K., Schall, T. J., Miyasaka, N., & Nanki, T. (2010, Nov). Pathogenic role of CXCR7 in rheumatoid arthritis. *Arthritis Rheum, 62*(11), 3211-3220. https://doi.org/10.1002/art.27650

Weber, C. (2005, Apr 1). Platelets and chemokines in atherosclerosis: partners in crime. *Circ Res, 96*(6), 612-616. https://doi.org/10.1161/01.Res.0000160077.17427.57

Weber, C., Meiler, S., Döring, Y., Koch, M., Drechsler, M., Megens, R. T., Rowinska, Z., Bidzhekov, K., Fecher, C., Ribechini, E., van Zandvoort, M. A., Binder, C. J., Jelinek, I., Hristov, M., Boon, L., Jung, S., Korn, T., Lutz, M. B., Förster, I., Zenke, M., Hieronymus, T., Junt, T., & Zernecke, A. (2011, Jul). CCL17-expressing dendritic cells drive atherosclerosis by restraining regulatory T cell homeostasis in mice. *J Clin Invest, 121*(7), 2898-2910. https://doi.org/10.1172/jci44925

Weber, C., & Noels, H. (2011, Nov 7). Atherosclerosis: current pathogenesis and therapeutic options. *Nat Med, 17*(11), 1410-1422. https://doi.org/10.1038/nm.2538

Werner, L., Elad, H., Brazowski, E., Tulchinsky, H., Vigodman, S., Kopylov, U., Halpern, Z., Guzner-Gur, H., & Dotan, I. (2011, Sep). Reciprocal regulation of CXCR4 and CXCR7 in intestinal mucosal homeostasis and inflammatory bowel disease. *J Leukoc Biol, 90*(3), 583-590. https://doi.org/10.1189/jlb.0111101

Wesley, R. B., 2nd, Meng, X., Godin, D., & Galis, Z. S. (1998, Mar). Extracellular matrix modulates macrophage functions characteristic to atheroma: collagen type I enhances acquisition of resident macrophage traits by human peripheral blood monocytes in vitro. *Arterioscler Thromb Vasc Biol, 18*(3), 432-440. https://doi.org/10.1161/01.atv.18.3.432

Wetzel-Strong, S. E., Li, M., Klein, K. R., Nishikimi, T., & Caron, K. M. (2014, Feb). Epicardial-derived adrenomedullin drives cardiac hyperplasia during embryogenesis. *Developmental dynamics : an official publication of the American Association of Anatomists, 243*(2), 243-256. https://doi.org/10.1002/dvdy.24065

Widney, D. P., Xia, Y.-R., Lusis, A. J., & Smith, J. B. (2000). The Murine Chemokine CXCL11 (IFN-Inducible T Cell α Chemoattractant) Is an IFN-γ- and Lipopolysaccharide- Inducible Glucocorticoid-Attenuated Response Gene Expressed in Lung and Other Tissues During Endotoxemia. *The Journal of Immunology, 164*(12), 6322. https://doi.org/10.4049/jimmunol.164.12.6322

Winter, C., Silvestre-Roig, C., Ortega-Gomez, A., Lemnitzer, P., Poelman, H., Schumski, A., Winter, J., Drechsler, M., de Jong, R., Immler, R., Sperandio, M., Hristov, M., Zeller, T., Nicolaes, G. A. F., Weber, C., Viola, J. R., Hidalgo, A., Scheiermann, C., & Soehnlein, O. (2018, Jul 3). Chrono-pharmacological Targeting of the CCL2-CCR2 Axis Ameliorates Atherosclerosis. *Cell Metab, 28*(1), 175-182.e175. https://doi.org/10.1016/j.cmet.2018.05.002

World Health Organization. (2020). *The top 10 causes of death*. https://www.who.int/news-room/fact-sheets/detail/the-top-10-causes-of-death

Wu, M. Y., Li, C. J., Hou, M. F., & Chu, P. Y. (2017, Sep 22). New Insights into the Role of Inflammation in the Pathogenesis of Atherosclerosis. *International journal of molecular sciences, 18*(10). https://doi.org/10.3390/ijms18102034

Würth, R., Bajetto, A., Harrison, J. K., Barbieri, F., & Florio, T. (2014). CXCL12 modulation of CXCR4 and CXCR7 activity in human glioblastoma stem-like cells and regulation of the tumor microenvironment. *Front Cell Neurosci, 8*, 144. https://doi.org/10.3389/fncel.2014.00144

Xin, H. B., Deng, K. Y., Rishniw, M., Ji, G., & Kotlikoff, M. I. (2002, Sep 3). Smooth muscle expression of Cre recombinase and eGFP in transgenic mice. *Physiol Genomics, 10*(3), 211-215. https://doi.org/10.1152/physiolgenomics.00054.2002

Yamada, K., Maishi, N., Akiyama, K., Towfik Alam, M., Ohga, N., Kawamoto, T., Shindoh, M., Takahashi, N., Kamiyama, T., Hida, Y., Taketomi, A., & Hida, K. (2015, Dec 15). CXCL12-CXCR7 axis is important for tumor endothelial cell angiogenic property. *Int J Cancer, 137*(12), 2825-2836. https://doi.org/10.1002/ijc.29655

Yamaguchi, J.-i., Kusano, K. F., Masuo, O., Kawamoto, A., Silver, M., Murasawa, S., Bosch-Marce, M., Masuda, H., Losordo, D. W., Isner, J. M., & Asahara, T. (2003, 2003/03/11). Stromal Cell–Derived Factor-1 Effects on Ex Vivo Expanded Endothelial Progenitor Cell Recruitment for Ischemic Neovascularization. *Circulation, 107*(9), 1322-1328. https://doi.org/10.1161/01.CIR.0000055313.77510.22

Yan, X., Cai, S., Xiong, X., Sun, W., Dai, X., Chen, S., Ye, Q., Song, Z., Jiang, Q., & Xu, Z. (2012, Apr). Chemokine receptor CXCR7 mediates human endothelial progenitor cells survival, angiogenesis, but not proliferation. *J Cell Biochem, 113*(4), 1437-1446. https://doi.org/10.1002/jcb.24015

Yao, Y., Zhou, Y., Liu, L., Xu, Y., Chen, Q., Wang, Y., Wu, S., Deng, Y., Zhang, J., & Shao, A. (2020, 2020-August-20). Nanoparticle-Based Drug Delivery in Cancer Therapy and Its Role in Overcoming Drug Resistance [Review]. *Frontiers in Molecular Biosciences, 7*. https://doi.org/10.3389/fmolb.2020.00193

Yellowley, C. (2013). CXCL12/CXCR4 signaling and other recruitment and homing pathways in fracture repair. *BoneKEy reports, 2*, 300-300. https://doi.org/10.1038/bonekey.2013.34

Yu, S., Crawford, D., Tsuchihashi, T., Behrens, T. W., & Srivastava, D. (2011). The chemokine receptor CXCR7 functions to regulate cardiac valve remodeling. *Developmental dynamics : an official publication of the American Association of Anatomists, 240*(2), 384-393. https://doi.org/10.1002/dvdy.22549

Yu, X. H., Fu, Y. C., Zhang, D. W., Yin, K., & Tang, C. K. (2013, Sep 23). Foam cells in atherosclerosis. *Clin Chim Acta, 424*, 245-252. https://doi.org/10.1016/j.cca.2013.06.006

Yusuf-Makagiansar, H., Anderson, M. E., Yakovleva, T. V., Murray, J. S., & Siahaan, T. J. (2002, Mar). Inhibition of LFA-1/ICAM-1 and VLA-4/VCAM-1 as a therapeutic approach to inflammation and autoimmune diseases. *Med Res Rev, 22*(2), 146-167. https://doi.org/10.1002/med.10001

Zabel, B. A., Wang, Y., Lewén, S., Berahovich, R. D., Penfold, M. E., Zhang, P., Powers, J., Summers, B. C., Miao, Z., Zhao, B., Jalili, A., Janowska-Wieczorek, A., Jaen, J. C., & Schall, T. J. (2009, Sep 1). Elucidation of CXCR7-mediated signaling events and inhibition of CXCR4-mediated tumor cell transendothelial migration by CXCR7 ligands. *J Immunol, 183*(5), 3204-3211. https://doi.org/10.4049/jimmunol.0900269

Zechner, R., Strauss, J., Frank, S., Wagner, E., Hofmann, W., Kratky, D., Hiden, M., & Levak-Frank, S. (2000, Nov). The role of lipoprotein lipase in adipose tissue development and metabolism. *Int J Obes Relat Metab Disord, 24 Suppl 4*, S53-56. https://doi.org/10.1038/sj.ijo.0801506

Zernecke, A., Shagdarsuren, E., & Weber, C. (2008, 2008/11/01). Chemokines in Atherosclerosis. *Arteriosclerosis, Thrombosis, and Vascular Biology, 28*(11), 1897-1908. https://doi.org/10.1161/ATVBAHA.107.161174

Zhang, S. H., Reddick, R. L., Piedrahita, J. A., & Maeda, N. (1992, Oct 16). Spontaneous hypercholesterolemia and arterial lesions in mice lacking apolipoprotein E. *Science, 258*(5081), 468-471. https://doi.org/10.1126/science.1411543

Zhao, D., Zhu, Z., Li, D., Xu, R., Wang, T., & Liu, K. (2015, 2015/11/17). Pioglitazone Suppresses CXCR7 Expression To Inhibit Human Macrophage Chemotaxis through Peroxisome Proliferator-Activated Receptor γ. *Biochemistry, 54*(45), 6806-6814. https://doi.org/10.1021/acs.biochem.5b00847

Zhao, Z., Ukidve, A., Kim, J., & Mitragotri, S. (2020, Apr 2). Targeting Strategies for Tissue-Specific Drug Delivery. *Cell, 181*(1), 151-167. https://doi.org/10.1016/j.cell.2020.02.001

Zhong, X., Li, X., Liu, F., Tan, H., & Shang, D. (2012, Aug 24). Omentin inhibits TNF-α-induced expression of adhesion molecules in endothelial cells via ERK/NF-κB pathway. *Biochem Biophys Res Commun, 425*(2), 401-406. https://doi.org/10.1016/j.bbrc.2012.07.110

Apendix A:

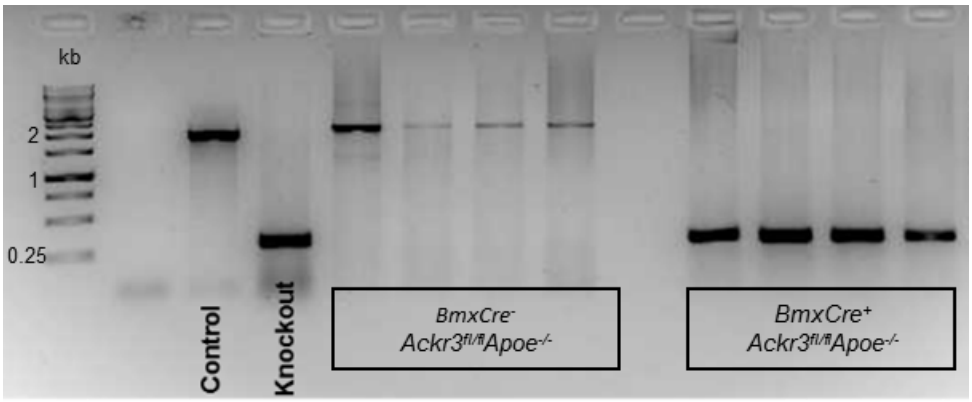

Figure 31: Genotyping of *Bmx*^{Cre} mediated deletion of *Ackr3* in *Apoe*$^{-/-}$ mice.

The control band is observed at 1.9 kb and the knockout band is observed at 0.3 kb.

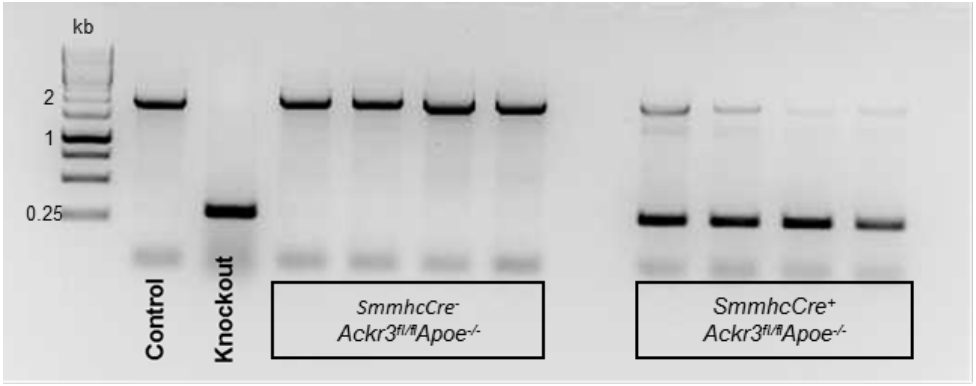

Figure 32: Genotyping of *Smmhc*^{Cre} mediated deletion of *Ackr3* in *Apoe*$^{-/-}$ mice.

The control band is observed at 1.9 kb and the knockout band is observed at 0.3 kb.

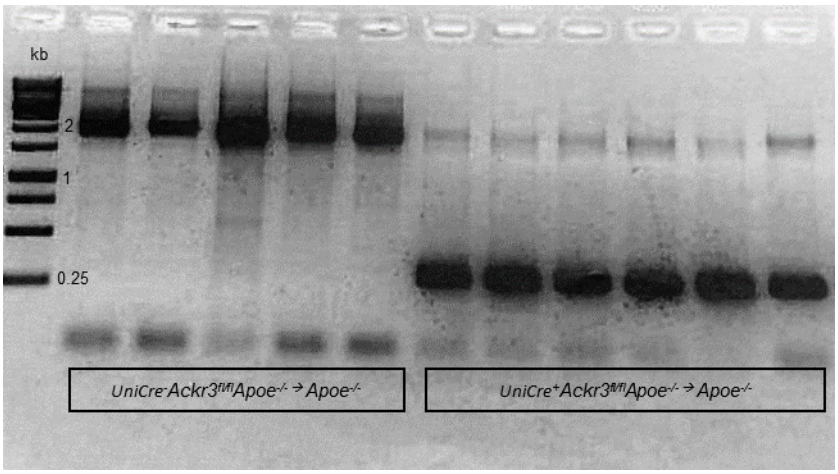

Figure 33: Genotyping of *Ackr3* deletion in bone marrow transplantation study.

The control band is observed at 1.9 kb and the knockout band is observed at 0.3 kb.

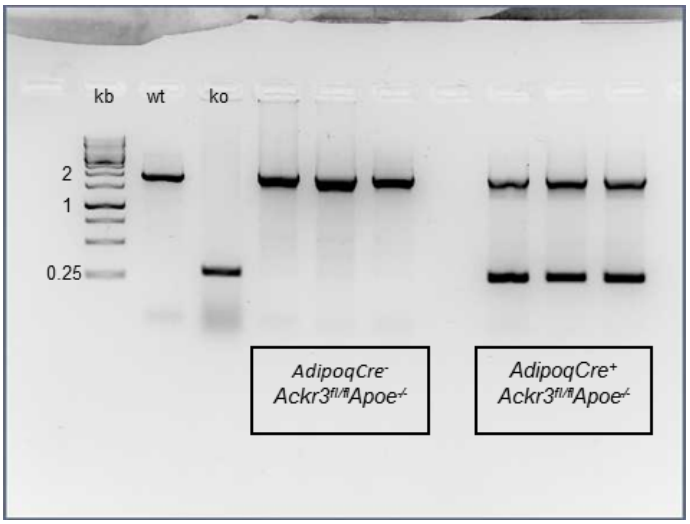

Figure 34: Genotyping of *Adipoq*^{Cre} mediated deletion of *Ackr3* in *Apoe*$^{-/-}$ mice.

The control band is observed at 1.9 kb and the knockout band is observed at 0.3 kb.

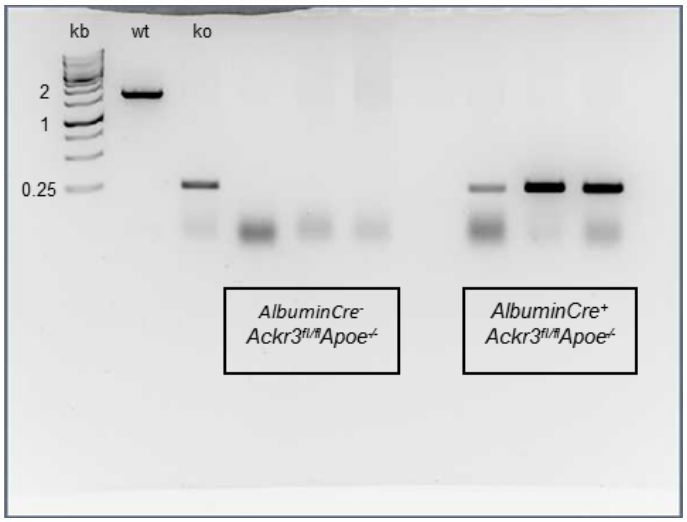

Figure 35: Genotyping of *Albumin*^{Cre} mediated deletion of *Ackr3* in *Apoe*$^{-/-}$ mice.

The control band is observed at 1.9 kb and the knockout band is observed at 0.3 kb.

Apendix B:

Table 6: Quantification of circulating leukocytes and leukocyte subsets via flow cytometry analysis in 4-week WD fed control and arterial endothelial ACKR3 deficient mice.

4 weeks WD	*BmxCre-* *Ackr3$^{fl/fl}$* *Apoe$^{-/-}$*	*BmxCre+* *Ackr3$^{fl/fl}$* *Apoe$^{-/-}$*	P-value
Leukocytes [x 10^6/ml]	1.9 ± 0.5	3.4 ± 0.8	0.15
Neutrophils [x 10^5/ml]	4.4 ± 1.4	10 ± 1.9	0.03*
Classical Monocytes [x 10^5/ml]	0.5 ± 0.1	1.0 ± 0.2	0.15
Non-classical Monocytes [x 10^4/ml]	7.1 ± 2.3	15 ± 4.0	0.09
B cells [x 10^5/ml]	8.6 ± 2.7	11.6 ± 3.7	0.5
T cells [x 10^5/ml]	3.6 ± 0.8	5.4 ± 1.3	0.42

Table 7: Quantification of circulating leukocytes and leukocyte subsets via flow cytometry analysis and quantification of plasma lipid levels in 12-week WD fed control and arterial endothelial deficient mice.

12 weeks WD	***BmxCre-*** ***Ackr3$^{fl/fl}$*** ***Apoe$^{-/-}$***	***BmxCre+*** ***Ackr3$^{fl/fl}$*** ***Apoe$^{-/-}$***	**P-value**
Leukocytes [x 10^6/ml]	1.3 ± 0.2	2.1 ± 0.2	0.011*
Neutrophils [x 10^5/ml]	3.5 ± 0.8	6.4 ± 0.8	0.017*
Classical Monocytes [x 10^5/ml]	1.0 ± 0.2	1.2 ± 0.1	0.541
Non-classical Monocytes [x 10^4/ml]	8.9 ± 1.9	8.2 ± 1.5	0.776
B cells [x 10^5/ml]	5.0 ± 1.0	8.2 ± 0.9	0.022*
T cells [x 10^5/ml]	1.8 ± 0.3	2.6 ± 0.3	0.072
Cholesterol [mg/dL]	1208.0 ± 100.9	984.8 ± 144.4	0.219
Triglycerides [mg/dL]	181.4 ± 17.8	132.2 ± 26.0	0.133

Table 8: Quantification of circulating leukocytes and leukocyte subsets via flow cytometry analysis and quantification of plasma lipid levels in 12-week WD fed control and SMC-ACKR3 deficient mice.

12 weeks WD	**SmmhcCre- Ackr3$^{fl/fl}$ Apoe$^{-/-}$**	**SmmhcCre+ Ackr3$^{fl/fl}$ Apoe$^{-/-}$**	**P-value**
Leukocytes [x 10^6/ml]	4.4 ± 0.5	2.5 ± 0.3	0.01*
Neutrophils [x 10^5/ml]	13.5 ± 2.7	4.3 ± 0.7	0.01*
Classical Monocytes [x 10^5/ml]	4.7 ± 1.3	3.1 ± 0.5	0.27
Non-classical Monocytes [x 10^5/ml]	2.5 ± 0.5	3.9 ± 0.6	0.13
B cells [x 10^5/ml]	16.9 ± 1.8	8.2 ± 1.1	0.002*
T cells [x 10^5/ml]	2.6 ± 0.4	1.8 ± 0.2	0.23
Cholesterol [mg/dL]	1293.0 ± 139.7	940.3 ± 180.4	0.14
Triglycerides [mg/dL]	107.5 ± 20.23	114.9 ± 13.79	0.76

Table 9: Quantification of circulating leukocytes and leukocyte subsets via flow cytometry analysis and quantification of plasma lipid levels, as well as plasma CXCL12 levels in 12-week WD fed control and htACKR3 (hematopoietic) deficient mice.

12-week WD	**Control**	**ht-ACKR3**	**P-value**
Leukocytes [x 10^6/ml]	2.9 ± 0.3	2.9 ± 0.3	0.91
Neutrophils [x 10^5/ml]	5.5 ± 0.6	7.0 ± 0.7	0.14
Classical Monocytes [x 10^5/ml]	1.7 ± 0.2	2.1 ± 0.2	0.22
Non-classical Monocytes [x 10^5/ml]	1.2 ± 0.1	1.7 ± 0.2	0.19
B cells [x 10^5/ml]	9.1 ± 0.9	11 ± 1.6	0.31
T cells [x 10^5/ml]	3.6 ± 0.4	3.9 ± 0.5	0.93
Cholesterol [mg/dL]	713.4 ± 77.8	656.3 ± 68.18	0.58
Plasma CXCL12 [pg/mL]	132.6 ± 11.68	128.9 ± 9.064	0.80

Table 10: Quantification of circulating leukocytes and leukocyte subsets via flow cytometry analysis and quantification of plasma lipid levels, as well as plasma CXCL12 levels in 4-week WD fed control and adipocyte ACKR3 deficient mice.

4-Week WD	***AdipoqCre-* *Ackr3*$^{fl/fl}$ *Apoe*$^{-/-}$**	***AdipoqCre+* *Ackr3*$^{fl/fl}$ *Apoe*$^{-/-}$**	**P-value**
Leukocytes [x 10^6/mL]	2.4 ± 0.2	2.1 ± 0.1	0.3445
Neutrophils [x 10^5/mL]	6.5 ± 0.5	5.8 ± 0.5	0.3701
Classical Monocytes [x 10^5/mL]	1.9 ± 0.3	2.1 ± 0.2	0.5925
Non-classical Monocytes [x 10^4/mL]	7.7 ± 1.3	9.3 ± 1.7	0.5826
B cells [x 10^5/mL]	8.7 ± 1.1	7.2 ± 0.6	0.2358
T cells [x 10^5/mL]	3.1 ± 0.3	2.5 ± 0.2	0.1476
Plasma CXCL12 [pg/mL]	452.1 ± 50.2	386.3 ± 66.08	0.4360
Mouse weight [g]	24.5 ± 0.5	25.6 ± 0.7	0.2575
wAT weight [mg]	341.6 ± 62.71	384.6 ± 72.18	0.6633

Table 11: Quantification of circulating leukocytes and leukocyte subsets via flow cytometry analysis in 4-week WD fed control and hepatic ACKR3 deficient mice.

4-week WD	**AlbuminCre- Ackr3$^{fl/fl}$ Apoe$^{-/-}$**	**AlbuminCre+ Ackr3$^{fl/fl}$ Apoe$^{-/-}$**	**P-value**
Leukocytes [x 10^6/ml]	2.6 ± 0.3	2.3 ± 0.3	0.5180
Neutrophils [x 10^5/ml]	5.8 ± 1.2	5.3 ± 1.6	0.8075
Classical Monocytes [x 10^5/ml]	1.7 ± 0.2	2.3 ± 0.7	0.6009
Non-classical Monocytes [x 10^4/ml]	9.9 ± 1.4	11.1 ± 2.8	0.7396
B cells [x 10^5/ml]	10.0 ± 1.5	7.7 ± 1.1	0.2094
T cells [x 10^5/ml]	4.2 ± 0.6	3.6 ± 0.6	0.4722

Apendix C:

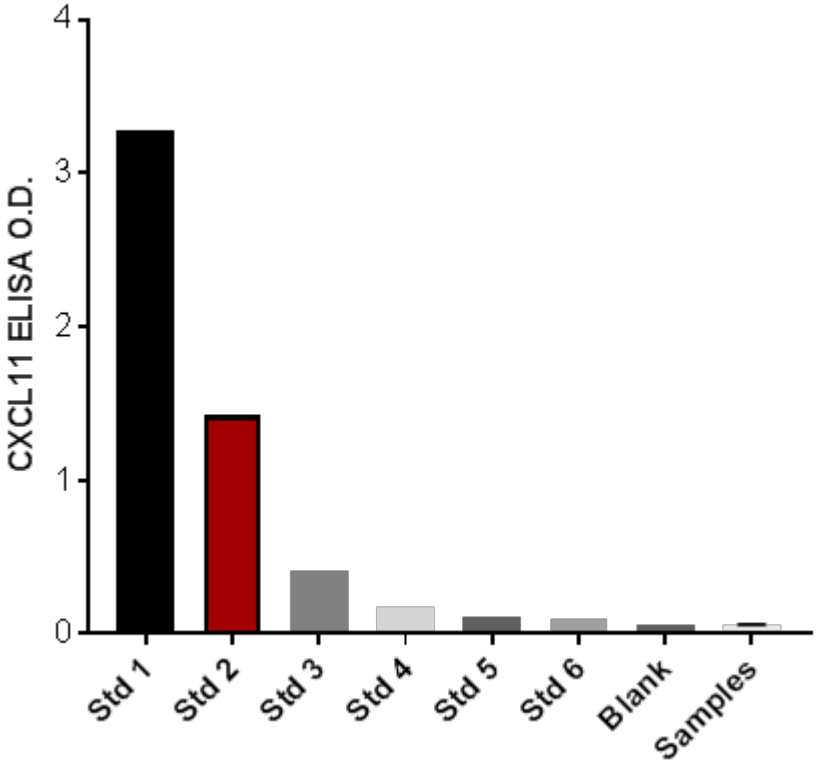

Figure 36: CXCL11 measurement in mouse plasma samples.

Apoe$^{-/-}$ mouse plasma samples were screened for the presence of CXCL11 in the plasma via ELISA (n=64). Std = standard, samples = mouse plasma samples. Error bar indicates ±SEM.

Apendix D:

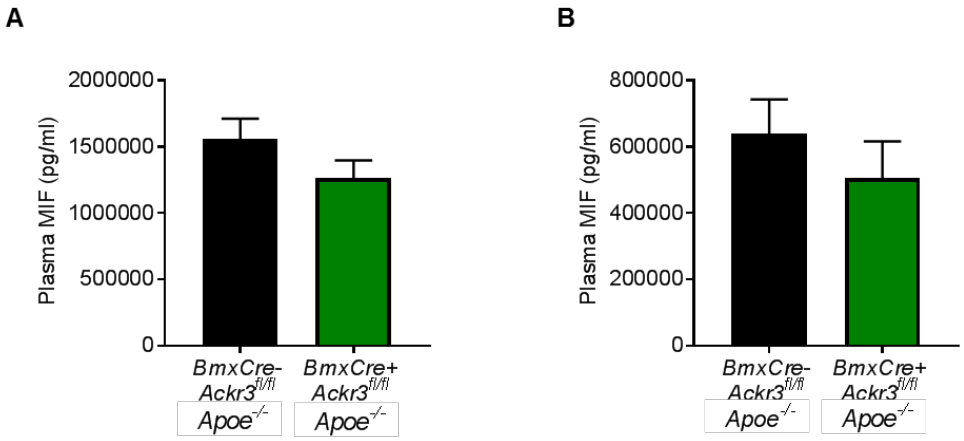

Figure 37: MIF levels in mouse plasma samples.

MIF was measured in the plasma of A. 4 week (n=9-11) and B. 12 week (n=12-13) WD fed control and aEC-ACKR3 mice. Error bars indicate ±SEM.

Acknowledgements

I would like to thank my principal investigators and supervisors Prof. Dr. Yvonne Döring and Prof. Dr. Christian Weber for giving me the opportunity to work on this project at IPEK, LMU and for supporting me in many ways throughout my PhD work! They both set out great examples to us in terms of a professional and successful career and I look up to their accomplishments.

I would like to express my gratitude to my daily supervisor Dr. Emiel van der Vorst for always supporting me in my endeavours and for all his time and efforts he has spent on teaching and guiding me. I would also like to thank Emiel for his patience, for always making time for me and for always being there regardless of the distance and the load of work he had on his plate. I have always wondered how he manages so much demanding work simultaneously.

I would like to thank our hard working and talented assistants Soyolmaa Bayasgalan and Yvonne Jansen, as well as our former assistant Sonja Mühlberger for always supporting me and assisting me in my PhD work throughout the years. Without their support, the PhD would surely take way longer! Yvonne J. has always been the master of techniques and a very good lab manager! Her speed and dedication has always impressed her colleagues. Soyolmaa was at all times happy to learn new experiments, she had a good eye for detail and she assisted us in so many ways! Special thanks to Soyolmaa, Yvonne and Olga Schengel for all the hard work they put in for the genotyping of our mouse lines!

I would like to extend my gratitude to our team members Dr. Yi Yan, Linsey Peters and Madeleine Müller for their kindness, support and friendship. We shared great times together and I am happy that we always keep in touch despite the distances and busy schedules.

I would like to thank my thesis advisory committee members Prof. Dr. Jürgen Bernhagen, Dr. Siegfried Ussar as well as my supervisors for their time, guidance and support.

I would like to thank Dr. Ismail Cimen for his friendship, kindness and for always supporting me at work like a voluntary supervisor. I always enjoyed our stimulating scientific discussions and I am looking forward to working with him and Professor Erbay on exciting projects coming up in the next step of my career!

I would also like to thank all of the co-authors in the publications arising from this work as well as other colleagues and scientists allowing me to be a part of their projects and publications.

Furthermore, I am thankful to the members of IPEK whose collaboration and team work helped us carry out our experiments and provided us a friendly environment. Thank you, Dr. Lucia Natarelli for staying on top of cell culture and making sure it always operates well up to standards! Many thanks to everyone taking part in the maintenance of the equipment and instruments!

All of the *in vivo* mouse work would not be possible without our animal facility ZVH team, thank you all very much for running the ZVH, for taking such good care of our mice and for supporting us with our mouse experiments!

A big thank you to the members of IRTG1123, specially to Prof. Dr. Sabine Steffens and to Catherine Gunczi for establishing, managing and coordinating the IRTG!

Thank you, Claudia Geißler, for always creating a friendly and social atmosphere on the second floor, engaging well with your colleagues and being so nice.

Many thanks to the IPEK Office team for always helping us with administrative matter very promptly! And many thanks to Herr Putz and Dr. Hundelshausen for extending their support in the demanding field of IT!

Last but not least, I would like to thank my family and my closest friends for always supporting me throughout my career. Special thanks to my mum and dad for enabling me to have such good education and for always supporting me emotionally and financially, no matter what. Many thanks to my sweet sister, my loving husband and my best friends for always being there through thick and thin! Success is more achievable and the journey is more meaningful with the support of the loved ones.

Affidavit

Affidavit

Gencer, Selin

Surname, first name

Street

Zip code, town, country

I hereby declare, that the submitted thesis entitled:

Cell-specific roles of ACKR3 in atherosclerosis

……

is my own work. I have only used the sources indicated and have not made unauthorised use of services of a third party. Where the work of others has been quoted or reproduced, the source is always given.

I further declare that the submitted thesis or parts thereof have not been presented as part of an examination degree to any other university.

_Munich, 20.01.2022 _____Selin Gencer_____

place, date Signature doctoral candidate

Confirmation of congruency

LMU LUDWIG-MAXIMILIANS-UNIVERSITÄT MÜNCHEN | Promotionsbüro Medizinische Fakultät | MMRS

Confirmation of congruency between printed and electronic version of the doctoral thesis

Gencer, Selin

Surname, first name

Street

Zip code, town, country

I hereby declare, that the submitted thesis entitled:

Cell-specific roles of ACKR3 in atherosclerosis

……

is congruent with the printed version both in content and format.

__ Munich, 20.01.2022 _Selin Gencer_____

place, date Signature doctoral candidate

List of publications

Hakeem Said, I., **Gencer, S.**, Ullrich, M. S., & Kuhnert, N. (2018, Jun). Tea and coffee time with bacteria - Investigation of uptake of key coffee and tea phenolics by wild type E. coli. *Food Res Int, 108*, 584-594. https://doi.org/10.1016/j.foodres.2018.03.023

Chilloux, J., Brial, F., Everard, A., Smyth, D., Zhang, L., Plovier, H., Myridakis, A., Hoyles, L., Fuchs, J. E., Blancher, C., **Gencer, S.**, Martinez-Gili, L., Fearnside, J. F., Barton, R. H., Neves, A. L., Rothwell, A. R., Gérard, C., Calderari, S., Boulangé, C. L., Patel, S., Scott, J., Glen, R. C., Gooderham, N. J., Nicholson, J. K., Gauguier, D., Liu, P. P., Cani, P. D., & Dumas, M.-E. (2018). Microbiome Inhibition of IRAK-4 by Trimethylamine Mediates Metabolic and Immune Benefits in High-Fat-Diet-induced Insulin Resistance. *bioRxiv*, 277434. https://doi.org/10.1101/277434

van der Vorst, E. P. C., Peters, L. J. F., Muller, M., **Gencer, S.**, Yan, Y., Weber, C., & Doring, Y. (2019). G-Protein Coupled Receptor Targeting on Myeloid Cells in Atherosclerosis. *Front Pharmacol, 10*, 531. https://doi.org/10.3389/fphar.2019.00531

Gencer, S., van der Vorst, E. P. C., Aslani, M., Weber, C., Döring, Y., & Duchene, J. (2019, Apr). Atypical Chemokine Receptors in Cardiovascular Disease. *Thromb Haemost, 119*(4), 534-541. https://doi.org/10.1055/s-0038-1676988

Döring, Y., van der Vorst, E. P. C., Duchene, J., Jansen, Y., **Gencer, S.**, Bidzhekov, K., Atzler, D., Santovito, D., Rader, D. J., Saleheen, D., & Weber, C. (2019, Mar 5). CXCL12 Derived From Endothelial Cells Promotes Atherosclerosis to Drive Coronary Artery Disease. *Circulation, 139*(10), 1338-1340. https://doi.org/10.1161/circulationaha.118.037953

van der Vorst, E. P. C., Mandl, M., Muller, M., Neideck, C., Jansen, Y., Hristov, M., **Gencer, S.**, Peters, L. J. F., Meiler, S., Feld, M., Geiselhoringer, A. L., de Jong, R. J., Ohnmacht, C., Noels, H., Soehnlein, O., Drechsler, M., Weber, C., & Doring, Y. (2019, Apr). Hematopoietic ChemR23 (Chemerin Receptor 23) Fuels Atherosclerosis by Sustaining an M1 Macrophage-Phenotype and Guidance of Plasmacytoid Dendritic Cells to Murine Lesions-Brief Report. *Arterioscler Thromb Vasc Biol, 39*(4), 685-693. https://doi.org/10.1161/ATVBAHA.119.312386

Gencer, S., Lacy, M., Atzler, D., van der Vorst, E. P. C., Döring, Y., & Weber, C. (2020, Dec). Immunoinflammatory, Thrombohaemostatic, and Cardiovascular Mechanisms in COVID-19. *Thromb Haemost, 120*(12), 1629-1641. https://doi.org/10.1055/s-0040-1718735

Doring, Y., Jansen, Y., Cimen, I., Aslani, M., **Gencer, S.**, Peters, L. J. F., Duchene, J., Weber, C., & van der Vorst, E. P. C. (2020, Mar 13). B-Cell-Specific CXCR4 Protects Against Atherosclerosis Development and Increases Plasma IgM Levels. *Circ Res, 126*(6), 787-788. https://doi.org/10.1161/CIRCRESAHA.119.316142

Gencer, S., Döring, Y., Jansen, Y., Bayasgalan, S., Schengel, O., Müller, M., Peters, L. J. F., Weber, C., & van der Vorst, E. P. C. (2021). Adipocyte-Specific ACKR3 Regulates Lipid Levels in Adipose Tissue. *Biomedicines, 9*(4), 394. https://www.mdpi.com/2227-9059/9/4/394

Gencer, S., Evans, B. R., van der Vorst, E. P. C., Döring, Y., & Weber, C. (2021, Jan 25). Inflammatory Chemokines in Atherosclerosis. *Cells, 10*(2). https://doi.org/10.3390/cells10020226

Sundararaman, S. S., Peters, L. J. F., Jansen, Y., **Gencer, S.**, Yan, Y., Nazir, S., Bonnin Marquez, A., Kahles, F., Lehrke, M., Biessen, E. A. L., Jankowski, J., Weber, C., Doring, Y., & van der Vorst, E. P. C. (2021, May 17). Adipocyte calcium sensing receptor is not involved in visceral adipose tissue inflammation or atherosclerosis development in hyperlipidemic Apoe(-/-) mice. *Sci Rep, 11*(1), 10409. https://doi.org/10.1038/s41598-021-89893-y

He, Y. Y., Xie, X. M., Zhang, H. D., Ye, J., **Gencer, S.**, van der Vorst, E. P. C., Döring, Y., Weber, C., Pang, X. B., Jing, Z. C., Yan, Y., & Han, Z. Y. (2021). Identification of Hypoxia Induced Metabolism Associated Genes in Pulmonary Hypertension. *Front Pharmacol, 12*, 753727. https://doi.org/10.3389/fphar.2021.753727

Patel, V. C., Lee, S., McPhail, M. J. W., Da Silva, K., Guilly, S., Zamalloa, A., Witherden, E., Støy, S., Manakkat Vijay, G. K., Pons, N., Galleron, N., Huang, X., **Gencer, S.**, Coen, M., Tranah, T. H., Wendon, J. A., Bruce, K. D., Le Chatelier, E., Ehrlich, S. D., Edwards, L. A., Shoaie, S., & Shawcross, D. L. (2022, Feb). Rifaximin-α reduces gut-derived inflammation and mucin degradation in cirrhosis and encephalopathy: RIFSYS randomised controlled trial. *J Hepatol, 76*(2), 332-342. https://doi.org/10.1016/j.jhep.2021.09.010